CSIRO PUBLISHING

Invertebrate Systematics, 2015, **29**, 124–163
http://dx.doi.org/10.1071/IS14041

Total evidence analysis of the phylogenetic relationships of Lycosoidea spiders (Araneae, Entelegynae)

Daniele Polotow[A,B,D], *Anthea Carmichael*[A] *and Charles E. Griswold*[A,C]

[A]Arachnology Laboratory, California Academy of Sciences, 55 Music Concourse Drive, San Francisco, CA 94118, USA.
[B]Present address: Laboratório Especial de Coleções Zoológicas, Instituto Butantan, Av. Vital Brasil, 1500, Butantã, São Paulo, SP, 05503-900.
[C]Department of Environmental Science, Policy and Management, University of California, Berkeley, CA 94720-3114, USA.
[D]Corresponding author. Email: danielepolotow@gmail.com

Abstract. Phylogenetic relationships within the superfamily Lycosoidea are investigated through the coding and analysis of character data derived from morphology, behaviour and DNA sequences. In total, 61 terminal taxa were studied, representing most of the major groups of the RTA-clade (i.e. spiders that have a retrolateral tibial apophysis on the male palp). Parsimony and model-based approaches were used, and several support values, partitions and implied weighting schemes were explored to assess clade stability. The morphological–behavioural matrix comprised 96 characters, and four gene fragments were used: 28S (~737 base pairs), actin (~371 base pairs), COI (~630 base pairs) and H3 (~354 base pairs). Major conclusions of the phylogenetic analysis include: the concept of Lycosoidea is restricted to seven families: Lycosidae, Pisauridae, Ctenidae, Psechridae, Thomisidae, Oxyopidae (but Ctenidae and Pisauridae are not monophyletic) and also Trechaleidae (not included in the analysis); the monophyly of the 'Oval Calamistrum clade' (OC-clade) appears to be unequivocal, with high support, and encompassing the Lycosoidea plus the relimited Zoropsidae and the proposed new family Udubidae (fam. nov.); Zoropsidae is considered as senior synonym of Tengellidae and Zorocratidae (syn. nov.); Viridasiinae (rank nov.) is raised from subfamily to family rank, excluded from the Ctenidae and placed in Dionycha. Our quantitative phylogenetic analysis confirms the synonymy of Halidae with Pisauridae. The grate-shaped tapetum appears independently at least three times and has a complex evolutionary history, with several reversions.

Additional keywords: 28S rRNA, actin, cladistic analysis, COI, Ctenidae, Dionycha, H3, Halidae, Lycosidae, Oxyopidae, Pisauridae, Senoculidae, systematic, taxonomy, Tengellidae, Thomisidae, Udubidae, Zorocratidae, Zoropsidae.

Received 25 July 2014, accepted 23 October 2014, published online 11 June 2015

Introduction

The superfamily Lycosoidea includes, to date, the wolf spiders and their relatives and it was defined by having a grate-shaped tapetum in the secondary eyes (Homann 1971). Most spiders have eight eyes, arranged roughly in two rows, where the first row contains the antero-median and antero-lateral eyes, and the second contains the postero-median and the postero-lateral eyes (Land 1985). The antero-median pair is usually referred to as the principal eyes, which differ from the remaining secondary eyes (Homann 1971; Land 1985). The secondary eyes usually have a tapetum, which consists of several layers of guanine crystals, acting as a colour-selective interference reflector (Land 1972). Its function is probably the same as that of vertebrate tapeta, at least in wandering spiders; that is, to reflect light back through the receptors, giving them a second opportunity to absorb photons (Land 1985), thereby improving the formation of images (Homann 1971). Homann (1971) presented descriptions of the tapeta of several families and classified the eyes according with the arrangement of the crystals layer, although by no means all secondary eyes fit Homann's classification (Land 1985).

A peculiar kind of tapetum is the grate-shaped type, which has the reflecting material arranged in strips that resembles the grill of an oven (Land 1985: figs 2a, c; Fenk and Schimid 2010: fig. 1). The rhabdomeric portion of each receptor sits on the tapetal strip as though on a chair, with the axon bending round and under the strip before leaving the eye (Baccetti and Bedini 1964). Another distinguished type is the canoe-shaped, which consists of two lateral walls that enclose the rhabdomeric regions of the receptors. At the base there is a slit through which the axons of the receptors penetrate (Land 1985: figs 2b, d). Some spiders present the tapeta as a reflecting sheet with pores in it where the axons of the receptors penetrate (Land 1985).

The grate-shaped tapetum was considered to be a synapomorphy for the superfamily Lycosoidea (Homann 1971; Griswold 1993) and can be found in the wandering spider families Lycosidae, Oxyopidae, Ctenidae, Pisauridae, Senoculidae, Trechaleidae, Psechridae, in some Zoropsidae and Stiphidiidae, in the genera *Miturga* Thorell, 1870, *Argoctenus* L. Koch, 1878 and *Odo* Keyserling, 1887 (Miturgidae) (Homann 1971; Griswold 1993). Several Thomisidae species were reported with a grate-shaped tapetum (Homann 1928; Barth 2002: 132; Ramírez 2014: fig. 12I), but it can only be observed by dissecting the eyes. Recent analyses using molecular data (Agnarsson *et al*. 2013*b*) place Thomisidae among the Lycosoidea, and it was also considered a near-optimal solution in the morphological analysis of Ramírez (2014: fig. 215D). Considering some recent cladistic analyses, the superfamily appears to be non-monophyletic and the grate-shaped tapetum probably evolved more than once in the phylogeny of spiders (Silva Dávila 2003; Griswold *et al*. 2005; Miller *et al*. 2010; Ramírez 2014: figs 194A, B).

Lycosoidea are placed in the RTA Clade, which also contains Dionycha, dictynoids and amaurobioids and their relatives (Forster 1970), the fused paracribellar clade (also called 'austral cribellates') and the oval calamistrum clade (Griswold 1993; Griswold *et al*. 2005; Spagna and Gillespie 2008; Miller *et al*. 2010). The RTA Clade is defined by the presence of a unique retrolateral tibial apophysis on the male palp (Coddington and Levi 1991; Griswold *et al*. 2005). The homology of the palpal elements, including the retrolateral tibial apophysis, of several families is discussed by Sierwald (1990). Lycosoid relationships have been repeatedly studied and with the exception of the results presented by Griswold (1993), all the subsequent phylogenetic analyses indicated that Lycosoidea is non-monophyletic (Griswold *et al*. 1999, 2005; Silva Dávila 2003; Spagna and Gillespie 2008). There is some evidence that the grate-shaped tapetum has little phylogenetic value and evolved at least three times in the phylogeny of spiders (Silva Dávila 2003; Griswold *et al*. 2005; Ramírez 2014).

Our main goal here is to test the monophyly and composition of Lycosoidea and propose a total-evidence (genomic, morphological and behavioural data) hypothesis of phylogenetic relationships of Lycosoidea and their kin. On the basis of previous cladistic analyses (Griswold 1993; Griswold *et al*. 1999, 2005; Silva Dávila 2003; Raven and Stumkat 2005; Spagna and Gillespie 2008; Miller *et al*. 2010; Agnarsson *et al*. 2013*a*, 2013*b*; Ramírez 2014), we include spiders from the RTA Clade with either a grate- or non-grate-shaped tapetum in the eyes to test the limits of Lycosoidea. Previous phylogenetic analyses of high-level relationships of spiders have included large numbers of cribellate taxa (Griswold *et al*. 1999, 2005; Spagna and Gillespie 2008; Miller *et al*. 2010) because these are reasoned to be more likely to straddle the basal nodes of the phylogeny of higher groups than are their relatives that have lost the cribellum (Griswold *et al*. 2005). In this analysis we include both cribellate and non-cribellate species, because many families assigned to Lycosoidea are entirely ecribellate and because, to date, there is a large literature about the relationships of the basal nodes of spider phylogeny, which permits and encourages the investigation of taxa rarely treated in a molecular phylogeny of higher groups, such as Dionycha and Lycosoidea.

Materials and methods

Taxon sampling

Choice of terminal taxa was based on previous studies, such as the lycosoid phylogeny proposed by Griswold (1993), the ctenoid phylogeny proposed by Silva Dávila (2003), the zoropsoid phylogeny proposed by Raven and Stumkat (2005) and the recent, wide-ranging studies of Agnarsson *et al*. (2013*b*) and Ramírez (2014). Our goal was to include representatives of all spider families with the grate-shaped tapetum, a derived condition of the tapetum of the indirect eyes (Fenk and Schmid 2010: fig. 1). All these taxa belong to a group named the 'RTA-clade' (Coddington and Levi 1991), an informal group that comprises spiders with retrolateral tibial apophysis (RTA) on the male palp. The taxa used to generate the data for this study are described in Appendix 1. A large proportion of the specimens were used to generate both the molecular and morphological data. Description of the morphological characters can be found in Appendix 2 and the morphological matrix in Table 1. Voucher specimens were provided by the following museums (curator in parentheses): AMNH, American Museum of Natural History, New York (N. Platnick); CAS, California Academy of Sciences, San Francisco (C. Griswold); IBSP, Instituto Butantan, São Paulo (D. M. Barros Battesti); MACN, Museo Argentino de Ciencias Naturales 'Bernardino Rivadavia', Buenos Aires (C. Scioscia); UFMG, Universidade Federal de Minas Gerais, Belo Horizonte (A. Santos).

Morphological and behavioural data

The specimens were preserved in 75–95% ethanol. Morphological observation and illustrations of external structures were made using a Leica MZ12 stereomicroscope with camera lucida. Digital scanning electron microscope (SEM) photographs were taken on a LEO 1450vp SEM at the Entomology Department of California Academy of Sciences, San Francisco, USA. Preparation of specimens for the SEM follows Álvarez-Padilla and Hormiga (2007). For SEM preparation, specimens were cleaned ultrasonically, transferred to 100% ethanol for at least 48 h, submitted to critical-point drying or air-dried. After drying, specimens were mounted on rivets using copper wire, then sputter-coated with gold. Epigyna were excised from the abdomens of adult females and cleaned by either immersion in a trypsin solution, digested with contact lens cleaner (ReNu®) overnight or cleared with clove oil in order to examine internal structures (Sierwald 1989).

The morphological and behavioural dataset included 96 characters, scored for 61 taxa (Appendix 2). Mesquite 2.5 (Maddison and Maddison 2011) was used to build and edit the character matrix. Inapplicable and unknown states are presented as '–' and '?', respectively. All characters were *a priori* equally weighted and all multistate characters were coded as non-additive (Fitch 1971; Swofford and Maddison 1987). An *a posteriori* implied weight scheme was applied during some searches with TNT 1.1 (Goloboff *et al*. 2008*a*). Ambiguous character optimisations were solved so as to favour reversal or

Table 1. Data matrix

Taxa	Characters									
	0000000001	1111111112	2222222223	3333333334	4444444445	5555555556	6666666667	7777777778	8888888889	999999
	1234567890	1234567890	1234567890	1234567890	1234567890	1234567890	1234567890	1234567890	1234567890	123456
Parazygiella_carpenteri	0000002000	-013311100	0000110000	000100010-	-0-1301001	00---0010-	----000000	00-2101000	0000110?1	0-0000
Megadictyna_thilenii	0000000000	-011000100	0001000000	0000----0-	-0-0001001	10---0000-	----0?3000	0100001000	0000100?1	110000
Vidole_capensis	2120000011	1013611100	0001110000	0001000010	0100200001	10---1000-	----0?3000	0100001000	0001110?1	100000
Callobius_nevadensis	1120000011	0013311100	1111110011	1001000010	0100200101	10---00010	1011113000	0100001100	0000100?1	100000
Cybaeus_sp	2100000011	1013411101	1000000000	0000----0-	-110300001	10---00010	1012113000	00-0000010	0001100?1	0-000?
Textrix_denticulata	2141000012	?012311100	1000000000	0000----0-	-110200001	10---00010	00111?3000	00-0001010	0001100?1	0-000?
Coelotes_terrestris	1120010012	?013301101	1000010000	000100000-	-110000001	10---00010	10111?3000	00-0001000	0000110?1	0-000?
Agelenopsis_pensylvanica	2132200011	1013311100	1000000000	0000----0-	-110300001	10---12010	1010112000	10-0001010	0000110?1	0-1000
Desis_formidabilis	1110000011	00142100-0	1000000000	000100000-	-110000001	00---00011	0011100000	00-0000010	0001110?1	0-0000
Stiphidion_facetum	2131121011	1013211100	1100010000	0000----0-	-110200001	10---10010	0012113000	1100010100	0000100?1	100000
Cambridgea_sp	2130000011	0012310100	1100000000	000100000-	-100200001	10---10010	0010113000	10-0010100	00001?00?1	0-0000
Trachelas_tranquilus	0020002011	1113211100	1000000000	0000----0-	-0-0302000	-110100011	100-100000	00-0000200	0000110?1	0-000?
Anyphaena_pacifica	0030202011	011361?100	1000000000	000100000-	-101200000	-110110011	1010102000	00-1000200	0000100?1	0-000?
Metaphidippus_manni	1130222101	0001111100	1000100000	0000----0-	-0-0302000	-111000010	1010102000	10-0001200	0000110?1	0-0000
Cheiracanthium_sp	1120000011	010311?100	1000011000	0001001010	00-1000001	011110??11	1010112000	00-1001100	0000000?1	0-100?
Cheiracanthium_mildei	1100000001	010321?100	1000011000	0001001010	00-1000000	-111000011	1011101000	00-100?100	0000100?1	0-1000
Mituliodon_tarantulinus	0030111011	1003211110	1000001000	0001001010	00-1010000	-110100011	1011101000	00-2001101	0000110001	0-100?
Argoctenus_9023609	0031121010	-0032010-0	1000001000	0001001010	00-1010000	-111102011	101110?0?0	00-2001???	????????00	--000?
Argoctenus_9019841	0031121011	1003211100	1000001000	0001001010	00-1010000	-111100011	1011102000	00-2001???	????????00	--000?
Vulsor_isaloensis	0031101011	1003211110	1010010010	1001001010	10-1000010	-111100011	1010103000	10-2001100	0010100?1	0-000?
Viridasius_9015404	0031101011	1003211110	1010010010	1001001010	10-1200010	-111100011	1010101000	10-2001101	00001?0?01	0-000?
Viridasius_9016432	0031101011	1003211110	1010010011	1001001010	10-1200010	-111110011	1010102031	10-2001100	00001?0??1	0-000?
Apollophanes_sp	0010002001	0011011100	1000000000	0000----0-	-0-0300200	-111100010	1011102000	10-0001100	0000000?0	--000?
Odo_abudi	0031101011	1003211110	1000000000	0001001010	00-1200000	-111100011	1011101000	10-200?101	00?0??0000	--000?
Odo_bruchi	0031100011	0003211100	1000000000	0001001010	00-1200000	-111100011	1010101000	10-200?101	00?0??0000	--000?
Raecius_asper	1120000011	1003301110	1100100000	10011-0010	0100200101	00---02011	0011102110	0110000100	00?0??0??1	110000
Uduba_sp	1120000011	1003301110	1100000100	1001000010	0101211001	00---02011	0011103110	00-0000100	1000110?1	0-0000
Zorodictyna_9031271	0030000011	1003301110	1100010010	1001000010	0100200101	00---02011	0011103110	0112000101	0000100?1	11000?
Zorodictyna_9035866	0030010011	1003311110	1100110010	1001000010	0100200101	00---02011	0011103110	00-2000100	1000100?1	0-000?
Zorodictyna_9029890	0030010011	100331111?	??????????	??????????	??????????1	00---02011	0011103?10	00-200?100	10?0??0?1	0-000?
Zorodictyna_9029889	0030010011	100331111?	??????????	??????????	??????????1	00---02011	0011103?10	00-200?100	0000100?1	0-000?
Tengella_sp	0030200011	1003411100	1010000010	1001000010	00-?200001	10---00011	0011113010	0112000100	0010110?1	10000?
Tengella_radiata	0030200011	1003411100	1010000010	1001000010	00-0200001	10---00011	0011113010	0112000100	0010110?1	100000
Zorocrates_fuscus	0030010011	1003301100	1000110000	1001000010	0101210001	0110100011	0011103010	0112000100	10?0??0021	100000
Zoropsis_spinimana	0030111011	1003311110	1000110111	1001010010	0100200200	-111100011	1011104131	0110000100	1000100011	100000
Titiotus_sp	0030010011	1003311110	1110100011	1001010010	0100200101	0111000011	1011103031	00-2000101	00?0??0011	0-?00?
Kilyana_hendersoni	0030101011	1003311110	1110110110	1001010110	0101210000	-111100111	1011103111	00-2000100	1000100?1	0-000?
Senoculus_3250	2011121010	-013311101	1010010000	0000----1?	0100200201	10---10011	1010104031	10-1000200	00?0??0021	0-?000
Uliodon_frenatus	0030010011	1003311110	1010110110	1001000010	0101200100	-0---00011	1011103010	00-2000100	0000100?1	0-000?
Austrotengella_toddae	0031100011	1002311110	1010100010	10011-0010	00-0200101	00---00011	1011103031	00-1000101	0010110?1	0-000?
Phanothea_digitata	0030012111	1003311110	1010100110	10011-0010	00-0200201	00---00011	1011103110	00-2000101	00101101?1	0-000?
Griswoldia_acaenata	0030111011	1003311110	1010110110	10011-0010	00-0200101	00---01111	1011103120	00-2000101	0000110?1	0-000?
Griswoldia_disparilis	0030111011	1003311110	1010100110	10011-0010	00-0200101	00---00111	1011103120	00-2000101	0000110?1	0-000?
Celaetycheus_abara	0031121011	1003501110	1010110010	1001000010	0100400001	0111000011	1011103021	00-1000101	0000110020	--000?
Ctenus_gr_crulsi	0031121011	100340?110	1010000011	10011-0010	0101200100	-111103011	1011103020	00-1000101	0000100021	0-0001
Enoploctenus_cyclothorax	0041121011	1003411110	1000000010	10011-0010	0100200001	011110??11	1011104031	?0-2000101	00?01?0021	0-0000
Caloctenus_oxapampa	0041121011	10133??110	1000010010	10011-0010	0101200201	0111010011	1011114031	?0-2000100	0000100?1	0-000?

(*continued next page*)

Table 1. (*continued*)

Taxa	Characters									
	0000000001	1111111112	2222222223	3333333334	4444444445	5555555556	6666666667	7777777778	8888888889	999999
	1234567890	1234567890	1234567890	1234567890	1234567890	1234567890	1234567890	1234567890	1234567890	123456
Ancylometes_bogotensis	0031121011	1003402110	1010000001	1001000010	0100400101	010–100011	1011112010	00–2000100	0010110021	0–0001
Acanthoctenus_sp	0041121011	1003311112	??????????	?0?????0?1	??????????1	0111000011	1011104231	0112002100	1000110021	110000
Psechrus_cebu	0032101011	1013411100	0000000112	1000––––12	00–0302001	1111000010	0011114020	0110000100	0000110021	100001
Cupiennius_salei	0031121011	1003411110	1000000000	0001000010	0101300201	0111100011	1010113010	00–1000100	0000111021	0–0002
Misumenoides_sp	2111011001	0013212102	??????????	?????????0	??????????0	–0–––00010	1001103210	00–0102200	0000120020	––000?
Tmarus_sp	0030111001	0010012101	1101110000	0000––––0–	00–1001000	–0–––00011	1001103000	20–0100200	0000000021	0–000?
Oxyopes_sp	0031211110	–012112100	1000000000	0001000010	0100200001	10–––00111	1110112000	00–1100100	0000000021	0–000?
Peucetia_rubrolineata	0031211110	–010012100	1000010000	0001000010	00–0400001	10–––00110	1110113000	00–1100200	0000?210?1	0–0000
Draposa_tenasserineasis	0030101011	1013311110	0000000000	0101000111	00–1301001	010–100011	1010113001	00–1100100	0000111021	0–0012
Alopecosa_kochi	0030101011	1013211110	0000000000	0101000111	00–1301001	010–100011	1010113000	00–1100100	0000111021	0–0012
Nilus_majunguensis	0031121011	1013311110	1000000000	0111000?12	00–1401201	10–––10011	1010113010	10–1100100	0000111021	0–0101
Thaumasia_hirsutochela	0030121011	1013311110	1010000000	0111000010	00–1000201	10–––10011	1010113010	?0–1100100	0100111021	0–010?
Architis_brasiliensis	0042121011	1013311100	1010000000	0000––––10	00–0201201	10–––10011	1010113011	10–1100100	0100101021	0–010?
Hala_cf_paulyi	0032121011	1013311100	1010000000	0110––––0–	00–1000001	10–––10011	1010113010	10–1100100	0001200021	0–010?

secondary loss over convergence (Farris optimisation or ACCTRAN).

Abbreviations

ALE, anterior lateral eyes; AME, anterior median eyes; BS, base of spermathecae; C, conductor; CD, copulatory ducts; Cy, cymbium; E, embolus; ELP, embolus laminar process; FD, fertilization ducts; HS, head of spermathecae; LL, locking lobes; LP, lateral process; LS, lateral sector; MA, median apophysis; MS, median sector; MTA, median tibial apophysis; MTP, membranous tegular process; Pa, patella; PaP, patellar process; PCP, prolateral cymbial process; PLE, posterior lateral eyes; PME, posterior median eyes; PP, pars pendula; RCP, retrolateral cymbial process; RTA, retrolateral tibial apophysis; S, spermathecae; ST, subtegulum; Te, tegulum; Ti, tibia; TP, tegular process; VTA, ventral tibial apophysis; VCP, ventral cymbial process; VTP, ventral tibial process.

References to figures published elsewhere are listed in lowercase type (fig.); references to figures in this paper are capitalised (Fig.).

Molecular protocols

Whole-genomic DNA was extracted from up to four legs with a DNEasy® kit (Qiagen Inc.) following the manufacturer's protocol for animal tissues. Specimens for molecular work were preferred preserved in 96–100% ethanol. If specimens preserved in 75% ethanol were used, they were no older than 5 years at the time of DNA extraction. All the protocols for DNA amplification, visualisation, purification and sequence reactions were carried out in the Center for Comparative Genomics of California Academy of Sciences.

Four gene fragments were amplified in 25-μL reactions: a ~540-bp region from cytochrome oxidase I (COI), a ~330-bp region of histone H3, a ~770-bp region of 28S rDNA, and a ~330-bp region of Actin. For most of the gene fragments, single amplicons were obtained. For some gene fragments of 28S, combinations of overlapping amplicons were used and the resulting sequences assembled later. These four gene fragments have been shown to be phylogenetically informative in many studies on arachnid systematics and have been reported to evolve at different rates, potentially providing phylogenetic resolution at different taxonomic levels (e.g. Arnedo *et al*. 2001; Hormiga *et al*. 2003; Prendini *et al*. 2003; Spagna and Gillespie 2008; Giribet *et al*. 2010; Miller *et al*. 2010). Primers and annealing temperatures for each locus are given in Table 2. Most reactions consisted of 2.5 μL of 10× Apex buffer® (Genesee Scientific, San Diego, USA), 0.42 μL of 10 mM dNTP, 2.4 μL of 25 mM $MgCl_2$, 1 μL each of forward and reverse 10 mM dNTP primers, between 1.5 and 2.5 μL of BSA, 0.3 μL Apex Taq DNA Polymerase® (Genesee Scientific, San Diego, USA), 1–4 μL of template DNA, and water to 25 μL. Reaction conditions included an initial denaturation step at 95°C for 2 min, followed by 35 cycles of 95°C for 30 s (annealing temperatures and times as reported in Table 2) and 72°C for 1 min (H3 and COI) or 1.5 min (Actin and 28S), followed by a final extension at 72°C for 7 min, and a hold at 4°C. The only significant exception to this protocol was for the amplifications of H3. These reactions used 2.5 μL of 10×

Table 2. Primer sequences, their sources and reaction conditions used to generate data for this study

Locus	Annealing temperature/time	Direction	Primer	Sequence	Reference
COI	50–54°/30s	Forward	LC011490-oono	CWA CAA AYC ATA RRG ATA TTG G	Modified from Folmer *et al.* (1994)
		Reverse	C1-N-2191	CCC GGT AAA ATT AAA ATA TAA ACT TC	Simon *et al.* (1994)
		Reverse	HC02198	TAAACTTCAGGGTGACCAAAAAATCA	Folmer *et al.* (1994)
H3	52°/30s	Forward	H3aF	ATG GCT CGT ACC AAG CAG ACV GC	Colgan *et al.* (1998)
		Reverse	H3aR	ATA TCC TTR GGC ATR ATR GTG AC	Colgan *et al.* (1998)
		Forward	H3nF	ATG GCT CGT ACC AAG CAG AC	Colgan *et al.* (1998)
28S	50–53°/30s	Forward	28S0cs	CGT GAA ACT GCT CAG AGG	Modified from Hedin and Maddison (2001)
		Reverse	28SC	GGT TCG ATT AGT CTT TCG CC	Hedin and Maddison (2001)
		Internal	28SA	GAC CCG TCT TGA AAC ACG GA	Whiting *et al.* (1997)
		Internal	28SR	CCG TGT TTC AAG ACG GGT CG – modified reverse of 28SA	Whiting *et al.* (1997)
Actin	58°/30s	Forward	F1	GTCGCCCTGGACTTCGAGCA	This study
		Reverse	R	TCCACATCTGCTGGAAGGTGGACA	This study

USB PCR reaction buffer (USB Corporation, Cleveland, USA), 0.5 µL of 10 mM dNTP, 1.5 µL of 25 mM $MgCl_2$, 0.2 µL each of forward and reverse 25 mM primers, 2 µL of BSA, 0.5 µL of HotStart-IT®™ Taq DNA Polymerase (USB Corporation, Cleveland, USA), up to 4 µL template DNA, and water to 25 µL. Reaction conditions followed the protocol of Latiolais *et al.* (2006). PCR products were purified using Exonuclease 1 (Exo1) and Shrimp Alkaline Phospatase (SAP). For every 1 µL of PCR product, 0.01 µL of Exo1, 0.02 µL of SAP, and 0.11 µL of H_2O was added. This mixture was incubated at 37°C for 15 min and 80°C for another 15 min.

The ABI BigDye® Terminator kit (ver. 3.1, Applied Biosystems Inc., Foster City, USA) was used to perform 10 µL cycle sequencing reactions using 1.63 µL 5× buffer, 0.5 µL 10 mM primer, and 0.75 µL BigDye® Terminator. Template DNA and water amounts were adjusted on the basis of the concentration of DNA in each sample. Cycle sequencing parameters followed the protocol of Platt *et al.* (2007) with a variable annealing temperature dependent on the melting temperature of the individual primer. Reaction sequences were obtained from an ABI 3130XL genetic analyser (Applied Biosystems Inc., Foster City, USA). For some 28S rDNA samples, internal primers were used in addition to external primers to provide redundant sequence coverage (see Table 2). Sequence reconciliation, edition and chromatogram evaluation were performed using Geneious 7.1.5 created by Biomatters and available from http://www.geneious.com/. To check for contamination, all edited sequences were BLASTed (Altschul *et al.* 1997, as implemented by the National Center for Biotechnology Information website http://ncbi.nlm.nih.gov) against the GenBank nucleotide database. GenBank accession numbers for all new sequence data generated for this study are given in Table 3, which also lists the sequence data generated in previous studies, as *Megadictyna thilenii* Dahl from Blackledge *et al.* (2009), *Coelotes terrestris* Blackwall, 1841, *Stiphidion facetum* Simon, 1912, *Tengella radiata* (Kulczyn'ski, 1909) and *Textrix denticulata* Sundevall, 1833 from Spagna and Gillespie (2008) and *Vidole capensis* (Pocock, 1900) from Miller *et al.* (2010). Morphological vouchers are deposited with the California Academy of Sciences (San Francisco, CA, USA) except if noted otherwise (Appendix 1). Extraction and PCR products are vouchered at the Center for Comparative Genomics at the California Academy of Sciences. All terminal taxa represent single exemplar specimens; no 'chimeras' or consensus sequences were produced from multiple specimens.

Alignment analysis

Alignments were built with MAFFT (MAFFT Multiple alignment program for amino acid or nucleo- tide sequences, version 6, available at http://align.bmr.kyushu-u.ac.jp/mafft/online/server/) (Katoh *et al.* 2002, 2005; Katoh and Toh 2008). MAFFT is one of the few available alignment programs that have been shown to produce relatively accurate and fast alignments (Golubchik *et al.* 2007). MAFFT implements three different algorithms, including the Needleman and Wunsch (1970) algorithm. The other algorithms use local alignments with affine gap costs and global alignments with generalised affine gap costs (Berger and Munson 1991; Gotoh 1993; Notredame *et al.* 2000; Katoh *et al.* 2002, 2005). We have used the E-INS-i strategy, which is one of the most exhaustive algorithms implemented, because it gives the most accurate results, with the least number of assumptions (MAFFT online documentation). Alignment indel opening penalty was set to a default value of 1.53. Gaps were treated as a fifth state during phylogenetic analyses to account for historical information contained in insertion and deletion events. This treatment maximises independence of characters and logical consistency of phylogenetic analyses, at the expense of upweighting otherwise potentially single events (Giribet and Wheeler 1999). The Actin, CO1 and H3 alignments were further tested by translating the sequences into amino acids and checking for inappropriately placed stop codons.

Phylogeny

Bayesian analysis

Bayesian analysis was performed using MrBayes 3.1.2 (Huelsenbeck and Ronquist 2001; Ronquist and Huelsenbeck

Table 3. GenBank accession numbers for the sequences generated for this study and sequences from previous studies

Species	H3	COI	28S	Actin	Collection/Publication
Acanthoctenus sp.	KM225189	KM225088	KM225033	KM225139	IBSP 162608
Agelenopsis pensylvanica	KM225190		KM225034	KM225140	CAS 9023843
Alopecosa kochi	KM225191	KM225089	KM225035	KM225141	CAS 9031448
Ancyometes bogotensis	KM225192	KM225090	KM225036	KM225142	CAS 9021737
Anyphaena pacifica	KM225194	KM225092	KM225038		CAS 9047622
Apollophanes sp.	KM225195	KM225093	KM225039	KM225144	CAS 9031470
Architis brasiliensis	KM225196	KM225094	KM225040	KM225145	IBSP 162612
Argoctenus sp.	KM225198	KM225096	KM225042	KM225147	CAS 9023609
Argoctenus sp.	KM225197	KM225095	KM225041	KM225146	CAS 9019841
Australotengella toddae	KM225199	KM225097	KM225043	KM225148	CAS 9023720
Callobius nevadensis		KM225098	KM225044	KM225149	CAS 9047621
Caloctenus oxapampa	KM225200	KM225099	KM225045	KM225150	CAS 9016460
Cambridgea sp.	KM225201		KM225046	KM225151	CAS 9047626
Celaetycheus abara	KM225202	KM225100	KM225047		IBSP 162605
Cheiracanthium mildei	KM225203	KM225102	KM225049	KM225153	CAS 9047623
Cheiracanthium sp.		KM225101	KM225048	KM225152	CAS 9029142
Coelotes terrestris	DQ628652	DQ628627	DQ628689		Spagna and Gillespie 2008
Ctenus gr. crulsi	KM225204	KM225103	KM225050	KM225154	CAS 9021733
Cupiennius salei		KM225104	KM225051		CAS 9047631
Cybaeus sp.	KM225205	KM225105	KM225052	KM225155	CAS 9030568
Desis formidabilis	KM225206	KM225106	KM225053	KM225156	CAS 9023617
Draposa tenasserineasis	KM225207	KM225107	KM225054	KM225157	CAS 9019243
Enoploctenus cyclothorax	KM225208	KM225108	KM225055	KM225158	IBSP
Griswoldia acaenata	KM225209	KM225109	KM225056	KM225159	CAS 9043202
Griswoldia disparilis	KM225210	KM225110	KM225057	KM225160	CAS 9024917
Hala cf. *paulyi*	KM225211	KM225111	KM225058	KM225161	CAS 9036016
Kilyana hendersoni	KM225212	KM225112	KM225059	KM225162	CAS 9023591
Megadictyna thilenii	FJ607608	FJ607570	FJ607535		Blackledge *et al*. 2009
Metaphidippus manni	KM225213	KM225113	KM225060		CAS 9031471
Misumenoides sp.	KM225226	KM225125	KM225074	KM225174	CAS 9030064
Mituliodon tarantulinus	KM225214	KM225114	KM225061	KM225163	CAS 9023729
Nilus majunguensis	KM225224		KM225072		CAS 9047628
Odo abudi	KM225215	KM225115	KM225062	KM225164	CAS 9047618
Odo bruchi	KM225216	KM225116	KM225063	KM225165	MACN 4024
Oxyopes sp.	KM225217	KM225117	KM225064	KM225166	CAS 9019264
Parazygiella carpenteri	KM225218		KM225065	KM225167	CAS 9031452
Peucetia rubrolineata	KM225219	KM225118	KM225066	KM225168	CAS 10668
Phanotea digitata	KM225220	KM225119	KM225067	KM225169	CAS 9043274
Psechrus cebu	KM225221	KM225120	KM225068	KM225170	CAS 9042449
Raecius asper	KM225222	KM225121	KM225069	KM225171	AMNH
Senoculus sp.		KM225122	KM225070		UFMG 3250
Stiphidion facetum	DQ628657	DQ628631	DQ628693		Spagna and Gillespie 2008
Tengella radiata	DQ628649	DQ628622	DQ628684		Spagna and Gillespie 2008
Tengella sp	KM225223	KM225123	KM225071	KM225172	CAS 9047627
Textrix denticulata	DQ628647	DQ628621	DQ628682		Spagna and Gillespie 2008
Thaumasia hirsutochela	KM225225	KM225124	KM225073	KM225173	IBSP 162615
Titiotus sp	KM225227	KM225126	KM225075	KM225175	CAS 9047630
Tmarus sp.	KM225228	KM225127	KM225076	KM225176	CAS 9035914
Trachelas tranquillus	KM225229	KM225128	KM225077	KM225177	CAS 9047624
Uduba sp.	KM225230	KM225129	KM225078	KM225178	CAS 9030253
Uliodon frenatus	KM225231	KM225130	KM225079	KM225179	CAS 9047620
Vidole capensis	FJ949059	FJ949022	FJ948982		Miller *et al*. 2010
Viridasius sp	KM225232	KM225131	KM225080	KM225181	CAS 9015404
Viridasius sp.	KM225193	KM225091	KM225037	KM225143	CAS 9016432
Vulsor isaloensis		KM225132	KM225081	KM225182	CAS 9047617
Zorocrates fuscus	KM225233	KM225133	KM225082	KM225183	AMNH
Zorodictyna	KM225234	KM225134	KM225083	KM225184	CAS 9029889
Zorodictyna	KM225235	KM225135	KM225084	KM225185	CAS 9029890
Zorodictyna	KM225236	KM225136	KM225085	KM225186	CAS 9035866
Zorodictyna	KM225237	KM225137	KM225086	KM225187	CAS 9031271
Zoropsis spinimana	KM225238	KM225138	KM225087	KM225188	CAS 9019845

2003). A mixed-model analysis was conducted for each of the four alignments. For the three protein-coding genes, each codon position was modelled independently; the ribosomal gene was modelled independently for a total of eight data partitions. Gaps were treated as missing, not as a fifth character state. Best-fit models for each partition were determined independently according to the non-hierarchical Akaike Information Criterion as implemented in MrModeltest (Nylander 2008). The SYM model was applied to the H3 Position 2 partition; the HKY + G model was applied to the COI Position 3 partition; the GTR + I + C model was applied to the remaining partitions. Parameters (character state frequencies, C-shape parameter, proportion of invariant sites, substitution rates of the GTR model, transition/transversion ratio) were estimated independently for each partition using the following command: unlink statefreq = (all) shape = (all) pinvar = (all) revmat = (all) tratio = (all). Analyses were run on the Phylocluster at the Center for Comparative Genomics, California Academy of Sciences. Tree search proceeded according to MrBayes defaults (two independent analyses consisting of one cold and three heated MCMC chains). Analyses proceeded at least until the deviation of split frequencies fell below 0.01. Trees were sampled every 1000 generations. Chain convergence was evaluated in Tracer (Rambaut and Drummond 2007). At least the first 10% of each search was discarded as 'burn-in'.

Parsimony analyses

Parsimony analyses were performed with TNT 1.1 (Goloboff *et al.* 2008*a*). All characters in this dataset were treated as unordered. Internal branches were considered unsupported and collapsed during searches if they were only supported ambiguously (that is, when some optimisation lacks support, i.e. when the minimum length is zero; Rule 1 of TNT; see discussion in Coddington and Scharff 1994).

Searches consisted of 1000 replicates of random addition sequences, followed by 500 interactions of tree bisection reconnection (TBR) and parsimony ratchet as implemented in TNT (alternating searches and perturbation phases, with periodic rounds of original weights) (Goloboff *et al.* 2003; program documentation), retaining 10 trees per replication (commands:

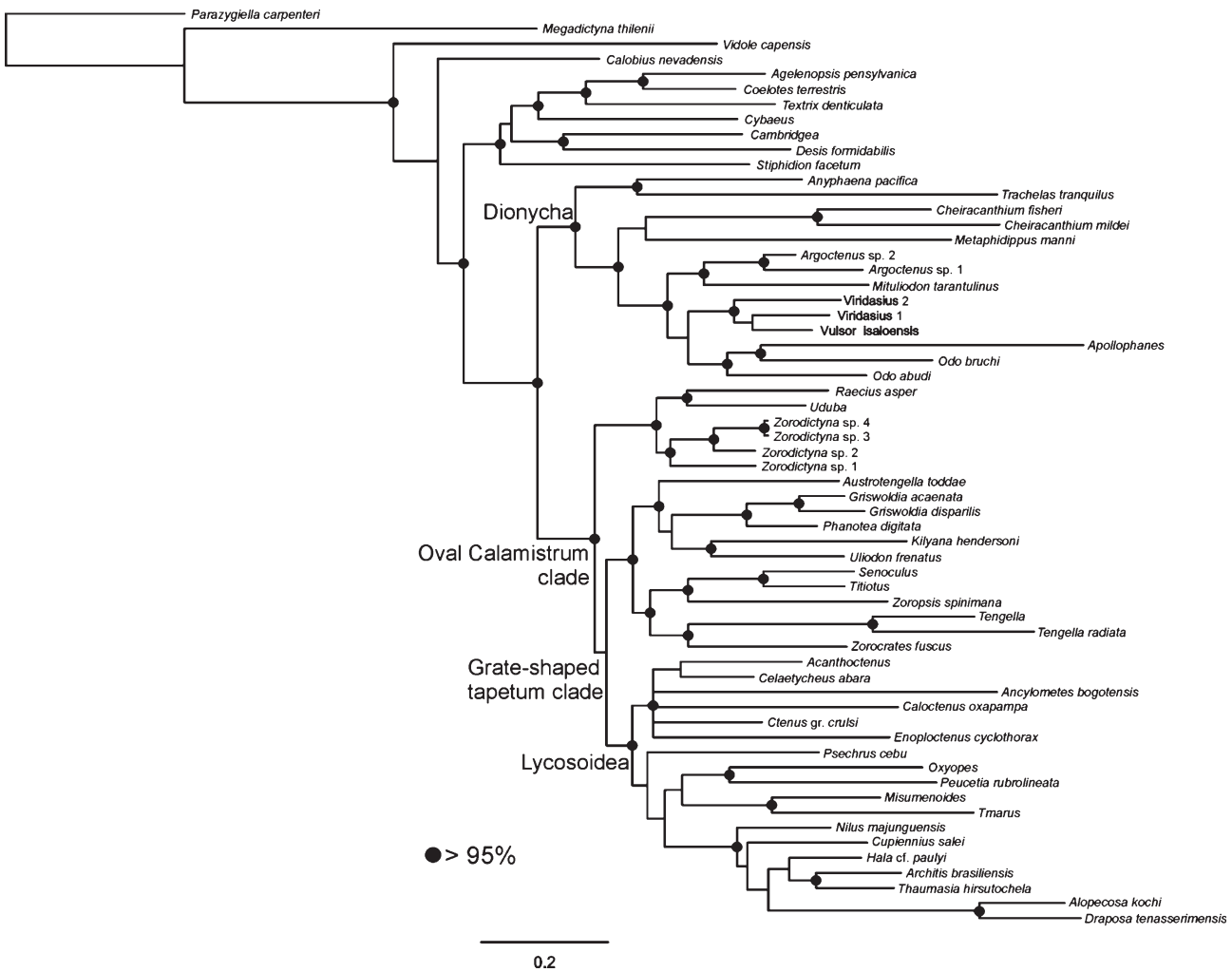

Fig. 1. Topology from Bayesian mixed-model analysis of total evidence. Black circles indicated branches with posterior probability higher than 95%.

ratchet: iter 500 equal; mult = ratchet replic 1000 tbr hold 10;). We also analysed the dataset under regimes weighting against homoplasy, using implied weighting (Goloboff 1993). This more-recent method of implied weights was given priority over successive weighting (Farris 1969) because implied weights is not affected by starting points or ambiguities in weights from multiple trees. Analyses under implied weights were conducted with TNT 1.1 (Goloboff *et al*. 2008*b*) with values of constant of concavity k = 1, 3, 6, 9, 20, 50, 99, using the same parameters described to perform equal-weight searches.

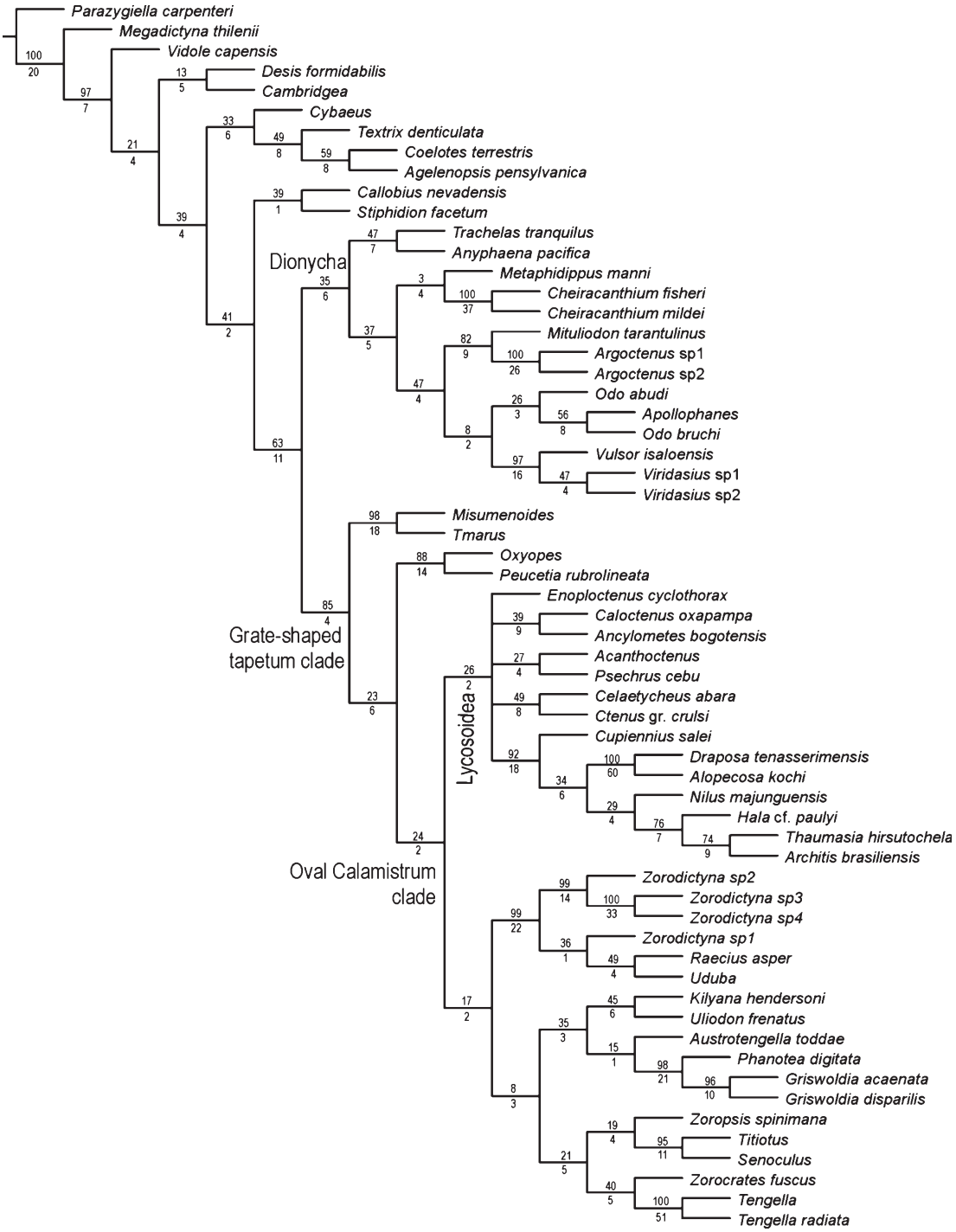

Fig. 2. Topology of the strict consensus of four most-parsimonious trees from the total evidence under equal-weights analysis. Values at nodes represent the branches' support from Bootstrap (top) and Bremer (below).

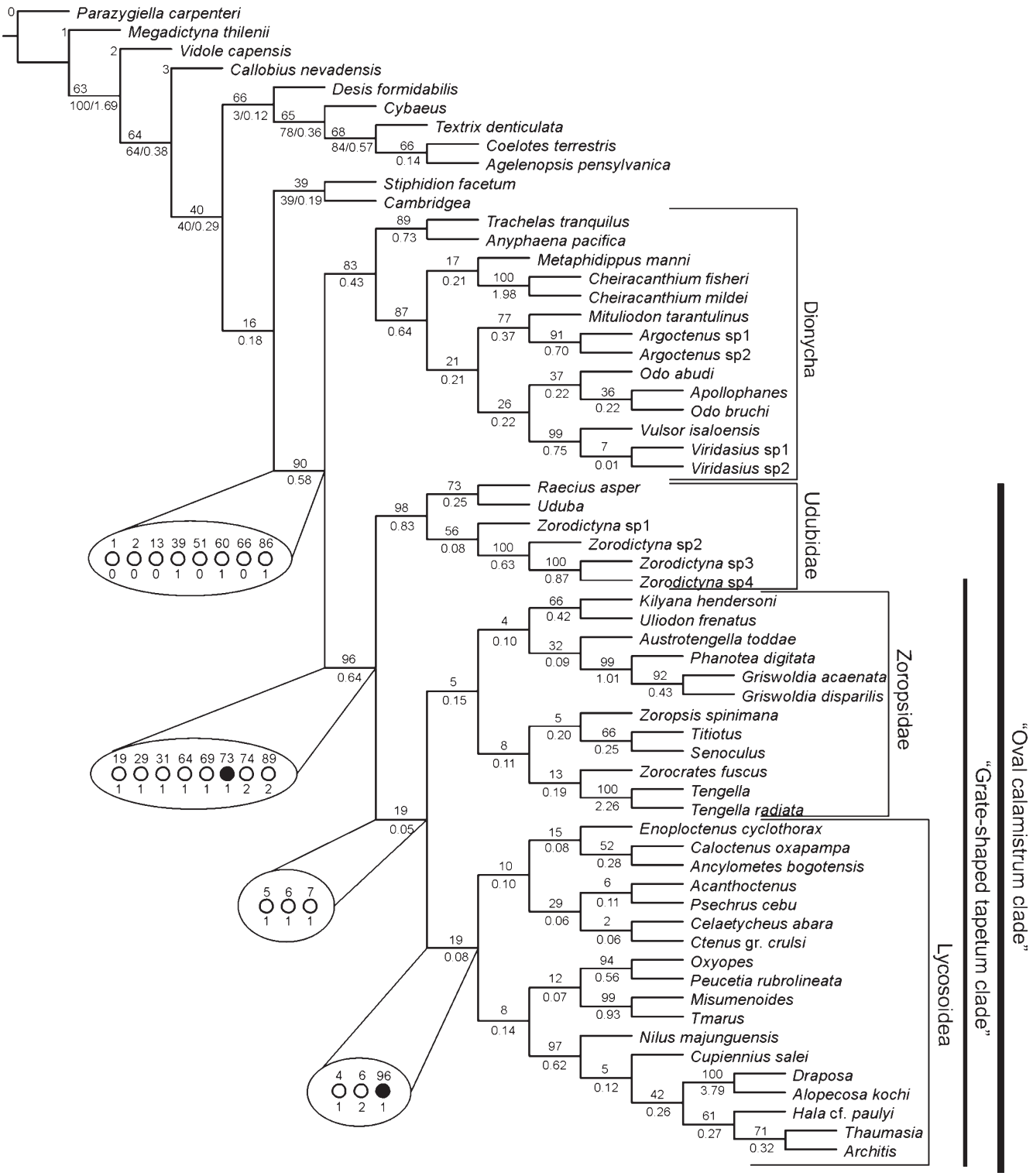

Fig. 3. Topology of the strict consensus tree under implied weights for constant of concavity k = 6. Character changes mapped on selected branches. Black circles indicate non-homoplastic synapomorphies. White circles indicate homoplastic synapomorphies. Branches with Bootstrap (top) and Bremer (below) values.

Sensitivity and stability of clades

In order to investigate the sensitivity of the data to different partitions schemes, six data partitions were defined: (1) all molecular data (28S, Actin, COI and H3); (2) nuclear gene fragments (28S, Actin and H3); (3) mitochondrial gene fragment (COI); (4) ribosomal gene fragment (28S); (5)

morphological and behavioural data; (6) protein-coding genes fragments (Actin, COI and H3). The partitioned data were analysed with the same parameters described for the parsimony and Bayesian analyses and the cladograms obtained were annotated with the results supported under different analysis parameters and represented as 'Navajo rugs' (Giribet and Edgecomb 2006).

Ancestral character reconstruction

In order to better understand the evolution of the tapetum, an ancestral character reconstruction was performed on this trait. The ancestral character reconstruction was performed using standard parsimony optimisations in Mesquite 2.75 (Maddison and Maddison 2011). The trace character function in Mesquite (Maddison and Maddison 2011) optimises most parsimonious character states at internodes; where multiple equally parsimonious solutions exist, the ancestral character state is equivocal (Fitch 1971; Swofford and Maddison 1987, 1992).

Support values

The following support measures were calculated for the parsimony analyses: absolute Bremer support (BS, Bremer 1994) and bootstrap (Felsenstein 1985). BS was calculated heuristically in TNT searching for suboptimal trees using the optimal trees as a starting point. TBR branch swapping was performed filling the tree-buffer, sequentially increasing the number of steps of suboptimal trees by one (1–2 steps), by five (5–50 steps) and by 10 (60–100 steps), retaining increasing numbers of trees by 3000 (from 2000 to 50 000) and running Bremer support with the saved trees. Support values for groups expressed as Bremer support in units of fit × 100 (BS, bottom) and GC (Group present/Contradicted) frequency differences (top) (Figs 2, 3). GC count the number of occurrences of individual cases of contradiction of a group in the consensus (thus counting cases where the group is unresolved in the consensus as neither favourable nor contradictory) (Goloboff *et al*. 2003).

Results

This section reports the results of all analyses performed in this study. Names of taxa in quotation marks, e.g. 'grate-shaped tapetum clade', refer to informal taxon names based on the preferred hypothesis of relationships (Fig. 3) (see below). Formal taxonomic hypotheses, nomenclatorial actions and diagnosis of groups will be presented in the section 'Systematics'. Original taxonomic names from previous works or that are formally addressed here are depicted without quotation marks.

Sequence data and alignments

This study produced a final aligned 2092-bp fragment for each taxon, consisting of 737 aligned bp for 28S, 371 aligned bp for Actin, 630 aligned bp for COI, and 354 aligned bp for H3. The analysis of the protein-coding genes was straightforward: Actin

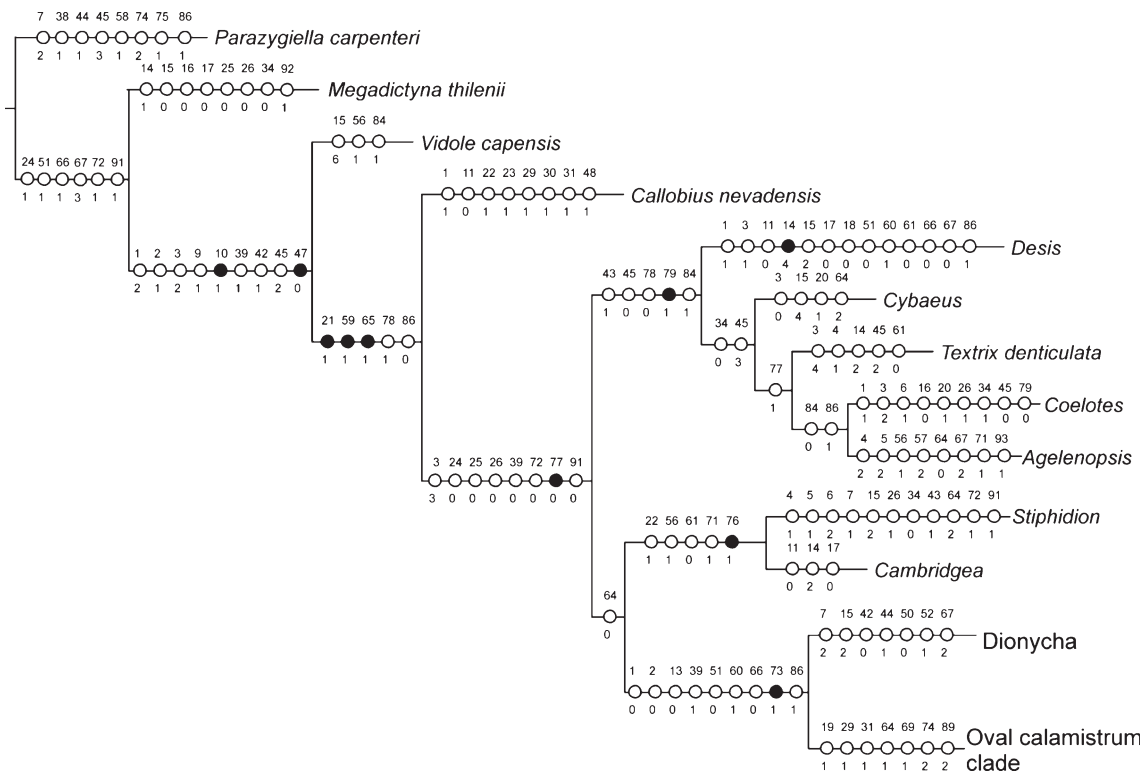

Fig. 4. Topology of the strict consensus tree under implied weights for constant of concavity k = 6. Character changes mapped on branches. Black circles indicate non-homoplastic synapomorphies. White circles indicate homoplastic synapomorphies.

and H3 required no gap insertions; COI required a single three-nucleotide deletion in two terminals (*Tengella radiata* and *Tengella* sp.), which can be considered a synapomorphy for the genus.

Phylogenetic analysis

The Bayesian analysis of the total evidence and the six data partitions was allowed to proceed for 50 000 000 generations. Results of the Bayesian analysis are shown in Fig. 1. The parsimony analysis of the total evidence under equal weights resulted in four trees of 8880 steps (CI = 0.23; RI = 0.36). Strict consensus of these parsimony results collapsed three branches and resulted in a tree of 8916 steps (CI = 0.23; RI = 0.36) depicted in Fig. 2. The parsimony analysis of the total evidence with values of the concavity k = 1, 3, 6, 9, 20, 50, 99 resulted in one tree in each of the analyses. The trees obtained by the constant k = 6 and 9 are identical (8906 L; CI = 0.23; RI = 0.36) and the results are selected as the working hypothesis to discuss the character evolution and to diagnose taxa. To facilitate the discussion, we refer to the tree resulting from the concavity value of k = 6 (Figs 3–7). The constant of concavity for the weighting function was also the same as determined in Ramírez (2003) (k = 6). Ramírez (2003) and Goloboff *et al.* (2008b) found that mild concavity values produced higher topological congruence indices for many morphological and molecular datasets. To explore congruence and sensitivity of different phylogenetic data, we ran analyses of six data partitions under parsimony and Bayesian analyses and summarised the results on the tree of concavity k = 6 as 'Navajo rugs' (Giribet and Edgecomb 2006) (Fig. 8). These analyses indicated that no partition reliably predicts the results of the total-evidence analysis. The ancestral character reconstruction of the tapetum shows that the grate-shaped kind evolved at least three times independently, with several reversions to primitive states (total of 13 steps) (Fig. 9).

Phylogenetic relationships

Three topologies will be considered for description of the results and further discussion: the tree generated by the Bayesian inference (Fig. 1), the consensus of four trees generated by the equal-weight analysis of parsimony (Fig. 2), and the only tree resulting from the parsimony analysis under implied weights with concavity constant of k = 6 (Figs 3–7). Both parsimony and Bayesian analyses show Lycosoidea to be monophyletic, composed by Lycosidae, Pisauridae, Oxyopidae, Thomisidae, Psechridae and Ctenidae. Pisauridae is monophyletic only in the equal-weight consensus (Fig. 2). Psechridae appears as sister-group of *Acanthoctenus* in both parsimony analyses (Figs 2, 3), but as sister group to Oxyopidae, Thomisidae, Pisauridae and Lycosidae in the Bayesian inference (Fig. 1). The 'GST clade' (grate-shaped tapetum) appears as sister-group of Udubidae (new family), together forming the 'Oval Calamistrum clade', in all three analyses. All three analyses show a clade formed with species currently placed in Zoropsidae, Zorocratidae, Tengellidae and Senoculidae. The expanded Zoropsidae appears as sister-group

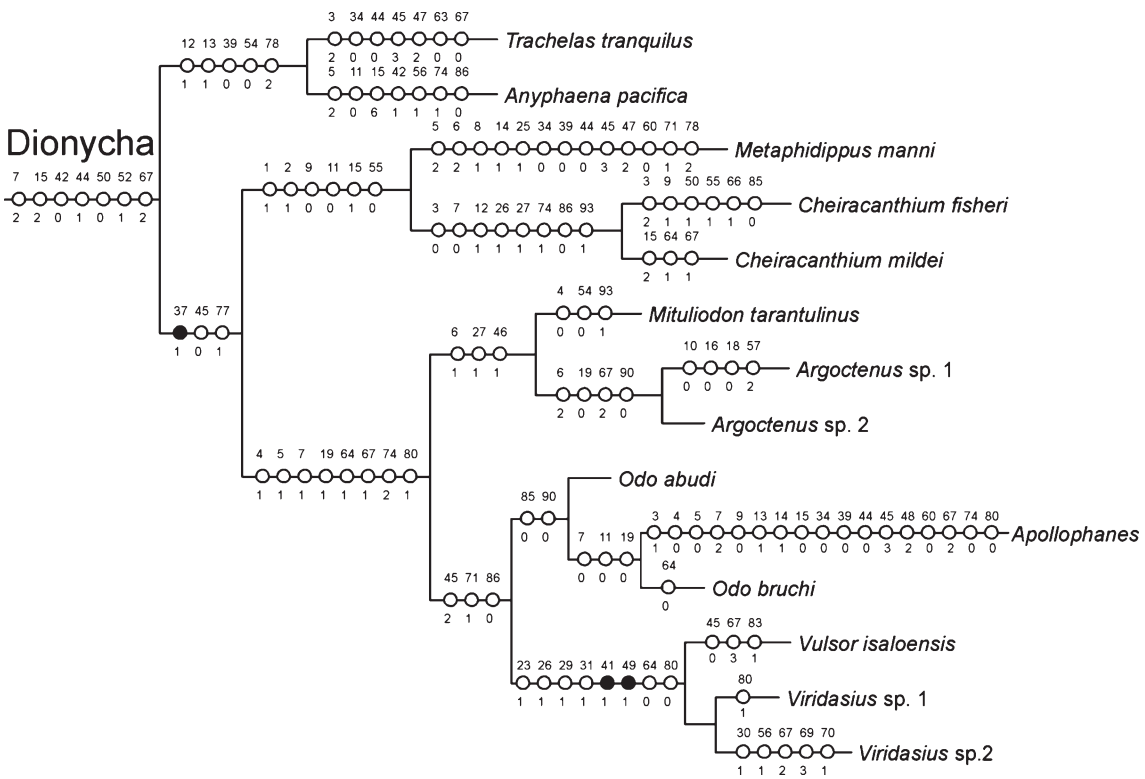

Fig. 5. Dionycha clade. Topology of the strict consensus tree under implied weights for constant of concavity k = 6. Character changes mapped on branches. Black circles indicate non-homoplastic synapomorphies. White circles indicate homoplastic synapomorphies.

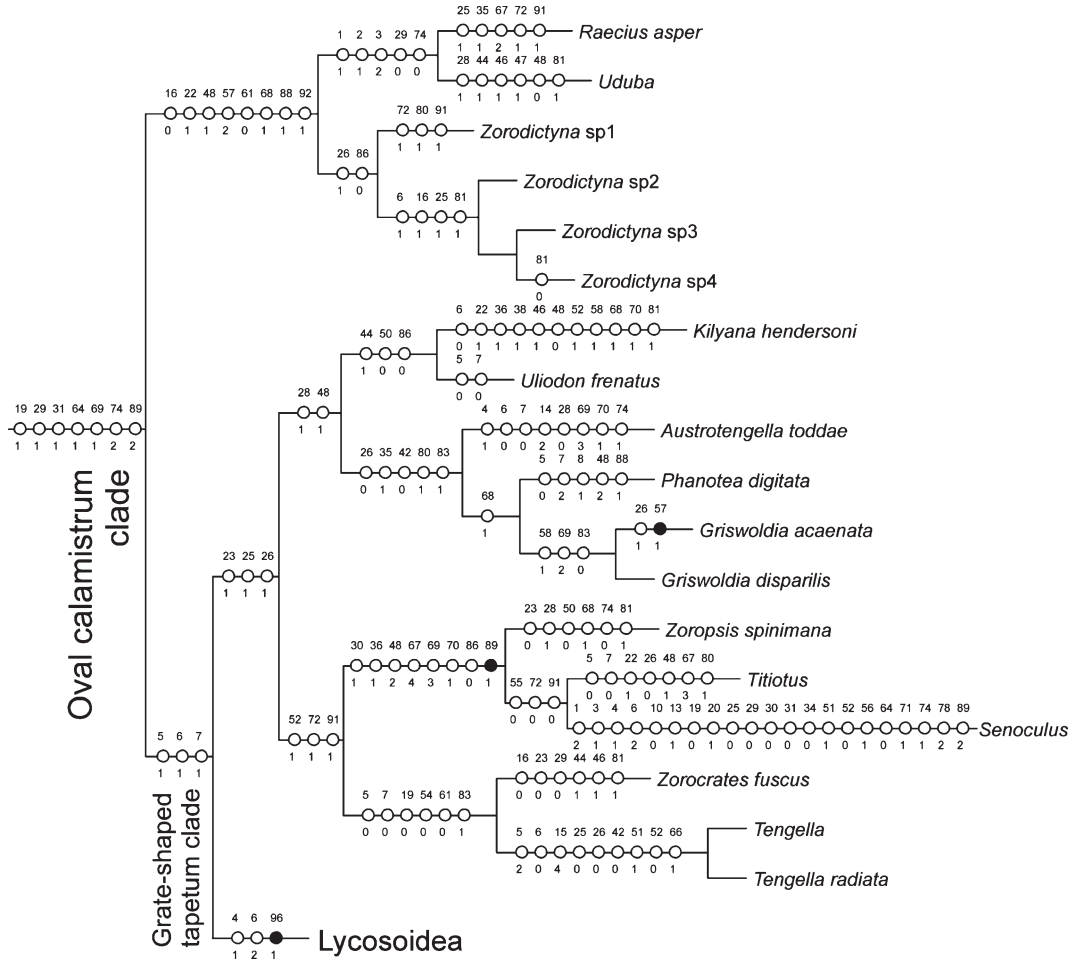

Fig. 6. Oval Calamistrum clade. Topology of the strict consensus tree under implied weights for constant of concavity k = 6. Character changes mapped on branches. Black circles indicate non-homoplastic synapomorphies. White circles indicate homoplastic synapomorphies.

of Lycosoidea in the Bayesian analysis and implied-weights parsimony k = 6 analysis (Figs 1, 3). Inferred phylogenetic trees revealed consistent relationships for most of the groups analysed. A monophyletic Lycosoidea clade, placed as sister-group of our expanded Zoropsidae, was recovered in both the k = 6 parsimony and Bayesian analyses (Figs 1, 3). Thomisidae and Oxyopidae appear as outgroups to the 'Oval Calamistrum clade' in the equal-weight parsimony analysis (Fig. 2) and in the analyses with the concavities k = 1, 3, 20, 50, 99, but in the Bayesian analysis and the parsimony analysis of concavity k = 6 and 9, Thomisidae and Oxyopidae appear within the Lycosoidea (Figs 1, 3).

Discussion

We base our following discussion on the results of the total-evidence analyses with parsimony (with implied weights k = 6) (Fig. 3) and Bayesian methods (Fig. 1), unless we state that we discuss a particular partitioned dataset. The morphological character state changes are shown on the tree obtained under concavity k = 6 (Figs 3–7).

Phylogenetic relationships

Outgroups

The relationships among the outgroups are not the primary focus of the present study, and accordingly the sample of character data for the outgroups is much less intensive than for the ingroup. Nevertheless, we believe it is worth commenting on the relationships of the basal groups on the cladogram. Following several previous phylogenetic hypotheses (Griswold *et al*. 1999; Miller *et al*. 2010), we root our analysis using an Orbicularian taxon (*Parazygiella carpenteri* Wunderlich). Our results corroborated the basal position of *Megadictyna thilenii* (Nicodamidae), *Vidole capensis* (Phyxelididae) and *Callobius nevadensis* Chamberlin, 1847 (Amaurobiidae) in relation to the remaining taxa used in the analysis (Figs 1–3).

'Fused Paracribellar clade' (Austral Cribellate clade)

The 'Fused Paracribellar clade' was proposed by Griswold *et al*. (1999) to include Amphinectidae, Stiphidiidae, Agelenidae (represented by the cribellate *Neoramia nana* Forster & Wilton, 1973) and Desidae. The name of the clade refers to the fused

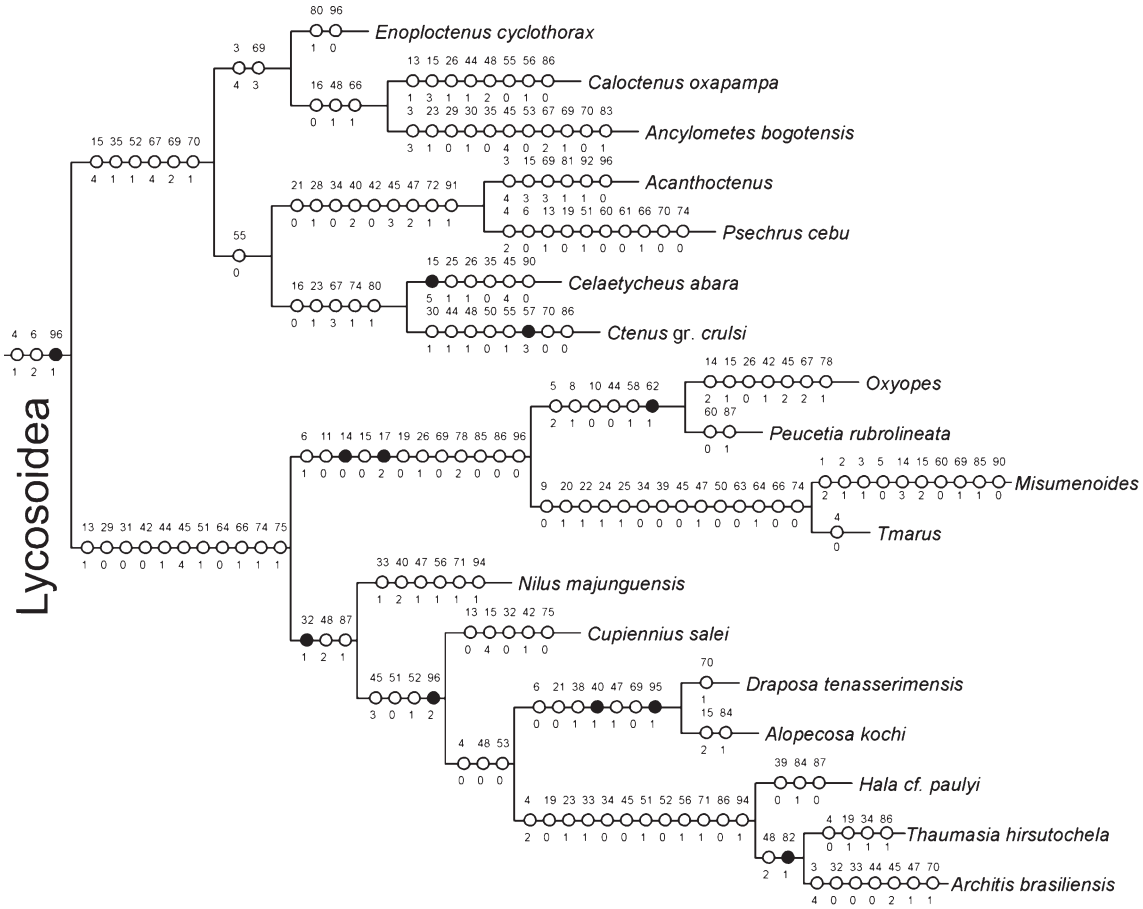

Fig. 7. Lycosoidea clade. Topology of the strict consensus tree under implied weights for constant of concavity k = 6. Character changes mapped on branches. Black circles indicate non-homoplastic synapomorphies. White circles indicate homoplastic synapomorphies.

spigot bases on the posterior median spinnerets, with two to several paracribellar shafts emerging from the same paracribellar base (Griswold *et al*. 2005: figs 66A, 68B, 73C, 87C). This clade, with the inclusion of cribellate Dictynidae, was corroborated by Spagna and Gillespie (2008) and Miller *et al*. (2010) as the 'austral cribellates' (though Agelenidae is no longer included: we now know that *Neorama*ia Forster & Wilton, 1973 is not related to true agelenids, e.g. *Tegenaria* Latreille, 1804, *Coelotes* Blackwall, 1841, *Agelenopsis* Giebel, 1869). Here, we do not use the paracribellar character in the matrix (we have only one cribellate spider from this group, *Stiphidion facetum*), but the name is still useful. Stiphidiidae do not cluster with the remaining taxa of the 'Fused Paracribellar clade' in our analyses.

Dionycha

Dionycha appears as sister-group of the 'Oval Calamistrum clade' (Fig. 1). Classical Dionycha taxa, including *Anyphaena* Sundevall, 1833 (Anyphaenidae), *Trachelas* L. Koch, 1872 (Trachelidae), *Metaphidippus* F. O. P.-Cambridge, 1901 (Salticidae), *Apollophanes* O. P.-Cambridge, 1898 (Philodromidae), *Cheiracanthium* C. L. Koch, 1839 (Eutichuridae) and *Mituliodon* Raven & Stumkat, 2003 (Miturgidae), cluster together in a well supported clade (Figs 1, 5). *Cheiracanthium* and *Mituliodon* were both formerly Miturgidae, but Ramírez (2014) recently moved *Cheiracanthium* into Eutichuridae, a result corroborated by our total-evidence analysis. *Odo* Keyserling, 1887, *Argoctenus* L. Koch, 1878 and the remaining Miturgidae do not form a monophyletic clade but cluster with the remaining Dionycha represented in our analysis (Figs 1, 5). The Viridasiinae clade, formed by two species of *Viridasius* Simon, 1889 and *Vulsor* Simon, 1889, cluster with *Apollophanes* (Philodromidae) and two species of *Odo* (Miturgidae), indicating that viridasiines arose independently of the remaining Ctenidae (Figs 1, 5). Bayer and Schönhofer (2013) used one species of *Viridasius* in their phylogenetic analysis and recover the same relation within the Dionycha. Viridasiinae were proposed by Lehtinen (1967) and comprise, to date, two genera, *Vulsor* and *Viridasius*. There are several new species and probably some new genera that belong to this clade, all from Madagascar (D. Silva Dávila, pers. comm.). Dionycha have separately been subject to an intensive, taxon-dense analysis (Ramírez 2014), so our conclusions must be

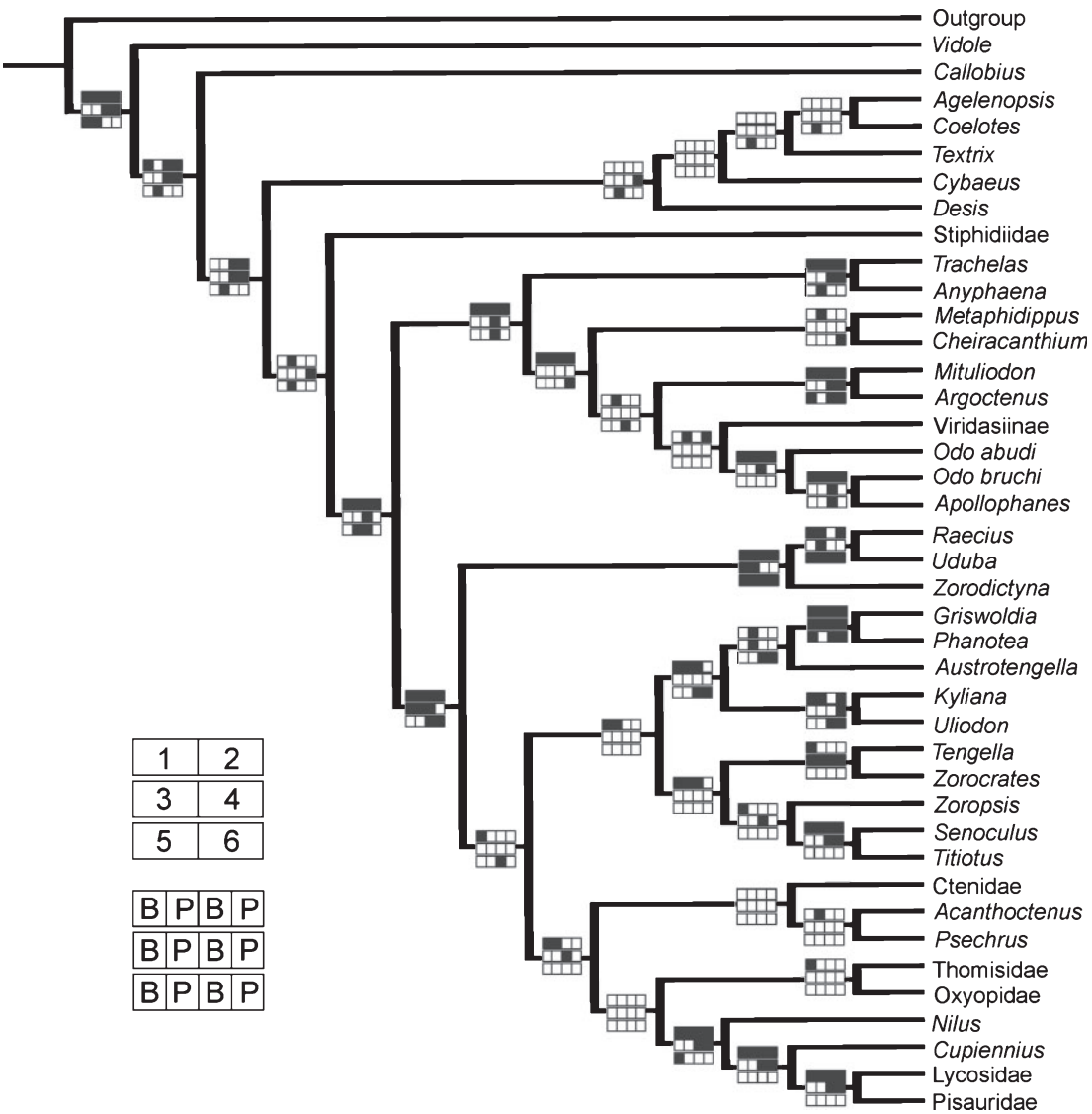

Fig. 8. Summary topology with congruence among data partitions and optimality. Topology and clade composition based on parsimony analysis of concavity k = 6. Boxes at nodes indicate each data partition (combined data or individual gene) subdivided by analysis method (B, Bayesian: left side; P, parsimony: right side). The data partitions were defined as: (1) all molecular data (28S, Actin, COI and H3); (2) nuclear gene fragments (28S, Actin and H3); (3) mitochondrial gene fragment (COI); (4) ribosomal gene fragment (28S); (5) morphological and behavioural data; (6) protein-coding gene fragments (Actin, COI and H3). Black squares indicate that the clade was recovered (regardless of support) in the given analysis, white squares indicate that the clade was not recovered.

considered provisional, but we believe that the monophyly and placement of the viridasiines are secure, and we suggest raising this taxon to family level (see Systematics).

'Oval Calamistrum clade'

The 'Oval Calamistrum clade' (OC clade) (Figs 1, 6) was proposed by Griswold (1993) to include spiders with an oval to rectangular arrangement of calamistral setae, which grouped Lycosoidea (from which only Peschridae and Ctenidae have cribellate members) with zoropsids, zorocratids and tengellids. This clade was recovered in Griswold *et al*. (1999) and Griswold *et al*. (2005). In the parsimony analysis of concavity k = 6 and Bayesian analysis (Figs 1, 3, 6) the 'OC clade' is sister-group of Dionycha and in the parsimony analysis with equal weights it is sister-group of Oxyopidae (Fig. 2). The 'OC clade' appears in almost all partitioned analyses of Bayesian inference and implied weights of concavity k = 6 (Fig. 8).

Udubids

Ububa Simon, 1880, *Raecius* Simon, 1892, *Zorodictyna* Strand, 1907 and three other undescribed species from Madagascar form a well supported clade (Figs 1, 6), which appears in all the analyses with different methods or weight

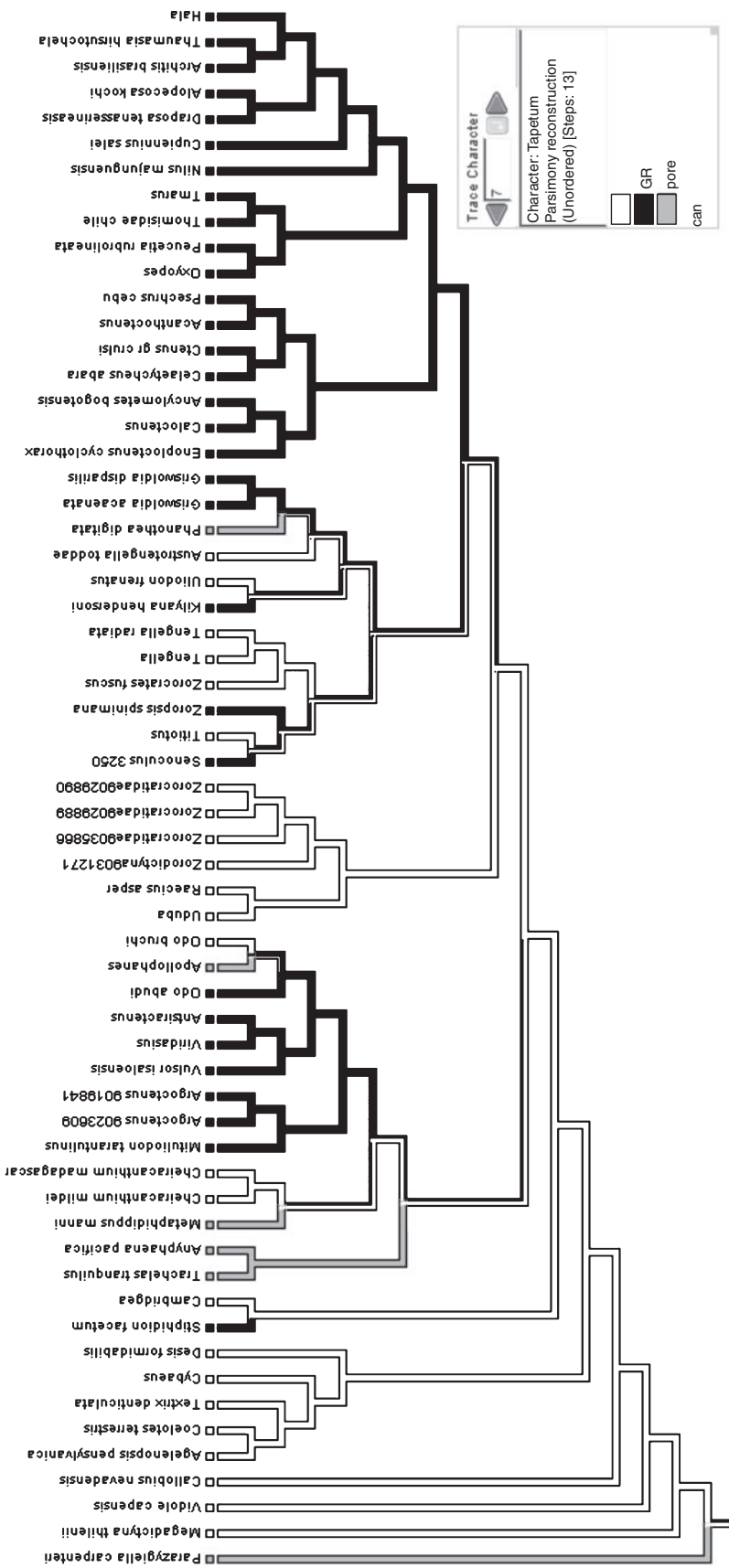

Fig. 9. Ancestral character state reconstruction of grate-shaped tapetum optimised on the parsimony analysis of concavity k = 6 (white: canoe-shaped tapetum; black: grate-shaped tapetum; grey: pore-shaped tapetum).

schemes. These genera are currently placed in Zorocratidae, but do not appear closely related to the type species of the family, *Zorocrates fuscus* Simon, 1888. Udubids are recovered in all the total-evidence analyses (Figs 1–3, 8) and the clade is supported by several homoplastic synapomorphies (Fig. 6). *Zorocrates* Simon, 1888 lacks these udubid synapomorphies. Udubids also appear in almost all partitioned analyses of Bayesian inference and implied weights of concavity k = 6 (Fig. 8). We suggest raising this taxon to family level (see Systematics).

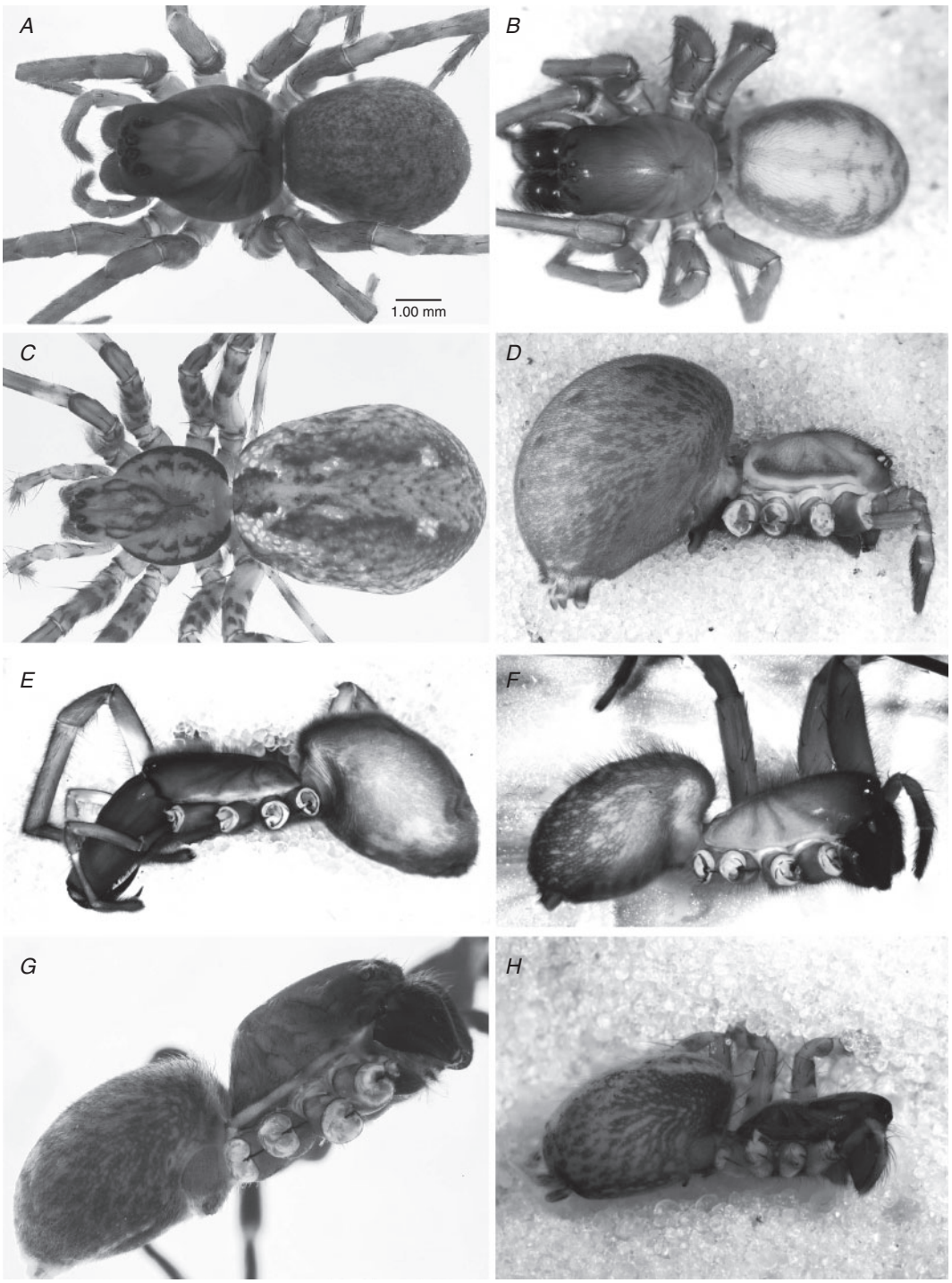

Fig. 10. *A–C*, dorsal view of the habitus; *D–H*, lateral view of the habitus. *A*, *Griswoldia acaenata*; *B*, *Callobius nevadensis*; *C*, *Stiphidion facetum*; *D*, *Megadictyna thilenii*; *E*, *Desis formidabilis*; *F*, *Vidole capensis*; *G*, *Kilyana hendersoni*; *H*, *Textrix denticulata*.

Lycosoidea

Lycosoidea was defined by Homann (1971) by the presence of a grate-shaped tapetum in the indirect eyes. Griswold (1993) presented a phylogeny with the families having a grate-shaped tapetum (including the stiphidiid *Stiphidion* Simon and miturgid *Mituliodon*) plus *Tengella* Dahl (Tengellidae), the latter of which share an oval calamistrum with the grate-shaped tapetum taxa. Analyses beginning with that of Griswold et al. (1999) suggested that Stiphidiidae were more closely related to the Agelenidae, Amphinectidae, Desidae and Neolanidae, and that the grate-shaped tapetum appears as convergent in Stiphidiidae and remaining Lycosoidea. Our results relimit the superfamily Lycosoidea, which now comprises species placed in Lycosidae, Pisauridae (including species placed in Halidae), Oxyopidae, Psechridae, Thomisidae and Ctenidae. In our analyses Pisauridae and Ctenidae are not monophyletic, and viridasiine ctenids are placed far from Lycosoidea. Trechaleidae, not included in our analysis, remains in Lycosoidea because of the similarities with the remaining lycosoids.

'GST clade'

The 'grate-shaped tapetum clade' (or 'GST clade') was proposed by Silva Dávila (2003) to include the lycosoids, tengelloids and ctenoids and was supported by the presence of the grate-shaped tapetum (with four reversals to canoe-shaped)

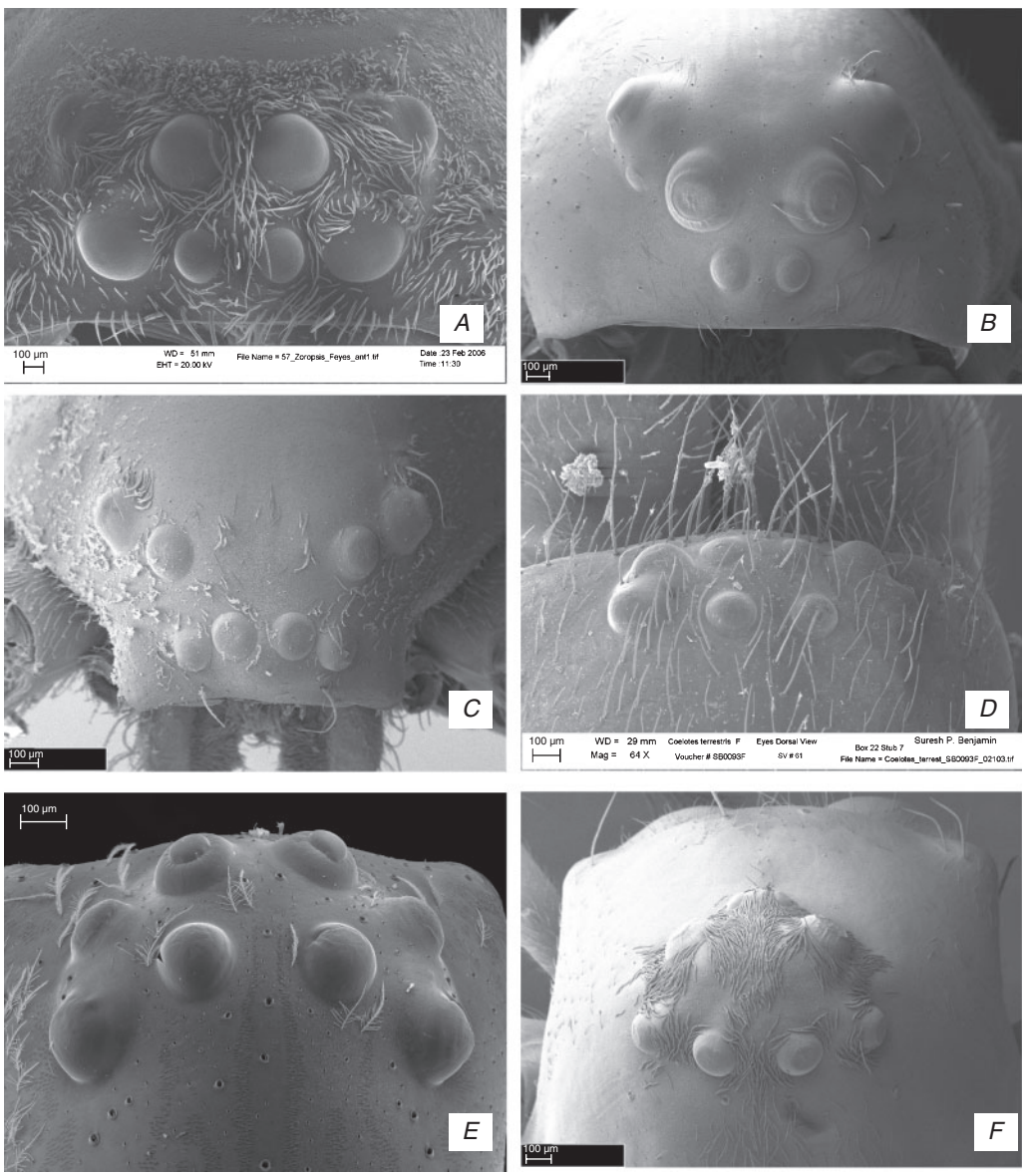

Fig. 11. Carapace, ocular area. *A*, *B*, anterior view of eyes area; *C–F*, dorsal view of eyes area. *A*, *Zoropsis spinimana* (CAS 9019845); *B*, *Celaetycheus abara* (IBSP 162605); *C*, *Hala* cf. *paulyi* (CAS 9036016); *D*, *Coelotes terrestris*; *E*, *Stiphidion facetum*; *F*, *Peucetia rubrolineata*.

and several other characters. In the parsimony analysis of concavity k = 6 and Bayesian inference (Figs 1, 3) we recover a similar group (with the exception of the udubids, miturgids and zorids), also supported by the presence of the grate-shaped tapetum. But our analyses suggest that evolutionary history of the grate-shaped tapetum is more complex than recovered by previous analyses (Griswold 1993; Silva Dávila 2003; Raven and Stumkat 2005). Not only does the grate-shaped tapetum reverse to a canoe shape within the 'GST clade', but the GST also appears at least two more times independently (Fig. 9).

Zoropsids

Under all total-evidence analyses, *Zorocrates*, *Tengella*, *Titiotus* Simon, 1897, and *Senoculus* Taczanowski, 1872 group with *Zoropsis* Simon, 1878, suggesting that these genera comprise a monophyletic group (Figs 1–3, 6, 8). Raven and Stumkat (2005) recently proposed expansion of Zoropsidae to include the taxa previously placed in Zorocratidae, but our analysis excludes from the zoropsids *Raecius*, *Uduba* and *Zorodictyna*, which comprise the core of our new Udubidae. Also associated with *Zoropsis* are *Austrotengella* Raven, 2012, the Griswoldiinae (*Griswoldia* Dippenaar-Schoeman & Jocqué and *Phanotea* Simon) and the Uliodoninae (*Uliodon* L. Koch and *Kilyana* Raven & Stumkat). We consider that there is enough evidence to support the synonymy of Zorocratidae and Tengellidae with Zoropsidae (the oldest family group name and the valid senior synonym). Morphological evidence to support our newly relimited Zoropsidae is weak, comprising only a few homoplastic synapomorphies: characters 23, 25 and

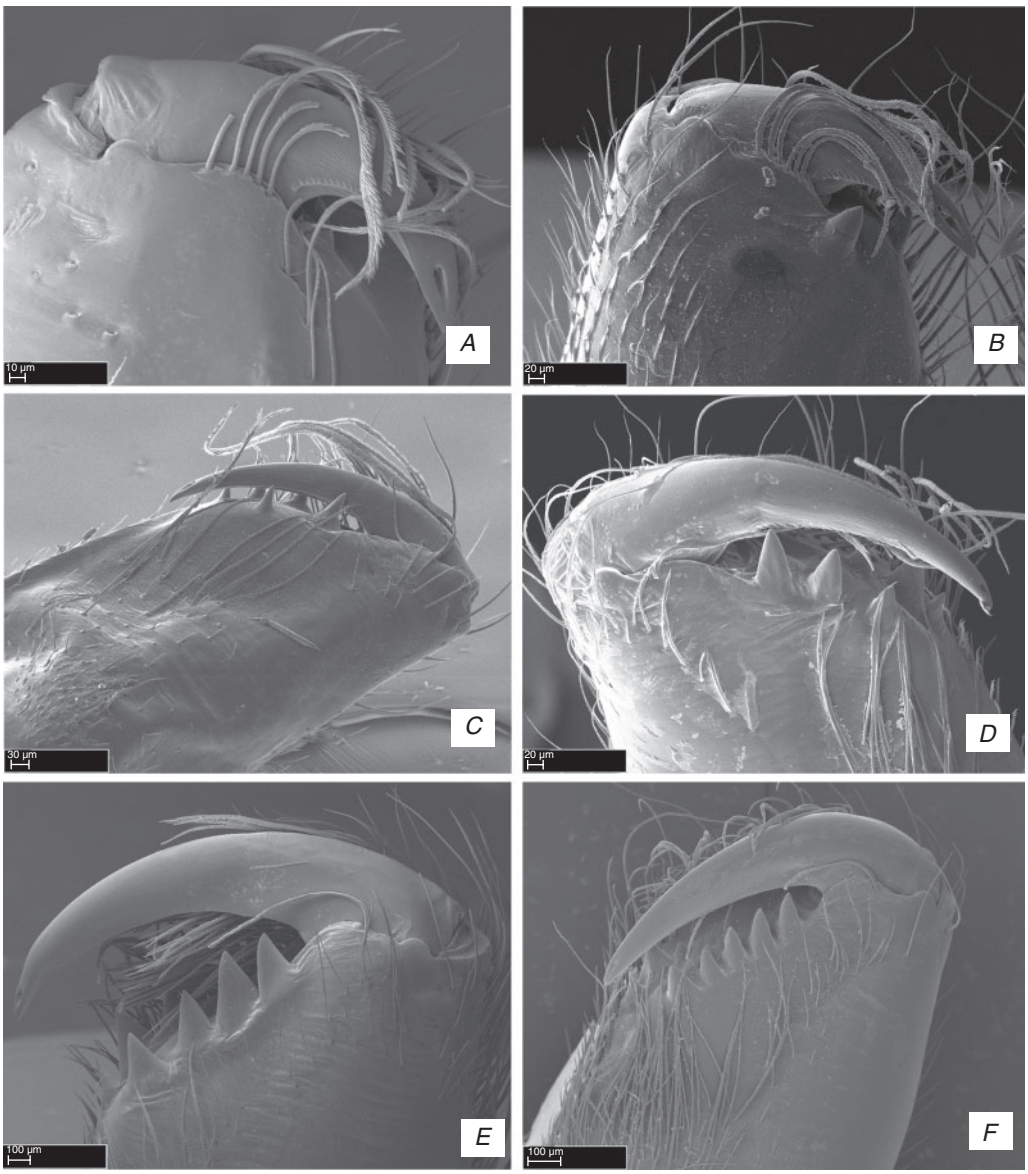

Fig. 12. Retrolateral view of the chelicerae. *A*, *Tmarus* sp.; *B*, *Oxyopes* sp.; *C*, *Argoctenus* sp.; *D*, *Hala* cf. *paulyi*; *E*, *Enoploctenus cyclothorax*; *F*, *Celaetycheus abara*.

26, in total-evidence analysis of concavity k = 6 (Fig. 6) and only character 23 in total-evidence with equal weights (Fig. 2). Whereas it is difficult to recover this clade using just morphological data, the total-evidence analyses are consistent in grouping *Zorocrates*, *Tengella*, *Titiotus* with *Zoropsis*.

The synonymy of Zoropsidae, a relimited Zorocratidae (without *Raecius*, *Uduba* and *Zorodictyna*), and Tengellidae would require a substantial expansion of Zoropsidae (which has priority over the other family names), to include ~25 genera, most of them not included in this analysis. Nevertheless, we see strong evidence grouping the unrepresented genera with our exemplars. From among the taxa assigned to Zoropsidae (World Spider Catalog 2015), *Akamasia* Bosselaers, 2002 and *Takeoa* Lehtinen, 1967 are similar to *Zoropsis* (Griswold 1993; Bosselaers 2002). *Cauquenia* Piacentini, Ramírez & Silva, 2013 (Piacentini *et al.* 2013), *Devendra* Lehtinen, 1967 (Griswold 1993) and *Itatiaya* Mello-Leitão, 1915 (Polotow and Brescovit 2010) have been confidently placed within the Griswoldiinae, represented in our matrix by *Griswoldia* and *Phanotea*. *Birrana* Raven & Stumkat, 2005, *Krukt* Raven & Stumkat, 2005, and *Megateg* Raven & Stumkat, 2005 have been placed near *Kilyana* (Raven and Stumkat 2005). *Huntia* Gray & Thompson, 2001, *Pseudoctenus* Caporiacco, 1949 and *Uliodon* have also been associated with the Zoropsinae (Raven and Stumkat 2005). From the taxa assigned to the Tengellidae (World Spider

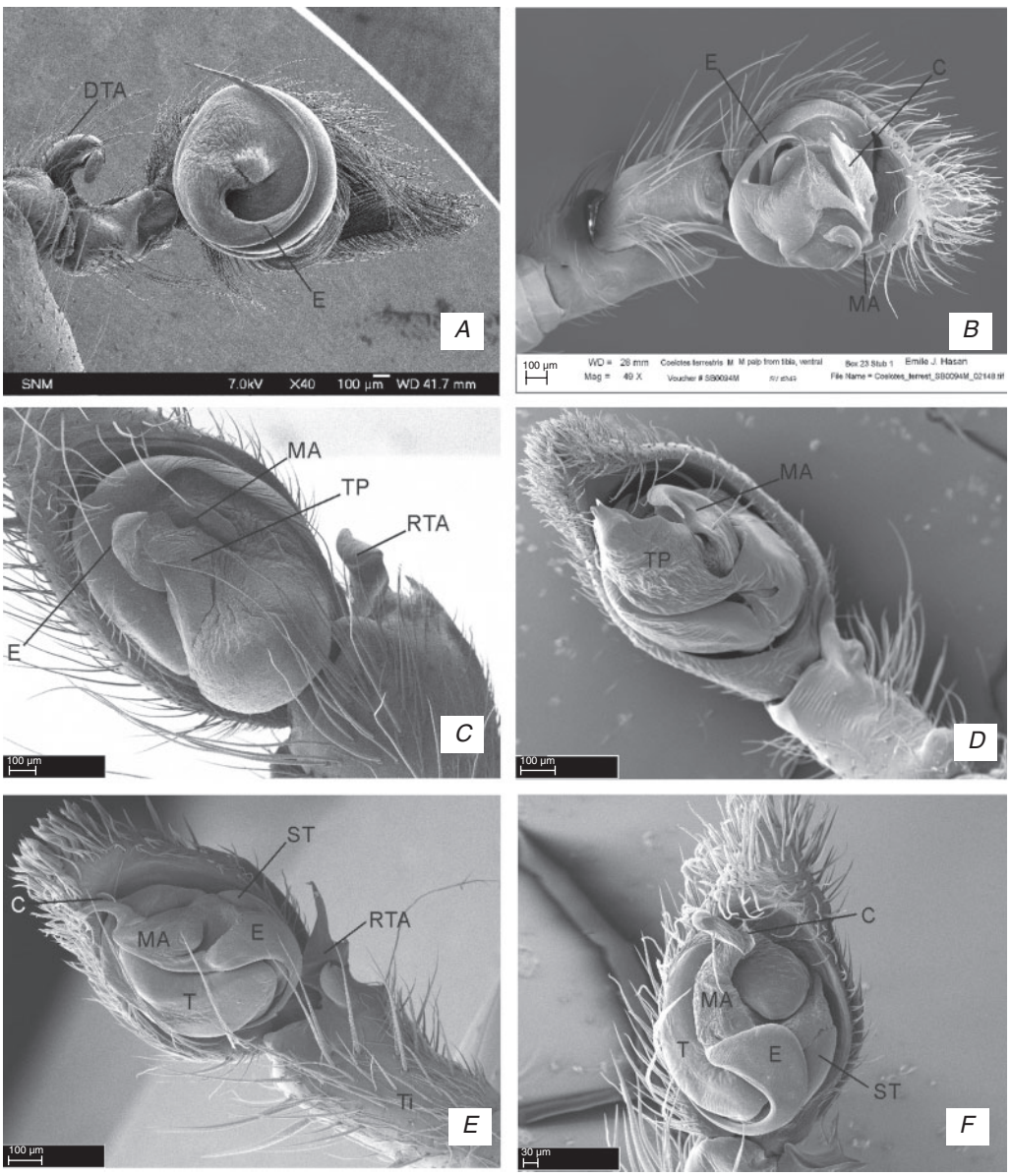

Fig. 13. Male palp, ventral view. *A*, *Megadictyna thilenii*; *B*, *Coelotes terrestris*; *C*, *Cambridgea* sp.; *D*, *Anyphaena pacifica*; *E*, *Argoctenus* sp.; *F*, *Argoctenus* sp. Abbreviations: C, conductor; DTA, dorsal tibial apophysis; E, embolus; MA, median apophysis; RTA, retrolateral tibial apophysis; ST, subtegulum; T, tegulum; Ti, tibia; TP, tegular process.

Catalog 2015) we have *Austrotengella*, *Tengella* and *Titiotus*. *Anachemmis* Chamberlin, 1919, *Liocranoides* Keyserling, 1881 and *Socalchemmis* Platnick & Ubick, 2001 are closely related to our exemplar *Titiotus* (Platnick and Ubick 2008). *Calamistrula* Dahl is a synonym of *Uduba* (Udubidae) (Griswold, pers. obs.). *Lauricius* Simon, 1888 and *Wiltonia* Koçak & Kemal, 2008 (Tengellidae) remain mysteries, but there is no better place for them than to accompany other tengellids into our newly circumscribed Zoropsidae. Previous analyses already suggest that the limits of Zoropsidae, Zorocratidae and Tengellidae are not well defined (Silva Dávila 2003; Raven and Stumkat 2005). Although our analyses fail to reveal many diagnostic characters to support the synonymy of these four families, they also fail to support the monophyly of, and provide diagnosis for, each family separately. Most problematic may be the position of Senoculidae within the Zoropsidae. This is unexpected, but supported both by Parsimony and Bayesian analyses (Figs 1–3). Some partitioned data, like the protein-coding gene fragments, show Senoculidae as a separate family within the Lycosoidea, a more conservative relationship for the family. *Senoculus* is on a long morphology branch (with 21 transformations), indicating that it might cluster with different clades when analysing only morphological characters. Despite our results, the synonymy of Senoculidae with Zoropsidae will

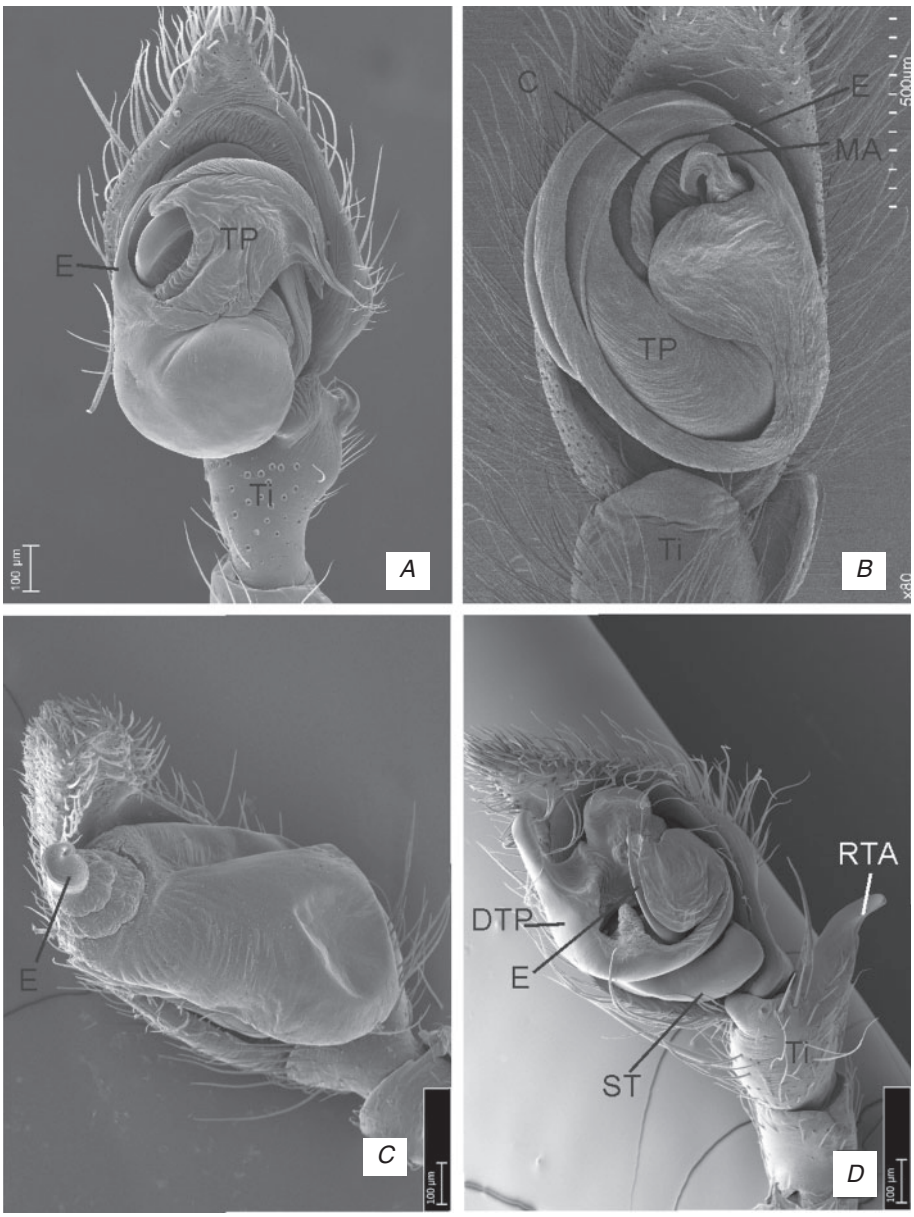

Fig. 14. Male palp, ventral view. *A*, *Stiphidion facetum*; *B*, *Desis formidabilis*; *C*, *Trachelas tranquillus*; *D*, *Hala* cf. *paulyi.* Abbreviations: C, conductor; DTP, distal tegular process; E, embolus; MA, median apophysis; RTA, retrolateral tibial apophysis; ST, subtegulum; T, tegulum; Ti, tibia; TP, tegular process.

be postponed, because this family is a classical Lycosoidea and this relation should be further explored.

Ctenids (tropical wolf spiders)

Ctenidae, as currently delimited, are polyphyletic in our results. Some previous phylogenetic analyses based only on morphology cluster Viridasiinae and *Cupiennius* Simon, 1891 with the remaining Ctenidae (Silva Dávila 2003; Polotow and Brescovit 2014) by several convergent traits, especially in the eye position and genital characters, though in other analyses (Ramírez 2014) viridasiines arise separately from other Ctenidae. In our results, all the total-evidence and partitioned analyses cluster Viridasiinae with Dionycha (Figs 1–3). The only exception was the morphological partition under equal-weights analysis of parsimony, which did not cluster Viridasiinae with the remaining Ctenidae or Dionycha. *Cupiennius* appears as sister-group of Lycosidae and part of Pisauridae (Figs 1–3, 7). The position of *Cupiennius* in the partitioned analyses is more complex, clustering with different clades in different partitions, but none of the analyses recover a monophyletic Ctenidae including *Cupiennius*. The remaining Ctenidae in our analysis cluster in a clade with low support in the parsimony analysis; this clade is not always present in the partitions (Fig. 8). Ctenidae (with a derived Psechridae as sister-group of *Acanthoctenus* Keyserling, 1877) are supported by six homoplastic synapomorphies in the parsimony analysis

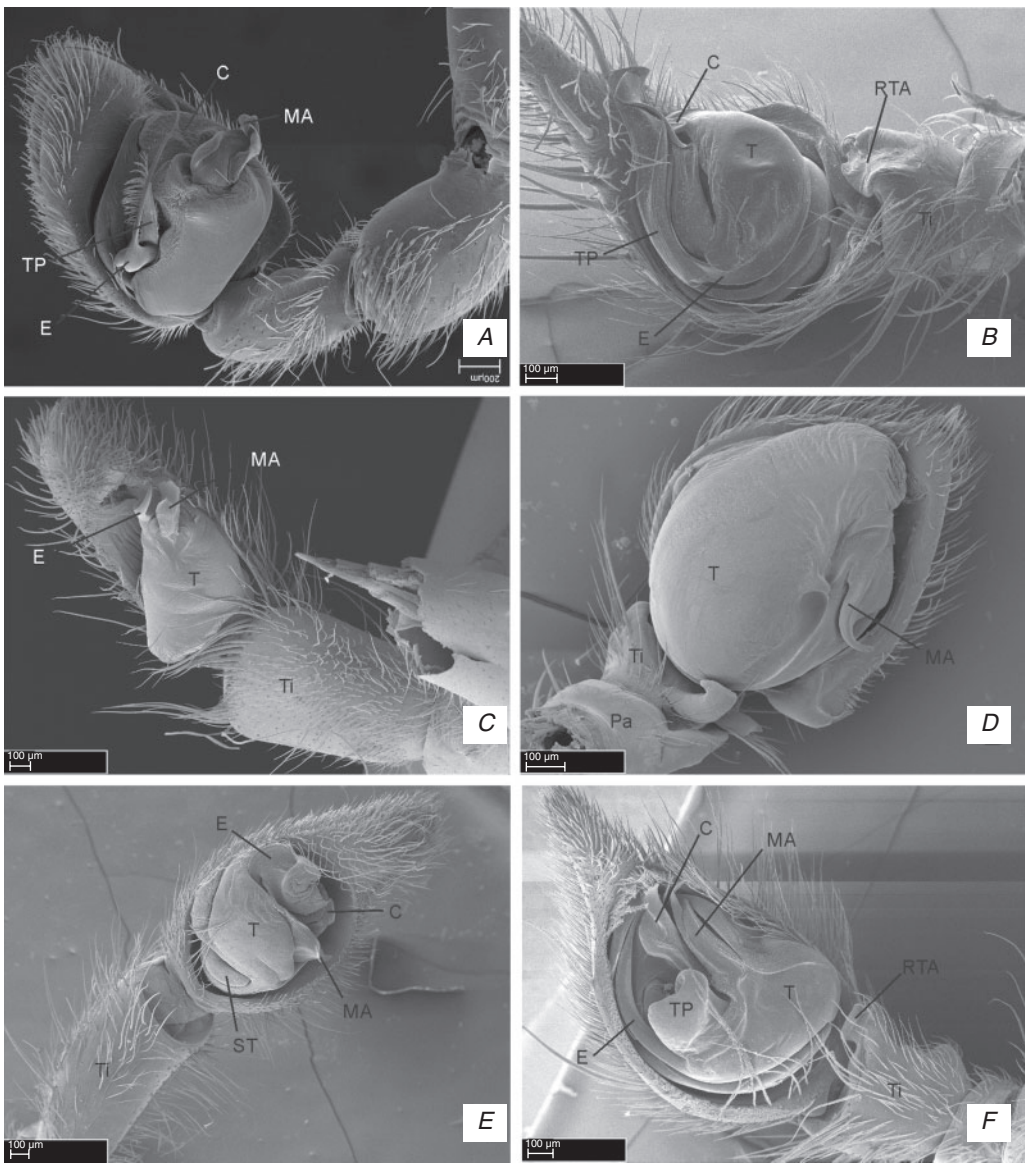

Fig. 15. Male palp, ventral view. *A*, *Kilyana hendersoni*; *B*, *Senoculus* sp.; *C*, *Psechrus cebu*; *D*, *Tmarus* sp.; *E*, *Alopecosa kochi*; *F*, *Oxyopes* sp. Abbreviations: C, conductor; DTP, distal tegular process; E, embolus; MA, median apophysis; Pa, patella; RTA, retrolateral tibial apophysis; ST, subtegulum; T, tegulum; Ti, tibia; TP, tegular process.

under implied weight k = 6 (Fig. 7): presence of four retromarginal teeth (character 15), cup-shaped median apophysis (character 35), presence of adhesive setae on tarsus (character 52), four or more pairs of spines on the ventral metatarsus of leg I and II (character 67), five pairs of spines on the ventral tibia of leg I and II (character 69) and overlapping spines on ventral tibia (character 70) (Fig. 7). The Bayesian analysis shows a Ctenidae clade (except Viridasiinae and *Cupiennius*) with posterior probability greater than 95% (Fig. 1).

Psechrids (giant funnel web and 'pseudo-orb' weavers)

The monophyly of Psechridae, comprising *Psechrus* Thorell, 1878 and *Fecenia* Simon, 1887, has been well established (Griswold 1993; Bayer and Schönhofer 2013; Agnarsson *et al.* 2013*b*). The grate-shaped tapetum of psechrids mandated inclusion in Lycosoidea (Homann 1971). In our analysis Psechridae (represented by *Psechrus*) cluster among the Lycosoidea, as has been the case in all previous quantitative analyses (Griswold 1993; Griswold *et al*. 1999; Silva Dávila 2003; Raven and Stumkat 2005; Griswold *et al.* 2005; Bayer and Schönhofer 2013; Agnarsson *et al.* 2013*a*; Agnarsson *et al.* 2013*b*). In our analyses psechrids appear as sister group of the clade formed by Oxyopidae, Thomisidae, Pisauridae, Lycosidae, *Cupiennius* and *Nilus* O. P.-Cambridge, 1876 in the Bayesian analysis (Fig. 1), and as a derived ctenid, sister group of *Acanthoctenus*, in the parsimony analyses with equal weights and implied weights concavity k = 6 (Figs 2, 3). Like Oxyopidae (Rovner 1980; Griswold 1983; Mora 1986), psechrids hang

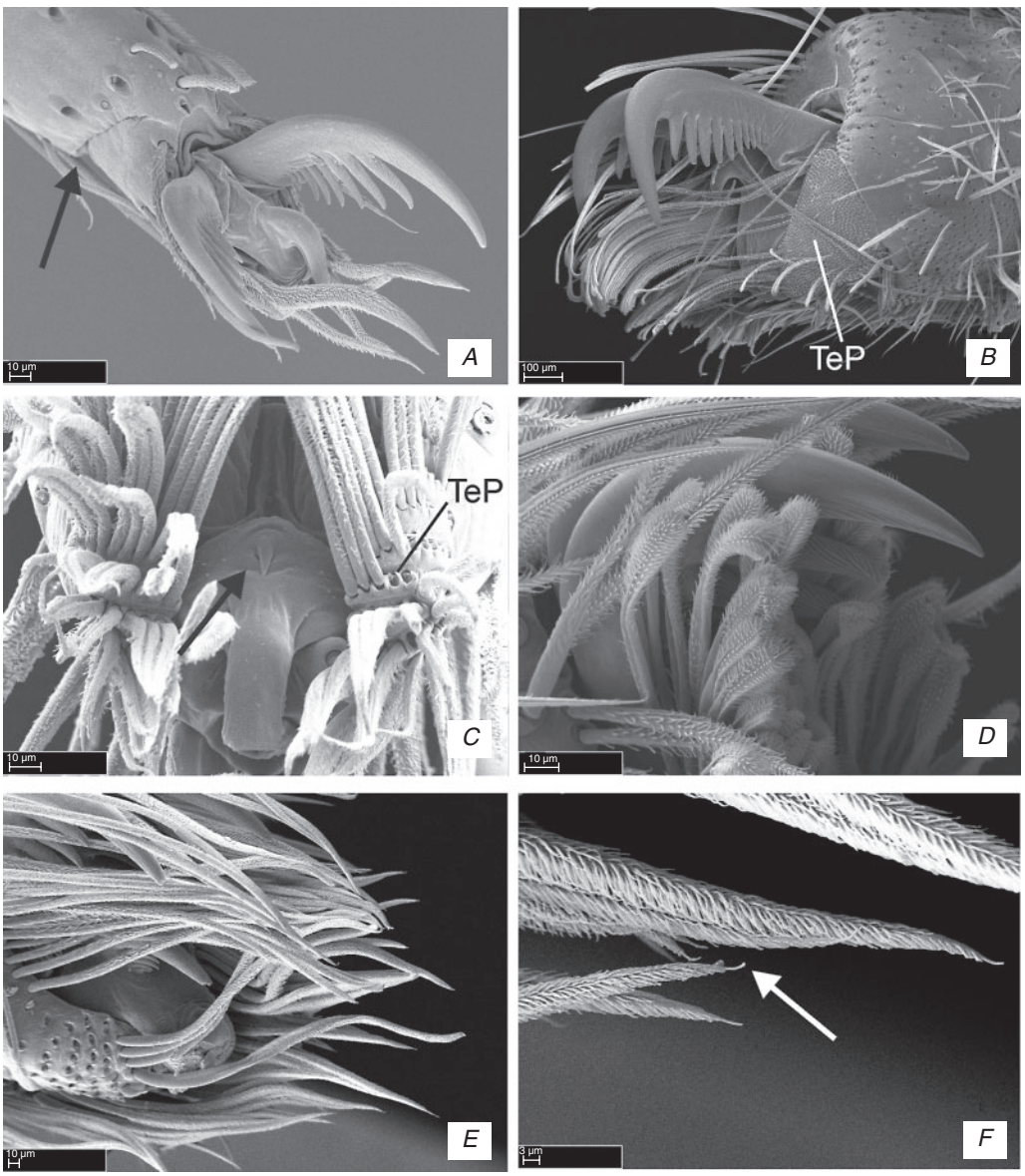

Fig. 16 Leg I, tip of the tarsus. *A*, *Architis brasiliensis*; *B*, *Cupiennius salei*; *C*, *Acanthoctenus* sp.; *D*, *Argoctenus*; *E*, *F*, *Tengella radiata*. Abbreviations: TeP, tenante plate. Arrow points the pseudosegmented tarsus.

beneath sheet webs. Even the so-called 'pseudo-orb' of *Fecenia* adults has been shown to develop from a juvenile conical sheet web (Robinson and Lubin 1979). Recently, Bayer and Schönhofer (2013) investigated the phylogenetic relationships of Psechridae, and their results also show Psechridae within Lycosoidea. The relation of Psechridae and Ctenidae was not tested in their analysis, because the only ctenid species that they used was a *Viridasius* Simon, 1889 (here placed in Dionycha) (Bayer and Schönhofer 2013). As cited above, Viridasiinae do not cluster with Ctenidae in any of our analyses; therefore is not possible to compare the two analyses in this regard.

Psechridae species present some morphological characters that could relate them to derived Ctenidae, as the parsimony analysis suggests, such as the third claw and claw tufts (as several species of Ctenidae), whereas the retention of cribellum and calamistrum (as *Acanthoctenus*) and separate lorum I and II of the pedicel (fused in most Lycosoidea) distinguish psechrids from most other Lycosoidea. The molecular partition under parsimony also clusters Psechridae with Ctenidae (Fig. 8), but no other partition recovered this relation. Our Bayesian analyses never clustered Psechridae with Ctenidae: psechrids appear at the base of Lycosoidea as sister group of Lycosidae, Pisauridae, *Cupiennius*, *Nilus*, Oxyopidae and Thomisidae (Fig. 1).

Pisaurids

Pisauridae is represented in this analysis by four terminals. Only parsimony analysis under equal weights shows *Nilus* clustered with the remaining Pisauridae, in a monophyletic clade (Fig. 2). *Thaumasia* Perty, 1833, *Hala* Jocqué, 1994 and *Architis* Simon, 1898, although not a highly supported clade, appears in all analyses and all partitions as sister-group of Lycosidae (Figs 1, 3, 7). The Madagascar-endemic family Halidae was proposed by Jocqué (1994) and comprises two genera (*Hala* and *Tolma* Jocqué, 1994) from Madagascar. Jocqué and Dippenaar-Schoeman (2006) suggested that Halidae is a junior synonym of Pisauridae, but this idea has not previously been tested phylogenetically. Our results under all total-evidence analyses and most of the partitions (Figs 1–3, 7–8) place *Hala* in the Pisauridae as sister-group of *Architis* and *Thaumasia*, thus confirming the family synonymy.

Cupiennius – a model spider

Cupiennius is one of the most intensively studied genera of spiders and can be considered a model organism for understanding the physiology, behaviour and morphology of spiders (Barth 2002, and references therein). The genus comprises large spiders from the Neotropics, which can be easily bred in laboratory conditions (Barth 2002). *Cupiennius* was described in Ctenidae and kept as part of this family since then (Simon 1891). Our results do not corroborate the position of *Cupiennius* within Ctenidae and consistently show this genus as sister-group of Lycosidae and Pisauridae (Figs 1–3).

Lynx spiders (Oxyopidae) and crab spiders (Thomisidae)

Oxyopidae and Thomisidae frequently form a clade in our analyses, but their position varies greatly according to the

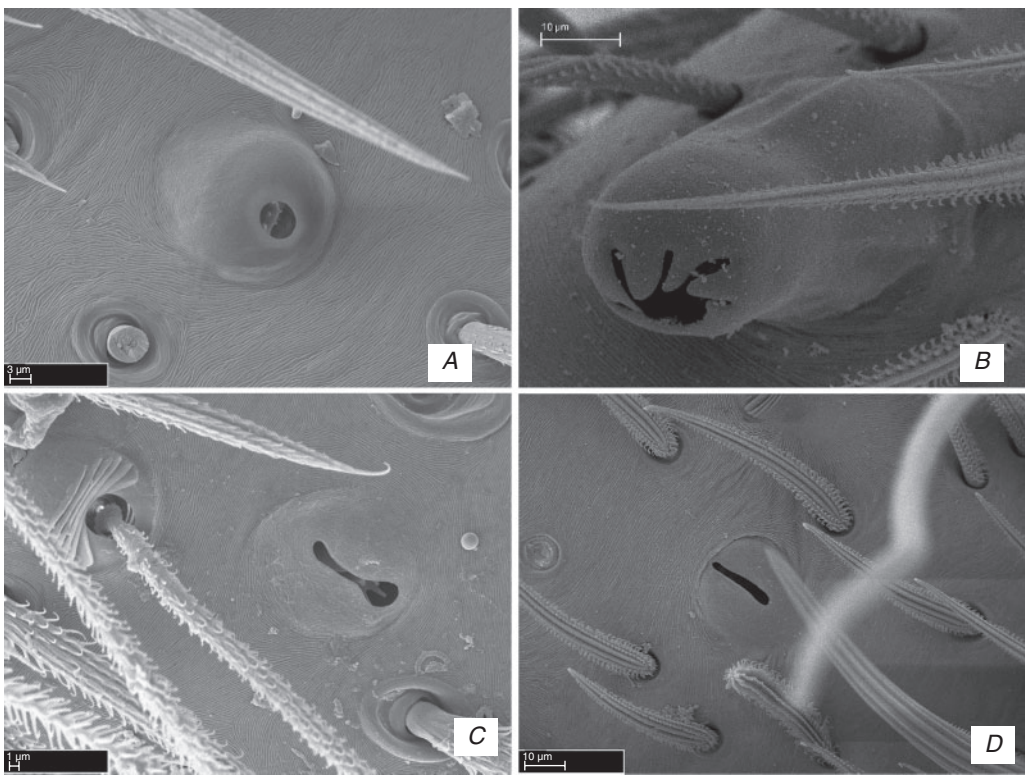

Fig. 17. Tarsal organ, leg I. *A*, *Phanotea digitata*; *B*, *Griswoldia acaenata*; *C*, *Zorodictyna* sp.; *D*, *Ctenus gr. crulsi*.

different analysis parameters. In the parsimony analysis with equal weights (and also with concavity values of k = 3, 20, 50 and 99) Thomisidae appear as sister-group of Oxyopidae plus the 'GST clade' (Fig. 2). In the parsimony analysis with concavity k = 1, both families form a clade, sister-group of the 'GST clade'. Thomisidae and Oxyopidae form a clade and appear in very different positions in the analyses using Bayesian and parsimony with concavity of k = 6 and 9, within the Lycosoidea and sister-group of the Lycosidae, Pisauridae, *Cupiennius* and *Nilus* (Figs 1, 3). None of the positions have strong support or are recovered by most partitions (Fig. 8). Bayer and Schönhofer (2013) and Agnarsson *et al.* (2013*b*) also recovered Thomisidae and Oxyopidae within Lycosoidea.

Systematics

In the following sections, we discuss morphological character support for certain groupings, suggesting how those groups might be diagnosed and identified. Also we present the taxonomic changes proposed on the basis of the results of this paper. The diagnoses are based on the results obtained by the parsimony analysis with concavity k = 6 (Figs 3–7).

Dionycha

The clade Dionycha (Fig. 5), represented in our analysis by exemplars from Anyphaenidae, Trachelidae, Eutichuridae, Mitugidae, Philodromidae, Salticidae, and the new family Viridasiidae, is supported by seven homoplastic synapomorphies,

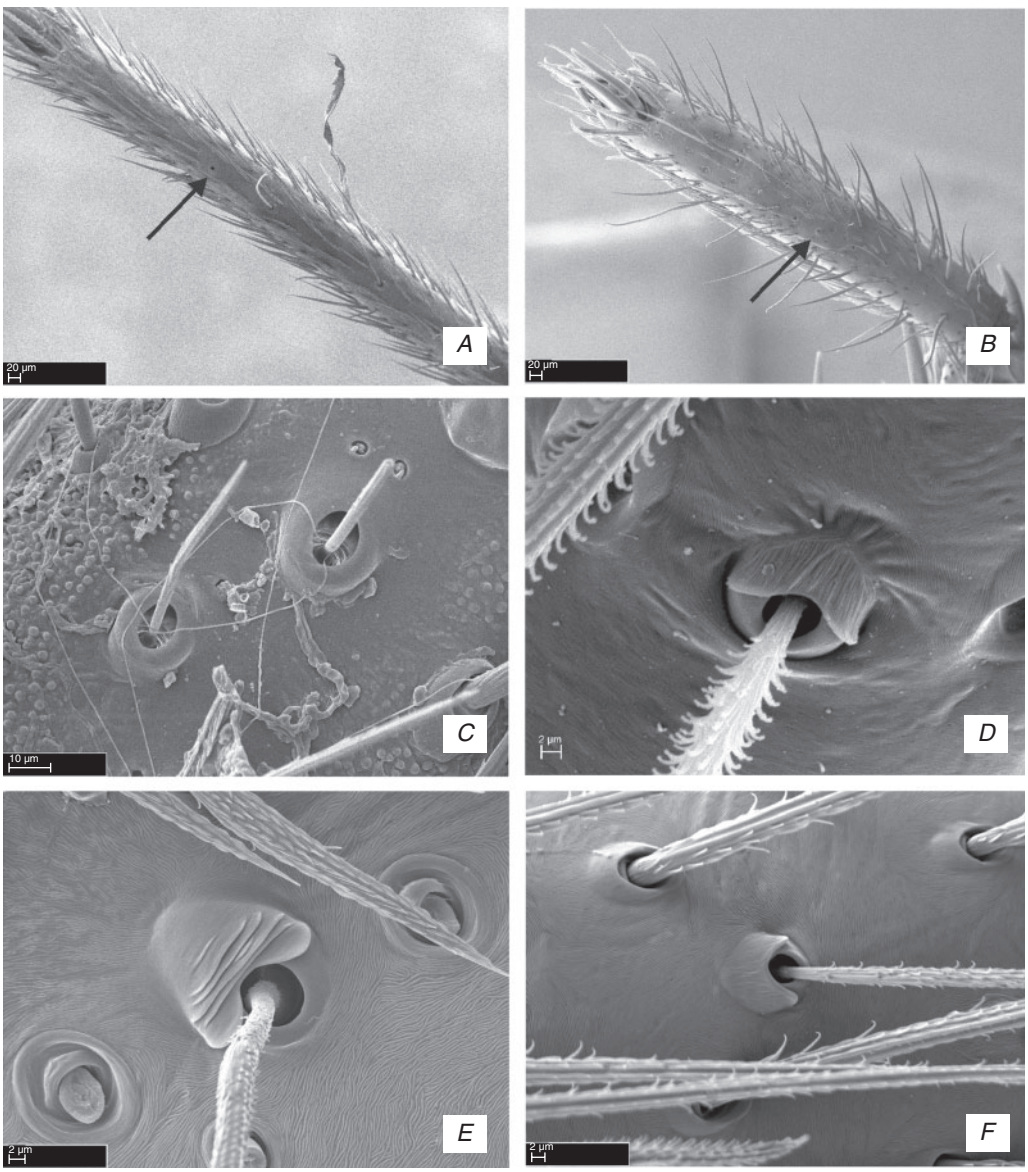

Fig. 18. Trichobothrium, leg I. *A*, *Oxyopes* sp.; *B*, *Griswoldia disparilis*; *C*, *Misumenoides* sp.; *D*, *Stiphidion facetum*; *E*, *Phanotea digitata*; *F*, *Anyphaena pacifica*. Arrows indicate the position of the tarsal organ.

which distinguish them from other 'RTA clade' taxa: tapetum perforated with pores (character 7), two retromarginal teeth on chelicerae (character 15), absence of an additional tegular process on male palp (character 42), embolus with flexible base (character 44), third claw absent (character 50), presence of adhesive setae on tarsus (character 52) and two pairs of ventral spines on metatarsus I (character 67).

'Oval Calamistrum clade'

The 'Oval Calamistrum clade' (Fig. 6), comprising Lycosoidea, our enlarged Zoropsidae and the new family Udubidae, is consistently recovered in our analyses and supported by seven homoplastic synapomorphies: subapical serrula (character 19), presence of locking lobes on the male palp (characters 29 and 31), tarsal trichobothrium proximal plate with transversal ridges (character 64), four pairs of ventral spines on tibia I (character 69), a unique oval calamistrum (character 73), trochanters of leg I with asymmetric and shallowly notched border (character 74) and minor ampullate gland spigots close together (character 89).

'Grate-shaped Tapetum clade' (GST clade)

This clade comprises seven family-level taxa (Fig. 6) – Zoropsidae (including Zorocratidae **syn. nov.** and Tengellidae **syn**. **nov**.), Lycosidae, Pisauridae, Oxyopidae, Thomisidae, Ctenidae and Trechaleidae (the latter not represented in our analysis) – and at least two genera that did not cluster with the former families – *Nilus* and *Cupiennius*. Our concept of the 'GST clade' differs from that of Silva-Dávila (2003) by including the Thomisidae but excluding some former zorocratids here placed in Udubidae, e.g. *Raecius*, *Uduba*, the viridasiines (formerly placed

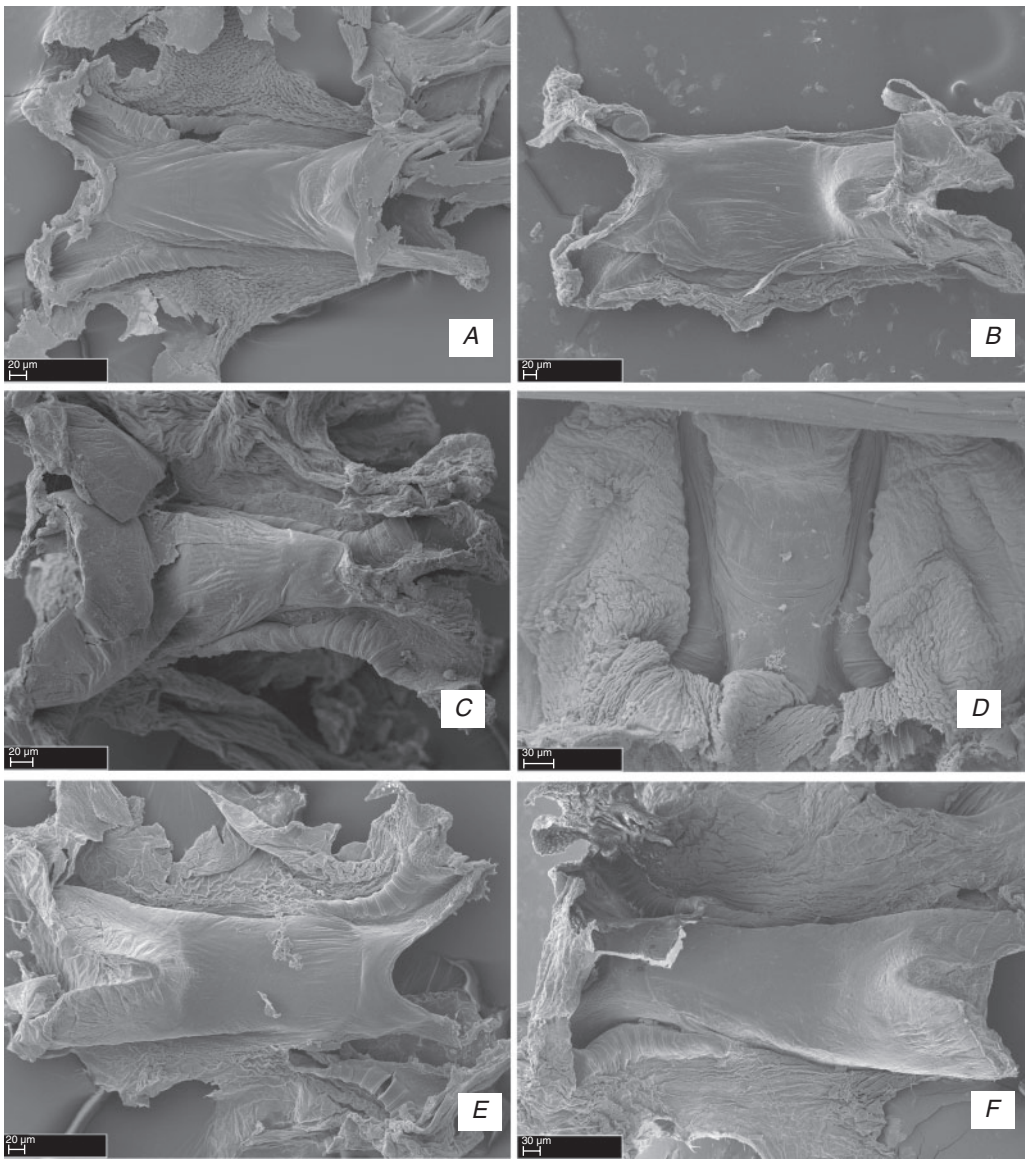

Fig. 19. Lorum of the pedicel, ventral view. *A*, *Tmarus* sp.; *B*, *Oxyopes* sp.; *C*, *Architis brasiliensis*; *D*, *Hala* cf. *paulyi*; *E*, *Draposa tenasserimensis*; *F*, *Alopecosa kochi*.

in Ctenidae, here proposed as the separate family Viridasiidae), and some miturgids and *Odo*. This clade is supported by three homoplastic synapomorphies (Fig. 6), which can be used to distinguish them from other 'RTA clade' taxa: posterior eye row recurved (character 5), ALE larger than AME (character 6) and presence of grate-shaped tapetum in the indirect eyes (character 7), reversed to canoe-shaped in some members.

Lycosoidea

Comprising seven families – Ctenidae, Oxyopidae, Thomisidae, Psechridae, Lycosidae, Pisauridae, Trechaleidae (not represented as a terminal in our analysis) – and at least two genera not clustered with the former families – *Nilus* and *Cupiennius* – our superfamily Lycosoidea differs from former concepts (Griswold 1993, Silva-Dávila 2003, Raven and Stumkat 2005) by including the Thomisidae but excluding Zoropsidae. The Lycosoidea are supported by one unique and two homoplastic synapomorphies (Fig. 7): egg sac carried by the chelicerae (later transformed to carried by the spinnerets) (character 96), anterior eye row (anterior view) recurved (character 4) and ALE smaller than AME (character 6).

A large clade of Lycosoidea excluding the Ctenidae (Pisauridae, including junior synonym Halidae, Lycosidae, Thomisidae, and Oxyopidae) is supported by several characters, four of them from the male pedipalp (Fig. 7): absence of the subtegulum lobe (character 29), absence of the lobe at the base of the embolus (character 31), absence of an additional tegular process (character 42), embolus with flexible base (character 44) and embolus with basal origin (character 45). The clade is also supported by six homoplastic somatic

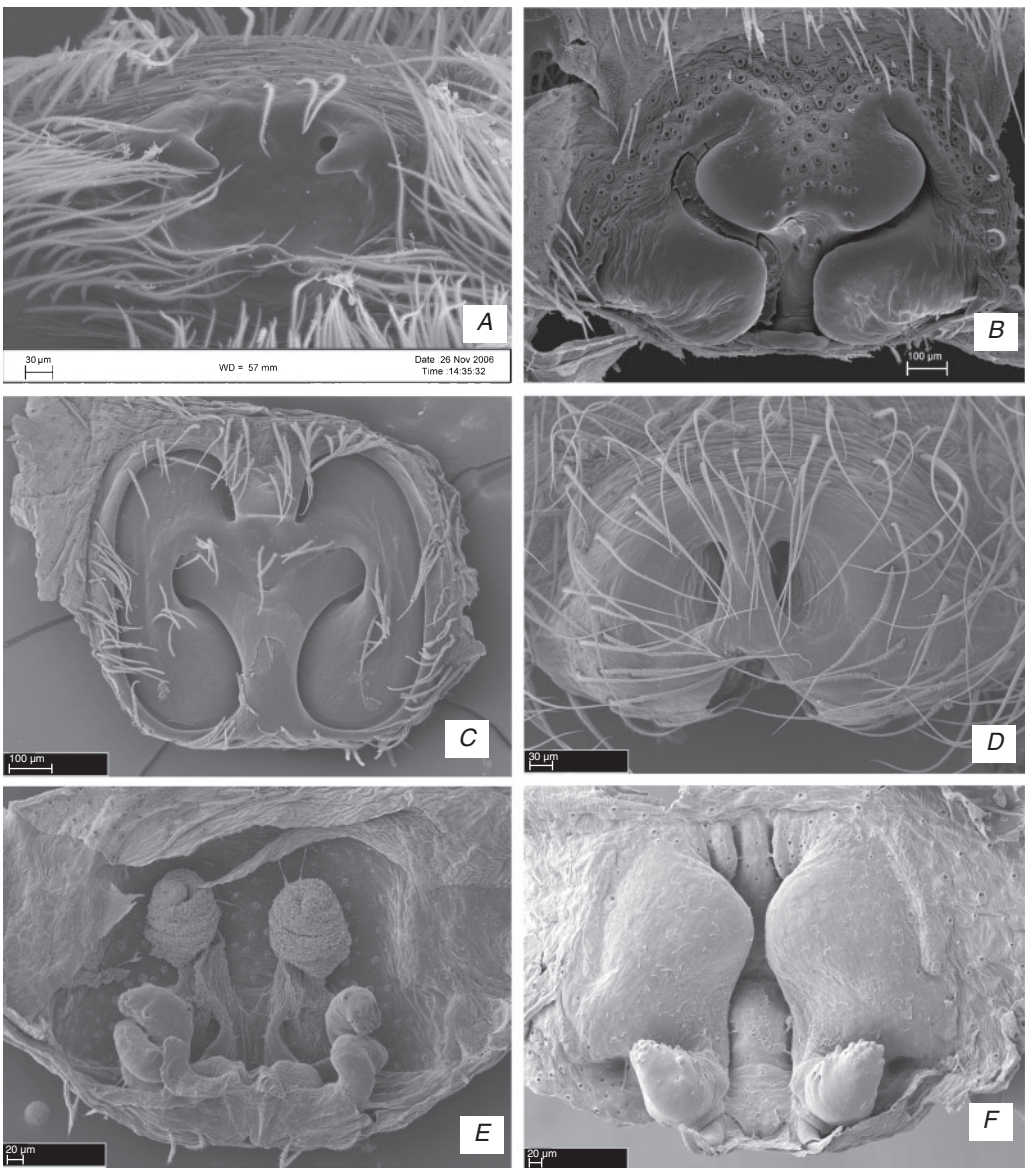

Fig. 20. Epigynum, ventral view. *A*, *Cheiracanthium fisheri*; *B*, *Desis formidabilis*; *C*, *Griswoldia acaenata*; *D*, *Acanthoctenus* sp.; *E*, *Architis brasiliensis*; *F*, *Austrotengella toddae*.

synapomorphies: sternum extending between coxae IV (character 13), presence of teeth on third claw (character 51), smooth proximal plate of the tarsal trichobothrium (character 64), presence of a distal spine on ventral metatarsus (character 66), border of trochanter on leg I deeply notched (character 74) and fused lorum I and II of the pedicel (character 75).

PISAURIDAE Simon, 1890

Types

Pisaura Simon, 1885.
Pisaura mirabilis (Clerck, 1757).
Araneus mirabilis Clerck, 1757: 108, plate 5, fig. 10.
Hala Jocqué, 1994.
Hala impigra Jocqué, 1994: 284, figs 7, 9, 12–19.

Notes, synonymy

Our analysis includes three traditional pisaurids (*Nilus*, *Thaumasia* and *Architis*) plus *Hala*, which was described in its own family (Jocqué 1994) and later placed as a junior synonym of Pisauridae (Jocqué and Dippenaar-Schoeman 2006). The clade (Fig. 7) containing *Nilus*, *Thaumasia* and *Architis* is paraphyletic with respect to Lycosidae (*Draposa* and *Alopecosa*) and *Cupiennius* (currently placed in Ctenidae: World Spider Catalog 2015). Our analysis contains no member of *Pisaura*, and the circumscription and composition of Pisauridae is beyond the scope of this contribution. At least *Hala* groups with the pisaurids *Thaumasia* and *Architis*, corroborating the synonymy of Halidae and Pisauridae.

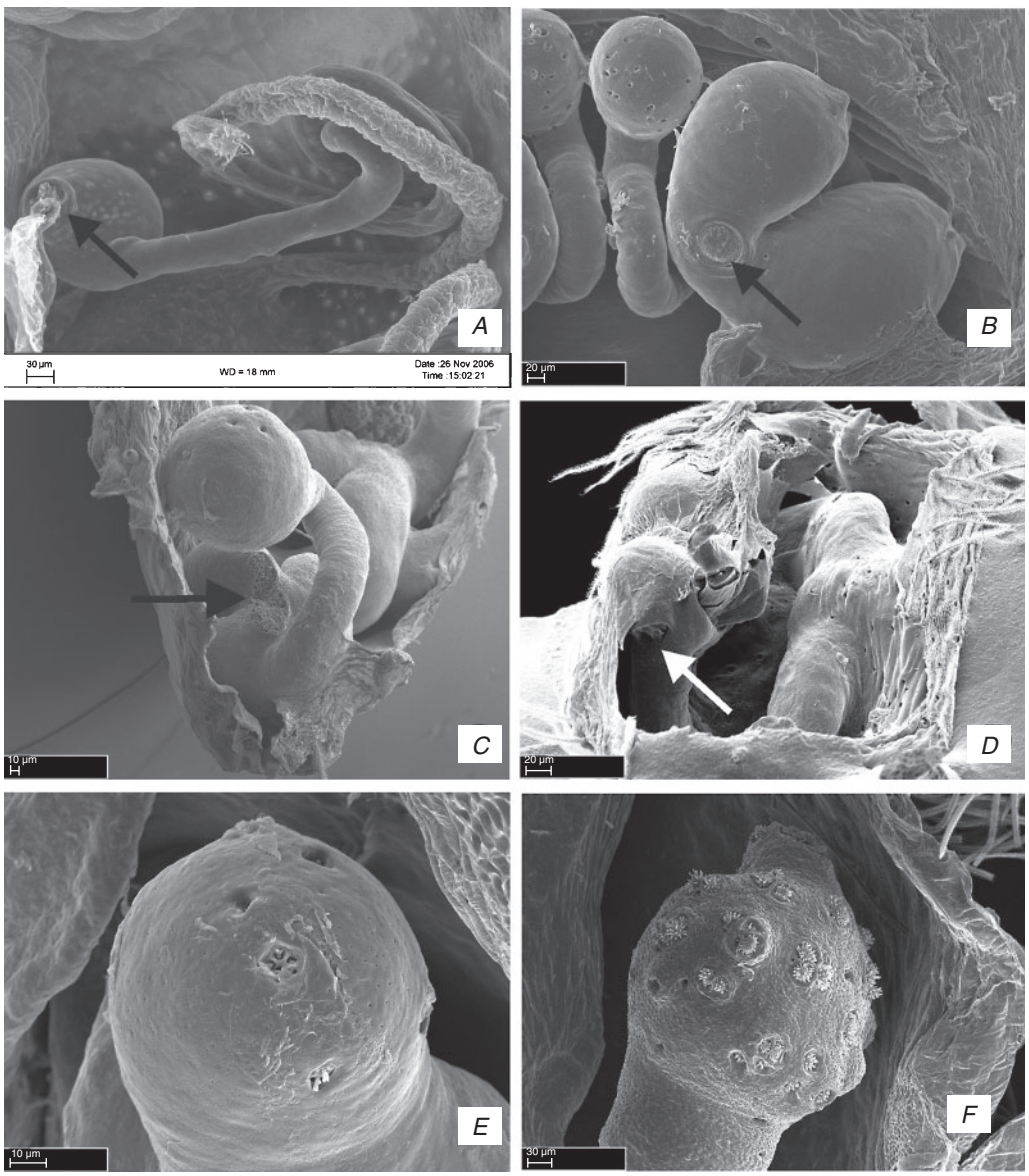

Fig. 21. Epigynum, dorsal view, spermathecae details. *A*, *Desis formidabilis*; *B*, *Cybaeus* sp.; *C*, *Alopecosa kochi*; *D*, *Hala* cf. *paulyi*; *E*, *Draposa tenasserimensis*; *F*, *Cupiennius salei*. Arrows indicate Bennett's gland.

Distribution

Worldwide.

UDUBIDAE Griswold & Polotow, fam. nov.

urn:lsid:zoobank.org:act:BEAA7711-93AF-496D-ADDB-B8DFFCF31364

Types

Uduba Simon, 1880, type genus.
Uduba madagascariensis (Vinson, 1863).
Olios madagascariensis Vinson, 1863: 100, 305; type species.

Diagnosis

The Udubidae (Figs 3, 6) are supported by several homoplastic synapomorphies, which can be used to distinguished them from other Oval Calamistrum clade families: absence of a serrula on the movable chela of the chelicerae (character 16), tibia of male palp with ventral apophysis (character 22), oval cross section of the embolus (character 48), tarsal organ with a keyhole-shaped opening (character 57), tarsal trichobothria of equal length (character 61), male leg tibiae with crack (character 68), uniquely textured spermathecae (character 88) and elongated posterior lateral spinnerets (character 92).

Composition

Compostichomma Karsch, 1891, *Raecius* Simon, 1892, *Uduba* Simon, 1880 and *Zorodictyna* Strand, 1907.

Distribution

Tropical and subtropical Africa, Madagascar, and Sri Lanka.

Note

Campostichomma was not included as a terminal in our analysis, but it presents the morphological diagnostic characters of Udubidae. The Udubidae fauna from Madagascar is diverse although only five species are currently recognised, i.e. *Calamistrula evanescens* Dahl, *Uduba dahli* Simon, 1903 and *U. madagascariensis* (Vinson, 1863), and *Zorodictyna inhonesta* (Simon, 1906) and *Z. oswaldi* (Lenz, 1891), there are nearly 100 new species to be described. *Calamistrula* Dahl 1901 is a junior synonym of *Uduba* (Griswold, pers. obs.), which genus is under revision (Griswold, Ledford and Ubick, in prep.).

VIRIDASIIDAE Lehtinen, 1967, rank.nov.

Types

Viridasius Simon, 1889, type genus.
Viridasius fasciatus (Lenz, 1886).
Phoneutria fasciata Lenz, 1886: 404, type species.

Notes

Although traditionally placed in Ctenidae, the peculiar nature of these spiders has been long recognised. Lehtinen considered Viridasiinae ‘a close relative of an extinct cribellate branch of Lycosoidea’ (Lehtinen 1967: 378). Viridasiinae were placed as

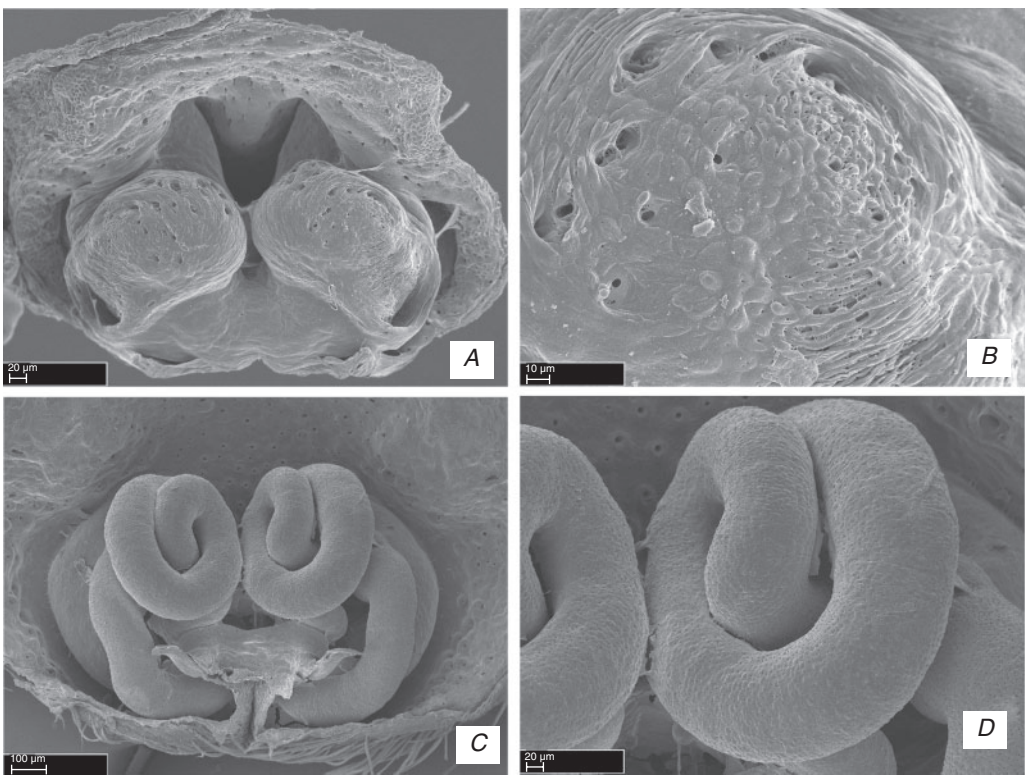

Fig. 22. Epigynum, dorsal view, spermathecae details. *A*, *B*, *Zorodictyna* sp.; *C*, *D*, *Uduba* sp.

a basal clade of Ctenidae by Silva Dávila (2003). In our analysis our three viridasiine exemplars, *Vulsor isaloensis* (Ono, 1993) and two species of *Viridasius*, cluster far from the other Ctenidae and nearer to Philodromidae and *Odo*, suggesting that viridasiines be excluded from Ctenidae (Figs 1–3).

Diagnosis

Several homoplasies and two unique synapomorphies support Viridasiidae. The unique synapomorphies are a tegular process at the conductor base (character 41) and the presence of a pars pendula on the embolus (character 49). Homoplasious synapomorphies include a type 2 ventral tibial process on the male palp (character 23), a cymbial retrolateral process (character 26), a subtegulum locking lobe (character 29), a locking lobe at the base of the embolus (character 31), tarsal trichobothrium with proximal plate smooth, more than three longitudinal rows of dorsal trichobothria on the metatarsus (character 65) and the epigynum lateral sector with a tooth (character 80).

Composition

Viridasius and *Vulsor*. There are many new species and some new genera that belong to this clade, all from Madagascar (D. Silva Dávila, pers. comm.).

Distribution

Madagascar.

ZOROPSIDAE Bertkau, 1882

Types

Zoropsis Simon, 1878, type genus.
Zoropsis spinimana (Dufour, 1820).
Dolomedes spinimanus Dufour, 1820: 204, plate 76, fig. 3.
Tengella Dahl, 1901, type genus.
Tengella perfuga Dahl, 1901: 252.
Zorocrates Simon, 1888, type genus.
Zorocrates fuscus Simon, 1888: 212.

Synonymy

We radically relimit this family and propose that Zorocratidae Dahl, 1913 (syn. nov.) and Tengellidae Dahl, 1908 (syn. nov.) be synonymised.

Diagnosis

This family circumscription is consistently supported by molecular data, as well as by three homoplastic morphological synapomorphies on the male palp (Fig. 6): presence of a type 2 ventral tibial process on the tibia (character 23), a rounded to oval cymbium (character 25) and a cymbial retrolateral process (character 26).

Composition

Included genera may be distributed among four subfamilies. Griswoldiinae Raven & Stumkat 2005, which are from south Asia (Sri Lanka), Australia, southern Africa and southern South America, comprise *Austrotengella*, *Cauquenia*, *Devendra*, *Griswoldia*, *Itatiaya* and *Phanotea*. Synapomorphies for Griswoldiinae comprise the absence of a cymbial retrolateral process (character 26), a cup-shaped median apophysis (character 35), no additional tegular process (character 42), a tooth on the epigynum lateral sector (character 80), and elongated gland tubes on the copulatory ducts (character 83). Uliodoninae Lehtinen, 1967, which are from Australia and New Zealand, comprise *Huntia* and *Uliodon*. Synapomorphies for Uliodoninae comprise a flexible embolic base (character 44), no inferior tarsal (third) claw (ITC) on leg I (character 50) and no gland tubes on the head of the spermathecae (character 86). *Kilyana* groups with Uliodoninae in this analysis, though in the more genera-rich analysis of Raven and Stumkat (2005), *Kilyana* groups with Zoropsinae. Also, following Raven and Stumkat (2005) and our analysis, we suggest that Zoropsinae Bertkau, 1882, which is a worldwide taxon, may comprise *Akamasia*, *Birrana*, *Kilyana*, *Krukt*, *Megateg*, *Takeoa* and *Zoropsis*. The 'tengellids' *Anachemmis*, *Liocranoides*, *Socalchemmis* and *Titiotus* may also be zoropsines. Synapomorphies for Zoropsinae comprise subtegulum with a shallow, cup-shaped excavation as a locking lobe (character 30), a hooked, bifid median apophysis apex (character 36) (Fig. 15*A*), embolus shape in cross-section laminar (character 48), highly spinose legs with four pairs of ventral spines on metatarsus I (character 67), six or more pairs of ventral spines on tibia I (character 69) and tibia I with ventral spines overlapping (character 70), with the head of the spermathecae lacking gland tubes (character 86) and the minor ampullate gland spigots separated by their diameter (character 89). Tengellinae Dahl comprise only the cribellate genera *Tengella* and *Zorocrates*. Synapomorphies for Tengellinae comprise some characters that may be considered reversals, e.g. posterior eye row (dorsal view) straight (Fig. 10*D*) (character 5), tapetum canoe-shaped (character 7), no tenant plates bearing claw tufts (character 54), and tarsal trichobothria lengths all equal (character 61); other synapomorphies include endite serrula position apical (character 19) and copulatory ducts with elongated gland tubes (character 83) (Fig. 20*F*). The single three-nucleotide gap in COI for the terminals *Tengella radiata* and *Tengella* sp. can be considered a synapomorphy for the genus *Tengella. Pseudoctenus*, *Lauricius* and *Wiltonia* are *incertae sedis* in our relimited Zoropsidae.

Distribution

Worldwide.

Conclusions

Results are consistent across several analytical parameters and methods for some of the groups found in the analyses. We recover the same clades and the same relations among clades in different analyses. These results imply that many morphological characters show substantial convergence. On the basis of the findings of this study, we provide additional evidence corroborating the non-monophyly of the grate-shaped tapetum. The reflective grate-shaped tapetum is related to a nocturnal and predatory behaviour and it appears to have evolved multiple times, through elongation of the canoe-shaped tapetum, which remains constrained by the diameter of the eye, which in turn leads to compression of the elongated tapetum as a series of loops or grids.

Based on the above analyses and discussion, our taxonomic conclusions can be summarised as follows:

(1) The monophyly of the Oval Calamistrum clade appears to be unequivocal, with high support.
(2) The grate-shaped tapetum appears independently at least three times and has a complex evolutionary history, with several reversions.
(3) The superfamily Lycosoidea should be restricted to seven families: Lycosidae, Pisauridae (including the junior synonym Halidae), Ctenidae, Psechridae, Thomisidae and Oxyopidae. Trechaleidae (not included in our dataset) is also a member of Lycosoidea.
(4) As currently circumscribed (World Spider Catalog 2015), the following families are not monophyletic: Ctenidae, Miturgidae, Pisauridae, Tengellidae, Zorocratidae and Zoropsidae.
(5) Senoculidae (*Senoculus*) do not cluster with the remaining Lycosoidea but instead as part of Zoropsidae.
(6) The parsimony analysis clusters Psechridae (*Psechrus*) within Ctenidae as sister-group of *Acanthoctenus*; this result is not supported by the Bayesian analysis. Placement of Psechridae within the Lycosoidea is unequivocal, but the sister group to Psechridae remains elusive.
(7) Ududibidae is proposed as a new family including the clade formed by former zorocratid genera *Uduba*, *Raecius* and *Zorodictyna*, plus the south Asian genus *Campostichomma*. These do not cluster with the zorocratid type species *Zorocrates fuscus*.
(8) Viridasiidae is proposed as a new family, comprising some former Ctenidae endemic to Madagascar.
(9) Zoropsidae is enlarged to include the genera of Zorocratidae and Tengellidae.

Acknowledgements

Financial support was provided by the Exline-Frizzell Fund for Arachnological Research and Lindsay Expedition Fund (both California Academy of Sciences, CAS) and by The Schlinger Foundation; DP is grateful for CNPq, Conselho Nacional de Desenvolvimento Científico e Tecnológico (PDE program) and a Bill and Maria Peck Fellowship (CAS); AC and CG thank the Hagey Research Investment Fund (CAS). The Lakeside Fund, CAS, supported the 'Lycosoidea Summit': including the authors and Lina Almeida, Estevam Cruz da Silva, Luis Piacintini, Diana Silva Dávila, Petra Sierwald and Darrell Ubick. Some of the ideas considered herein were spawned by the fruitful encounter in September 2011. Aspects of this research were supported by NSF grants: DEB-0072713 – 'Terrestrial Arthropod Inventory of Madagascar' (to CG and Brian Fisher), DEB 9296271 – 'Systematics and Biogeography of Afromontane Spiders' (to CG), DEB-0613775 'PBI: Collaborative Research – The Megadiverse, Microdistributed Spider Family Oonopidae' (to CG) and EAR-0228699 – 'Assembling the Tree of Life: Phylogeny of Spiders' (Ward Wheeler, PI). The program TNT was made available by the Willi Hennig Society. Specimens were provided by Martín Ramírez, Adalberto Santos and Darci Battesti. Professor Dr Wolfgang Nentwig from University of Bern kindly sent us the specimen of *Cupiennius salei*. We are thankful to Mark Harvey, Martin Ramírez and Cor Vink for the helpful comments and corrections in this manuscript.

References

Agnarsson, I., Gregorič, M., Blackledge, T. A., and Kuntner, M. (2013*a*). The phylogenetic placement of Psechridae within Entelegynae and the convergent origin of orblike spider webs. *Journal of Zoological Systematics and Evolutionary Research* **51**, 100–106. doi:10.1111/jzs.12007

Agnarsson, I., Coddington, J., and Kuntner, M. (2013*b*). Systematics – progress in the study of spider diversity and evolution. In 'Spider Research in the 21st Century: Trends and Perspectives'. (Ed. D. Penney.) pp. 58–111. (Siri Scientific Press: Rochdale, UK.)

Altschul, A. F., Madden, T. L., Schäffer, A. A., Zhang, J., Zhang, Z., Miller, W., and Lipman, D. J. (1997). Gapped BLAST and PSI-BLAST: a new generation of protein database search programs. *Nucleic Acids Research* **25**, 3389–3402.

Álvarez-Padilla, F., and Hormiga, G. (2007). A protocol for digesting internal soft tissues and mounting spiders for scanning electron microscopy. *The Journal of Arachnology* **35**, 538–542. doi:10.1636/Sh06-55.1

Arnedo, M., Oromi, P., and Ribera, C. (2001). Radiation of the spider genus *Dysdera* (Araneae, Dysderidae) in the Canary Islands: cladistic assessment based on multiple data sets. *Cladistics* **17**, 313–353. doi:10.1111/j.1096-0031.2001.tb00129.x

Baccetti, B., and Bedini, C. (1964). Research on the structure and physiology of the eyes of a lycosid spider. I. Microscopic and ultramicroscopic structure. *Archives Italiennes de Biologie* **102**, 97–122.

Barth, F. G. (2002). 'A Spider's World. Senses and Behavior.' (Springer-Verlag: Heidelberg.)

Bayer, S., and Schönhofer, A. L. (2013). Phylogenetic relationships of the spider family Psechridae inferred from molecular data, with comments on the Lycosoidea (Arachnida: Araneae). *Invertebrate Systematics* **27**, 53–80. doi:10.1071/IS12017

Bennett, R. G. (1992). The spermathecal pores of spiders with special reference to dictynoids and amaurobioids (Araneae, Araneomorphae, Araneoclada). *Proceedings of the Entomological Society of Ontario* **123**, 1–21.

Berger, M. P., and Munson, P. J. (1991). A novel randomized iterative strategy for aligning multiple protein sequences. *Computer Applications in the Biosciences* **7**, 479–484.

Bertkau, P. (1882). Über das Cribellum und Calamistrum. Ein Beitrag zur Histologie, Biologie und Systematik der Spinnen. *Archiv für Naturgeschichte* **48**, 316–362.

Blackledge, T. A., Scharff, N., Coddington, J. A., Szüts, T., Wenzel, J. W., Hayashi, C. Y., and Agnarsson, I. (2009). Reconstructing web evolution and spider diversification in the molecular era. *Proceedings of the National Academy of Sciences of the United States of America* **106**, 5229–5234. doi:10.1073/pnas.0901377106

Bremer, K. (1994). Branch support and tree stability. *Cladistics* **10**, 295–304.

Bosselaers, J. (2002). A cladistic analysis of Zoropsidae (Araneae), with the description of a new genus. *Belgian Journal of Zoology* **132**, 141–154.

Clerck, C. (1757). 'Svenska spindlar, uti sina hufvud-slågter indelte samt under några och sextio särskildte arter beskrefne och med illuminerade figurer uplyste.' (Stockholmiae.)

Coddington, J. A., and Levi, H. W. (1991). Systematics and evolution of spiders (Araneae). *Annual Review of Ecology and Systematics* **22**, 565–592. doi:10.1146/annurev.es.22.110191.003025

Coddington, J., and Scharff, N. (1994). Problems with zero-length branches. *Cladistics* **10**, 415–423. doi:10.1111/j.1096-0031.1994.tb00187.x

Colgan, D. J., McLauchlan, A., Wilson, G. D. F., Livingston, S. P., Edgecombe, G. D., Macaranas, J., Cassis, G., and Gray, M. R. (1998). Histone H3 and U2 snRNA DNA sequences and arthropod molecular evolution. *Australian Journal of Zoology* **46**, 419–437. doi:10.1071/ZO98048

Dahl, F. (1901). Nachtrag zur Uebersicht der Zoropsiden. *Sitzungs-Berichte der Gesellschaft Naturforschender Freunde, Berlin* **1901**, 244–255.

Dahl, F. (1908). Die Lycosiden oder Wolfsspinnen Deutschlands und ihre Stellung im Haushalt der Natur. Nach statistichen Untersuchungen dargestellt. *Nova Acta Academiae Caesareae Leopoldino-Carolinae Germanicae Naturae Curiosorum* **88**, 175–678.

Dahl, F. (1913). 'Vergleichende Physiologie und Morphologie der Spinnentiere unter besonderer Berucksichtigung der Lebensweise. 1. Die Beziehungen des Körperbaues und der Farben zur Umgebung.' (Jena.) pp. 1–113.

Dufour, L. (1820). Descriptions de cinq arachnides nouvelles. *Annales générales des Sciences physiques* **5**, 198–209.

Farris, J. S. (1969). A successive approximations approach to character weighting. *Systematic Zoology* **18**, 374–385.

Felsenstein, J. (1985). Phylogenies and the comparative method. *American Naturalist* **125**, 1–15.

Fenk, L. M., and Schmid, A. (2010). The orientation-dependent visual special cut-off frequency in a spider. *The Journal of Experimental Biology* **213**, 3111–3117. doi:10.1242/jeb.041939

Fitch, W. M. (1971). Toward defining the course of evolution: minimal change for a specific tree topology. *Systematic Zoology* **20**, 406–416. doi:10.2307/2412116

Foelix, R. F. (2011). 'Biology of Spiders.' 3rd edn. (Oxford University Press: New York.)

Folmer, O., Black, M., Hoeh, W., Lutz, R., and Vrijenhoek, R. (1994). DNA primers for the amplification of mitochondrial cytochrome *c* oxidase subunit I from diverse metazoan invertebrates. *Molecular Marine Biology and Biotechnology* **3**, 294–299.

Forster, R. R. (1970). The spiders of New Zealand. Part III. *Otago Museum Bulletin* **3**, 1–184.

Forster, R. R., and Wilton, C. L. (1973). The spiders of New Zealand. Part IV. *Otago Museum Bulletin* **4**, 1–309.

Giribet, G., and Wheeler, W. C. (1999). On gaps. *Molecular Phylogenetics and Evolution* **13**, 132–143.

Giribet, G., and Edgecomb, G. (2006). Conflict between datasets and phylogeny of centipedes: an analysis based on seven genes and morphology. *Proceedings. Biological Sciences* **273**, 531–538. doi:10.1098/rspb.2005.3365

Giribet, G., Vogt, L., Pérez González, A., Sharma, P., and Kury, A. B. (2010). A multilocus approach to harvestmen (Arachnida: Opiliones) phylogeny with emphasis on biogeography and the systematics of Laniatores. *Cladistics* **26**, 408–437.

Goloboff, P. A. (1993). Estimating character weights during tree search. *Cladistics* **9**, 83–91.

Goloboff, P. A., Farris, J. S., Källersjö, M., Oxelman, B., Ramírez, M. J., and Szumik, C. A. (2003). Improvements to resampling measures of group support. *Cladistics* **19**, 324–332. doi:10.1111/j.1096-0031.2003.tb00376.x

Goloboff, P. A., Farris, J. S., and Nixon, K. (2008*a*). TNT, a free program for phylogenetic analysis. *Cladistics* **24**, 774–786.

Goloboff, P. A., Carpenter, J. M., Arias, J. S., and Miranda Esquivel, D. R. (2008*b*). Weighting against homoplasy improves phylogenetic analysis of morphological data sets. *Cladistics* **24**, 758–773. doi:10.1111/j.1096-0031.2008.00209.x

Golubchik, T., Wise, M. J., Easteal, S., and Jermiin, L. S. (2007). Mind the gaps: evidence of bias in estimates of multiple sequence alignments. *Molecular Biology and Evolution* **24**, 2433–2442. doi:10.1093/molbev/msm176

Gotoh, O. (1993). Optimal alignment between groups of sequences and its application to multiple sequence alignment. *Computer Applications in the Biosciences* **9**, 361–370.

Griswold, C. E. (1983). *Tapinillus longipes* Taczanowski, a web-building lynx spider from the American tropics (Araneae: Oxyopidae). *Journal of Natural History* **17**, 979–985. doi:10.1080/00222938300770751

Griswold, C. E. (1993). Investigations into the phylogeny of the lycosoid spiders and their kin (Arachnida: Araneae: Lycosoidea). *Smithsonian Contributions to Zoology* **539**, 1–39. doi:10.5479/si.00810282.539

Griswold, C. E., Coddington, J. A., Platnick, N. I., and Forster, R. R. (1999). Towards a phylogeny of Entelegyne spiders (Araneae, Araneomorphae, Entelegynae). *The Journal of Arachnology* **27**, 53–63.

Griswold, C. E., Ramírez, M. J., Coddington, J. A., and Platnick, N. I. (2005). Atlas of phylogenetic data for entelegyne spiders (Araneae: Araneomorphae: Entelegynae) with comments on their phylogeny. *Proceedings of the California Academy of Sciences* **56**, 1–324.

Hedin, M. C., and Maddison, W. P. (2001). A combined molecular approach to phylogeny of the jumping spider subfamily Dendryphantinae (Araneae: Salticidae). *Molecular Phylogenetics and Evolution* **18**, 386–403. doi:10.1006/mpev.2000.0883

Homann, H. (1928). Beiträge zur Physiologie der Spinnenaugen. I. Untesuchungsmethoden. II. Das Sehvermögen der Salticiden. *Zeitschrift fur Vergleichende Physiologie* **7**, 201–268. doi:10.1007/BF00339163

Homann, H. (1971). Die Augen der Araneae: Anatomie, Ontogenie und Bedeutung für die Systematik (Chelicerata, Arachnida). *Zeitschrift für Morphologie der Tiere* **69**, 201–272. doi:10.1007/BF00277623

Hormiga, G., Arnedo, M., and Gillespie, R. (2003). Speciation on a conveyor belt: sequential colonization of the Hawaiian Islands by *Orsonwelles* spiders (Araneae, Linyphiidae). *Systematic Biology* **52**, 70–88. doi:10.1080/10635150390132786

Huelsenbeck, J. P., and Ronquist, F. (2001). MRBAYES: Bayesian inference of phylogenetic trees. *Bioinformatics* **17**, 754–755. doi:10.1093/bioinformatics/17.8.754

Jocqué, R. (1994). Halidae, a new spider family from Madagascar (Araneae). *Bulletin of the British Arachnological Society* **9**, 281–289.

Jocqué, R., and Dippenaar-Schoeman, A. S. (2006). 'Spider Families of the World.' (Musée Royal de l'Afrique Central: Tervuren.)

Katoh, K., Misawa, K., Kuma, K., and Miyata, T. (2002). MAFFT: a novel method for rapid multiple sequence alignment based on fast Fourier transform. *Nucleic Acids Research* **30**, 3059–3066.

Katoh, K.,, Kuma, K., Toh, H., and Miyata, T. (2005). MAFFT version 5: improvement in accuracy of multiple sequence alignment. *Nucleic Acids Research* **33**, 511–518.

Katoh, K., and Toh, H. (2008). Recent developments in the MAFFT multiple sequence alignment program. *Briefings in Bioinformatics* **9**, 286–298.

Land, M. F. (1972). The physics and biology of animal reflectors. *Progress in Biophysics and Molecular Biology* **24**, 75–106. doi:10.1016/0079-6107(72)90004-1

Land, M. F. (1985). The morphology and optics of spider eyes. In 'Neurobiology of Arachnids'. (Ed. F. G. Barth.) pp. 53–76. (Spring-Verlag: Berlin, Heidelberg.)

Latiolais, J. M., Taylor, M. S., Kaustuv, R., and Hellberg, M. E. (2006). A molecular phylogenetic analysis of strombid gastropod morphological diversity. *Molecular Phylogenetics and Evolution* **41**, 436–444.

Lehtinen, P. T. (1967). 'Classification of the Cribellate Spiders and some Allied Families: with Notes on the Evolution of the Suborder Araneomorpha.' (Societas Zoologica Botanica Fennica Vanamo: Helsinki.)

Lenz, H. (1886). Beiträge zur Kenntniss der Spinnenfauna Madagascars. *Zoologische Jahrbucher. Abteilung fur Systematik, Ökologie und Geographie der Tiere* **1**, 379–408.

Lenz, H. (1891). Spinnen von Madagascar und Nossi-Bé. *Jahrbuch der Hamburgischen Wissenschaftlichen Anstalten* **9**, 153–181.

Maddison, W. P., and Maddison, D. R. (2011). 'Mesquite: a Modular System for Evolutionary Analysis.' Version 2.75. Available at http://mesquiteproject.org

Miller, J. A., Carmichael, A., Ramírez, M. J., Spagna, J. C., Haddad, C. R., Rezac, M., Johannesen, J., Kral, J., Wang, X., and Griswold, C. E. (2010). Phylogeny of entelegyne spiders: affinities of the family Penestomidae (new rank), generic phylogeny of Eresidae, and asymmetric rates of change in spinning organ evolution (Araneae, Araneoidea, Entelegynae). *Molecular Phylogenetics and Evolution* **55**, 786–804. doi:10.1016/j.ympev.2010.02.021

Mora, G. (1986). Use of web by *Tapinillus longipes* (Araneae: Oxyopidae). In 'Proceedings of the Ninth International Congress of Arachnology, Panama 1983'. (Eds W. G. Eberhard, Y. D. Lubin and B. C. Robinson.) pp. 173–175. (Smithsonian Institution Press: Washington, DC.)

Needleman, S. B., and Wunsch, C. D. (1970). A general method applicable to the search for similarities in the amino acid sequence of two proteins. *Journal of Molecular Biology* **48**, 443–453.

Notredame, C., Higgins, D. G., and Heringa, J. (2000). T-Coffee: a novel method for fast and accurate multiple sequence alignment. *Journal of Molecular Biology* **302**, 205–217.

Nylander, J. A. A. (2008). MrModeltest Version 2.3. Evolutionary Biology Centre, Uppsala University. Available from: http://www.abc.se/~nylander/.

Ono, H. (1993). Spiders (Araneae) from Madagascar. *Acta Arachnologica Tokyo* **42**, 55–67.

Piacentini, L. N., Ramírez, M. J., and Silva, D. (2013). Systematics of *Cauquenia* (Araneae: Zoropsidae), with comments on the patterns of evolution of cribellum and male tibial crack on Lycosoidea. *Invertebrate Systematics* **27**, 567–577. doi:10.1071/IS13031

Platnick, N. I. (1977). The hypochiloid spiders: a cladistic analysis, with notes on the Atypoidea (Arachnida, Araneae). *American Museum Novitates* **2627**, 1–23.

Platnick, N. I., and Gertsch, W. J. (1976). The suborders of spiders: a cladistic analysis. *American Museum Novitates* **2607**, 1–15.

Platnick, N. I., and Ubick, D. (2008). A revision of the endemic Californian spider genus *Titiotus* Simon (Araneae, Tengellidae). *American Museum Novitates* **3608**, 1–33. doi:10.1206/0003-0082(2008)3608[1:AROTEC]2.0.CO;2

Platt, A. R., Woodhall, R. W., and George, A. L. J. (2007). Improved DNA sequencing quality and efficiency using an optimized fast cycle sequencing protocol. *BioTechniques* **43**, 58–62.

Polotow, D., and Brescovit, A. D. (2010). Phylogenetic relationships of the Neotropical spider genus *Itatiaya* (Araneae). *Zoologica Scripta* **40**, 187–193.

Polotow, D., and Brescovit, A. D. (2014). Phylogenetic analysis of the tropical wolf spider subfamily Cteninae (Arachnida, Araneae, Ctenidae). *Zoological Journal of the Linnean Society* **170**, 333–361.

Prendini, L., Crowe, T., and Wheeler, W. (2003). Systematics and biogeography of the family Scorpionidae (Chelicerata: Scorpiones), with a discussion on phylogenetic methods. *Invertebrate Systematics* **17**, 185–259. doi:10.1071/IS02016

Rambaut, A., and Drummond, A. J. (2007). Tracer: MCMC Trace Analysis Tool. Version 1.4. Available at http://beast.bio.ed.ac.uk/Tracer

Ramírez, M. J. (2003). The spider subfamily Amaurobioidinae (Araneae, Anyphaenidae): a phylogenetic revision at the generic level. *Bulletin of the American Museum of Natural History* **277**, 1–262. doi:10.1206/0003-0090(2003)277<0001:TSSAAA>2.0.CO;2

Ramírez, M. J. (2014). The morphology and phylogeny of dionychan spiders (Araneae: Araneomorphae). *Bulletin of the American Museum of Natural History* **390**, 1–374. doi:10.1206/821.1

Raven, R. J., and Stumkat, K. S. (2005). Revisions of Australian ground-hunting spiders: II. Zoropsidae (Lycosoidea: Araneae). *Memoirs of the Queensland Museum* **50**, 347–423.

Robinson, M. H., and Lubin, Y. D. (1979). Specialists and generalists: the ecology and behavior of some web-building spiders from Papua New Guinea. II. *Psechrus argentatus* and *Fecenia* sp. (Araneae: Psechridae). *Pacific Insects* **21**, 133–164.

Ronquist, F., and Huelsenbeck, J. P. (2003). MRBAYES 3: Bayesian phylogenetic inference under mixed models. *Bioinformatics* **19**, 1572–1574.

Rovner, J. S. (1980). Adaptations for prey capture in oxyopid spiders: phylogenetic implications. In '8th International Congress of Arachnology, Vienna'. (Ed. J. Gruber.) pp. 233–237.

Sierwald, P. (1989). Morphology and ontogeny of female copulatory organs in American Pisauridae, with special reference to homologous features (Arachnida: Araneae). *Smithsonian Contributions to Zoology* **484**, 1–24. doi:10.5479/si.00810282.484

Sierwald, P. (1990). Morphology and homologous features in the male palp organ in Pisauridae and other spider families, with notes on the taxonomy of Pisauridae (Arachnidae: Araneae). *Nemouria* **35**, 1–59.

Silva Dávila, D. (2003). Higher-level relationships of the spider family Ctenidae (Araneae: Ctenoidea). *Bulletin of the American Museum of Natural History* **274**, 1–86. doi:10.1206/0003-0090(2003)274<0001:HLROTS>2.0.CO;2

Simon, E. (1880). Révision de la famille des Sparassidae (Arachnides). *Actes de la Société linnéenne de Bordeaux* **34**, 223–351.

Simon, E. (1891). Descriptions de quelques arachnides du Costa Rica communiqués pa M. A. Getaz (de Genève). *Bulletin de la Société Zoologique de France* **16**, 109–112.

Simon, E. (1906). Etude sur les araignées de la section des cribellates. *Annales de la Société Entomologique de Belgique* **50**, 284–308.

Simon, C., Frati, F., Beckenbach, A., Crespi, B., Liu, H., and Flook, P. (1994). Evolution, weighting, and phylogenetic utility of mitochondrial gene sequences and a compilation of conserved polymerase chain reaction primers. *Annals of the Entomological Society of America* **87**, 651–701. doi:10.1093/aesa/87.6.651

Spagna, J. C., and Gillespie, R. G. (2008). More data, fewer shifts: molecular insights into the evolution of the spinning apparatus in non-orb-weaving spiders. *Molecular Phylogenetics and Evolution* **46**, 347–368. doi:10.1016/j.ympev.2007.08.008

Strand, E. (1907). Diagnosen neuer Spinnen aus Madagaskar und Sansibar. *Zoologischer Anzeiger Leipzig* **31**, 725–748.

Swofford, D. L., and Maddison, W. P. (1987). Reconstructing ancestral character states under Wagner parsimony. *Mathematical Biosciences* **87**, 199–229. doi:10.1016/0025-5564(87)90074-5

Swofford, D. L., and Maddison, W. P. (1992). Parsimony, character-state reconstructions, and evolutionary inferences. In 'Systematics, Historical Ecology, and North American Freshwater Fishes'. (Ed. R. L. Mayden.) pp. 187–223. (Stanford University Press: Stanford.)

Vinson, A. (1863). Aranéides des îles de la Réunion. *Maurice et Madagascar. Paris* **i-cxx**, 1–337.

Whiting, M. F., Carpenter, J. M., Wheeler, Q. D., and Wheeler, W. C. (1997). The Strepsiptera problem: phylogeny of the holometabolous insect orders inferred from 18S and 28S ribosomal DNA sequences and morphology. *Systematic Biology* **46**, 1–68.

Wolff, J. O., and Gorb, S. N. (2012). Comparative morphology of pretarsal scopulae in eleven spider families. *Arthropod Structure & Development* **41**, 419–433.

Wolff, J. O., Nentwig, W., and Gorb, S. N. (2013). The great silk alternative: multiple co-evolution of web loss and sticky hairs in spiders. *PLoS One* **8**(5), e62682. doi:10.1371/journal.pone.0062682

World Spider Catalog (2015). World Spider Catalog. Natural History Museum Bern. Online at http://wsc.nmbe.ch, [version 16, accessed January 2015]

Appendix 1. Terminal taxa

Family placement (in parentheses) reflects assignments supported by this analysis. All specimens are deposited in the California Academy of Sciences unless otherwise noted

Acanthoctenus sp. (Ctenidae): IBSP 162608; Brazil, Bahia, Wenceslau Guimarães, Estação Ecológica Wenceslau Guimarães, 13°34′50″S, 39°42′17″W, 23.x.2010, D. Polotow.

Agelenopsis pennsylvanica (C. L. Koch, 1843) (Agelenidae): CAS 9023843; USA, Maryland, Prince George Co., University Park, 38°58′17″N, 76°56′32″W, 25.ix.2005, G. Hormiga.

Alopecosa kochi (Keyserling, 1877) (Lycosidae): CAS 9031448; USA, CA, Siskiyou Co., 41°46′16″N, 122°06′50″W, 11.viii.2008, F. Alvarez Padilla.

Ancylometes bogotensis (Keyserling, 1877) (Ctenidae): CAS 9021737; French Guiana, Montenéry Emerald Jungle Village, inside building surrounding by secondary tropical rainforest, 04°47′02″N, 52°25′19.6″W, 34 m night, 18.vi.2005, D. Silva Dávila.

Anyphaena pacifica (Banks, 1896) (Anyphaenidae): CAS 9047622; USA, California, San Francisco, 5.viii.2012, D. Ubick.

Apollophanes sp. (Philodromidae): CAS 9031470; USA, CA, Siskiyou Co., Marble Mountains, Lovers campground, 25.14 km W Fort Jones, 41°35.684′N, 123°08.569′W, 1270 m, 12–13.viii.2008, F. Alvarez Padilla, A. Carmichael, D. Dimitrov, C. Griswold, G. Hormiga, A. Saucedo.

Architis brasiliensis (Mello-Leitão, 1940) (Pisauridae): IBSP 162612; Brazil, Bahia, Wenceslau Guimarães, Estação Ecológica Wenceslau Guimarães, 13°34′50″S, 39°42′17″W, 23.x.2010, D. Polotow.

Argoctenus sp. 1 (Miturgidae): CAS 9023609; Australia, Western Australia, Two Road, Walpole–Nornalup N.P., 34°57′51″S, 116°36′34″E, elev. 40 m, 25–26.ii.2006, C. Griswold, D. Silva Dávila, L. J. Boutin, G. Hormiga, N. Scharff.

Argoctenus sp. 2 (Miturgidae): CAS 9019841; New Zealand, South Island, near Otuwhero River, 41°00′54″S, 172°59′30″E, 29.iii.2003, C. J. Vink.

Austrotengella toddae Raven, 2012 (Zoropsidae): CAS 9023720; Australia, Queensland, Boombana, Brisbane Forest Park, 27°24′5.5″S, 152°47′35″E, 440 m, 26.iii.2006, C. Griswold, D. Silva Dávila, R. Raven, B. Baehr.

Callobius nevadensis (Amaurobiidae): CAS 9047621; USA, California, Mendocino Co., Angelo Reserve, 39°43′28″N, 123°38′39″W, 28–30.iv.2009, L. Almeida.

Caloctenus oxapampa Silva, 2004 (Ctenidae): CAS 9016460; Peru, Oxapampa, Rio San Alberto, 1909 m, 10°34′50″S, 75°23′46″W, 14.i.2004, J. Bottger.

Cambridgea sp. (Stiphidiidae): CAS 9047626; New Zealand, South Is., Otago Prov., Catlins Coastal Rainforest Park, Matai Falls, 14.8 km SWS Owaka, 46°30′21″S, 169°29′8.5″E, 18.ii.2005, C. Griswold, D. Silva Dávila, H. Wood.

Celaetycheus abara Polotow & Brescovit, 2013 (Ctenidae): IBSP 162605; Brazil, Bahia, Wenceslau Guimarães, Estação Ecológica Wenceslau Guimarães, 13°34′50″S, 39°42′17″W, 23.x.2010, D. Polotow.

Cheiracanthium fisheri Lotz, 2014 (Eutichuridae): CAS 9029142; Madagascar, Toliara, Foret de Kirindy, 46 km NE Morondava, 20°04.02′S, 44°39.43′E, 20–30.i.2006, H. Wood.

Cheiracanthium mildei L. Koch, 1864 (Eutichuridae): CAS 9047623; USA, CA, Petaluma, suburbs, 38°47′5.9″N, 122°58′36″W, elev. 18 m, Oct. 2012, C. Griswold.

Ctenus gr. *crulsi* Mello-Leitão, 1930 (Ctenidae): CAS 9021733; French Guiana, Montenéry Emerald Jungle Village, secondary tropical rainforest, 04°47′02″N, 52°25′19″W, 34 m, ground, night, 18.vi.2005, D. Silva Dávila.

Cupiennius salei (Keyserling, 1877) (Ctenidae): CAS 9047631; Switzerland, Bern, 16.xii.2013, laboratory-reared stock in the University of Bern, collected from banana trade from Central America, exact location unknown.

Cybaeus sp. (Cybaeidae): CAS 9030568; USA, CA, Siskiyou Co., Marble Mountains, Stream at road, 22.68 km W Fort Jones, 41°36′56″N, 123°06′54″W, elev. 950 m, 12–13.viii.2008, F. Alvarez Padilla, A. Carmichael, D. Dimitrov, C. Griswold, G. Hormiga, A. Saucedo.

Desis formidabilis (O.-P. Cambridge, 1890) (Desidae): CAS, South Africa, Western Cape, Table Mountain National Park, Kommetjie, 34°08′25″S, 18°19′19″E, 1.iii.2006, J. Miller, H. Wood, N. Larsen.

Draposa tenasserimensis (Thorell, 1895) (Lycosidae): CAS 9019243; Myanmar, Bago Division, Moeyingyi Wildlife Reservation, 17°35′53″N, 96°35′53″E, 5.x.2003, C. Griswold, D. Ubick.

Enoploctenus cyclothorax (Bertkau, 1880) (Ctenidae): IBSP; Brazil, Rio de Janeiro, Rio de Janeiro.

Griswoldia acaenata (Griswold, 1991) (Zoropsidae): CAS 9043202; South Africa, Western Cape Prov., Groeneweide Nature Walk, 7.99 km 80°E George, 33°57′15″S, 22°32′6.7″E, 141 m, 20.x.2011, L. Almeida, C. Griswold, T. Meikle, E. & D. van der Westhuizen.

Griswoldia disparilis (Lawrence, 1952) (Zoropsidae): CAS 9024917; South Africa, Eastern Cape, Kai Mouth, 58 km NE East London, dune forest, 32°41′12″S, 28°22′37″E, 15 m, 11–13.ii.2006, J. Miller, H. Wood, L. Lotz.

Hala cf. *paulyi* Jocqué, 1994 (Pisauridae): CAS 9036016; Madagascar: Toamasina Province, Station Forestier Analamazaotra, 0.75 km N Andasibe, elev 964m, 31.I–3.ii.2009, 18°55′46″S, 48°24′41″E, C. Griswold, A. Saucedo, H. Wood.

Kilyana hendersoni Raven & Stumkat, 2005 (Zoropsidae): CAS 9023591; Australia, Queensland, Boombana, Brisbane Forest Park, 27°24′5.5″S, 152°47′35″E, 440 m, Berlese, 26.iii.2006, C. Griswold, D. Silva Dávila, R. Raven, B. Baehr.

Metaphidippus manni (Peckham & Peckham, 1901) (Salticidae): CAS 9031471; USA, CA, Siskiyou Co., Marble Mountains, Lovers Campground, 25.14 km W Fort Jones, 41°35′41″N, 123°08′34″W, 1270 m, 12–13.viii.2008, F. Alvarez Padilla, A. Carmichael, D. Dimitrov, C. Griswold, G. Hormiga, A. Saucedo.

Misumenoides sp. (Thomisidae): CAS 9030064; Chile, X Region de Los Lagos, Chiloé Is., outside of P.N. Chiloé, 1.69 km N Cucao, 42°37′1.6″S, 74°05′56″W, 1.iii.2008, C. Griswold.

Mituliodon tarantulinus (L. Koch, 1873) (Miturgidae): CAS 9023729; Australia, Queensland, Stradbroke, Brown Lake, 2.96 km 053° ENE Dunwich, 27°29′20″S, 153°25′49″E, elev. 50 m, 25.iii.2006, C. Griswold, D. Silva Dávila, R. Raven & B. Baehr.

Nilus majunguensis (Strand, 1907) (Pisauridae): CAS 9047628; Madagascar, Toliara, Foret de Kirindy, 46 km NE Morondava, 20°04′1.5″S, 44°39′26″E, 20–30.i.2006, H. Wood, J. Miller.

Odo abudi Alayón, 2002 (Miturgidae): CAS 9047618; Dominican Republic, near El Rio, Cordillera Central, 19.00953°N, 70.32429°W, elev. 3489 ft, Jul. 2004, J. Huff.

Odo bruchi (Mello-Leitão, 1938) (Miturgidae): MACN 4024; Argentina, Buenos Aires Prov., Tomquist, Ruta Provincial 76, Abra del Pantanoso, 30 km N Sierra de la Ventana, 37°58′45″S, 61°52′47″W, 400 m, 19–21.vi.2009, C. Grismado, M. Izquierdo, L. Piacentini, A. Ojanguren.

(*continued next page*)

Appendix 1. (*continued*)

Oxyopes sp. (Oxyopidae): CAS 9019264; Myanmar, Bago Division, Moeyingyi Wildlife Reserve, 17°35′22″N, 96°34′32″E, 3.x.2003, C. Griswold, P. Sierwald, D. Ubick, Tin Mya Soe, Zaw Min.

Parazygiella carpenteri (Araneidae): CAS 9031452; USA, CA, Siskiyou Co., Juanita Lake Campground, 23.55 km SW Dorris, 41°49′4.6″N, 122°07′26″W, 1500 m, 9.viii.2008, F. Alvarez Padilla, A. Carmichael, D. Dimitrov, C. Griswold, G. Hormiga, A. Saucedo.

Peucetia rubrolineata Keyserling, 1877 (Oxyopidae): UFMG 10668; Brazil, Bahia, Una, Estação Experimental Lemos Maia (CEPLAC), 15°16′22″S, 39°5′31″W, 7–12.xii.2010, G. H. F. Azevedo, A. J. Santos.

Phanotea digitata Griswold, 1994 (Zoropsidae): CAS 9043274; South Africa, Western Cape Prov., Grootvaderbosh Nature Reserve, 14.97 km 316° NE Heidelberg, 33°59′1.4″S, 20°49′55″E, elev. 338 m, 17.x.2011, L. Almeida, C. Griswold, T. Meikle.

Psechrus cebu Murphy, 1986 (Psechridae): CAS 9042449; Philippines, Luzon Is., Camarines Sur Prov., Mt Isarog, 9.3 km E Naga City, 918 m, 13°39′55″N, 123°21′14″E, 31.v.–2.vi.2011, M.Yngente, N. Chousou-Polydouri, C. Griswold.

Raecius asper (Thorell, 1899) (Udubidae): AMNH; Cameroon, 7.5 km E Ndu on Road to Sabongari, 4.x.2002, R. West.

Senoculus sp. (Senoculidae): UFMG 3250; Brazil, Minas Gerais, Belo Horizonte, Estação Ecológica da UFMG, 19°58′S, 43°58′W, 10.ix.2009, B. T. Faleiro.

Tengella sp. (Zoropsidae): CAS 9047627; Panama, Prov. Coclé, 50 km west of Penonomé via El Copé (Omar Torrijos) 8°40′5″N, 80°35′33″W, 760 m, 3–8.vi.2008, G. Hormiga, L. Benavides.

Thaumasia hirsutochela Silva & Carico, 2012 (Pisauridae): IBSP 162615; Brazil, Bahia, Wenceslau Guimarães, Estação Ecológica Wenceslau Guimarães, 13°34′50″S, 39°42′17″W, 23.x.2010, D. Polotow.

Titiotus sp. (Zoropsidae): CAS 9047630; USA, CA, Contra Costa Co., Concord, 7.v.2013, M. Bation.

Tmarus sp. (Thomisidae): CAS 9035914; Madagascar, Toamasina Prov, Station Forest Analamazaotra, 18°55′46″S, 48°24′41″E, 31.i.–3.ii.2009, C. Griswold.

Trachelas tranquillus (Hentz, 1847) (Trachelidae): CAS 9047624; USA, CA, Petaluma, suburbs, 38°47′5.9″N, 122°58′36″W, elev. 18 m, Oct. 2012, C. Griswold.

Uduba sp. (Udubidae): CAS 9030253; Madagascar, Toamasina, Mikira forest, 2.5 h hike from Andaparaty, 29 km N Maroantsetra, 195 m, 10–12.xii.2008, 15°12′2″S, 49°36′55″E, F. Alvarez-Padilla, H. Wood.

Uliodon frenatus (L. Koch, 1873) (Zoropsidae): CAS 9047620; New Zealand, South Is., Marlborough Prov., Queen Charlotte Track, 41°15′8.2″S, 173°56′26″E, elev. 15 m, 26.ii.2005, C. Griswold, D. Silva Dávila, H. Wood.

Vidole capensis (Phyxelididae): CAS 9023622; South Africa, Eastern Cape, Grahamstown, Dassiekrans, 33°19′40″S, 26°30′0.2″E, 715 m, 20.ii.2006, J. Miller, H. Wood

Viridasius sp. 1 (Viridasiidae): CAS 9015404; Madagascar, Toamasina Prov., Parc National Masoala, Ambohitsitondroina Mt, Ambanizana 15°34′9″S, 50°00′12″E, 750–800 m, 01.iii.2003, D. Andriamalala, D. Silva Dávila.

Viridasius sp. 2 (Viridasiidae): CAS 9016432; Madagascar, Toliara, Foret Classé Tsikongambarika Ivolo Forest, Andily, ca. Fort Dauphin, 24°56′13″S, 46°55′58″E, 13.iii.2003, D. Adriamalala, D. Silva Dávila.

Vulsor isaloensis (Viridasiidae): CAS 9047617; Madagascar: Toliara, Fôret de Kirindy field station, 46 km NE Morondava, 20°04′3″S, 44°39′26″E, 50 m, 20–30.i.2006, H. Wood, J. Miller.

Zorocrates fuscus (Zoropsidae): AMNH; Mexico, Oaxaca, 3.7 km N El Moral, 17°30′7″N, 96°56′5″W, 2050 m, 23.vii.2002, L. Prendini, O. Francke, E. Gonzalez, J. Ponce.

Zorodictyna sp. 1 (Udubidae): CAS 9031271; Madagascar, Mahajanga Prov., Ampijoroa, National Park Ankarafantsika, near Lake Ravelobe, 16°17′48.7″S, 46°48′50″E, 26–28.i.2009, C. Griswold, A. Saucedo, H. Wood.

Zorodictyna sp. 2 (Udubidae): CAS 9035866; Madagascar, Mahajanga Prov., Ampijoroa, National Park Ankarafantsika, near Lake Ravelobe, 16°17′48″S, 46°48′50″E, 26–28.i.2009, C. Griswold, A. Saucedo, H. Wood.

Zorodictyna sp. 3 (Udubidae): CAS 9029890; Madagascar, Fianarantsoa Prov., National Park Andrigitra, 34 km S Ambalavao, elev. 1580 m, 22°08′48″S, 46°57′03″E, 7.i.2009, H. Wood.

Zorodictyna sp. 4 (Udubidae): CAS 9029889; Madagascar, Fianarantsoa Prov., National Park Andrigitra, 34 km S Ambalavao, elev. 1580 m, 22°08′48″S, 46°57′03″E, 7.i.2009, H. Wood.

Zoropsis spinimana (Zoropsidae): CAS 9019845; USA, California, Santa Clara Co., Sunnyvale, 12.i.2004, M. Nachand.

Appendix 2. Character descriptions

Prosoma

(*1*) *Carapace shape (dorsal view):* 0, piriform (Fig. 10*A*); 1, rectangular (Fig. 10*B*); 2, ampullate (Fig. 10*C*).
(L = 9; CI = 22; RI = 50)
A piriform carapace is narrow in the ocular area and oval in the thoracic area (Fig. 10*A*). The rectangular carapace presents the anterior and posterior areas approximately with same width (Fig. 10*B*). An ampullate carapace is similar to the piriform, but the difference between the pars cephalica and pars thoracica is accentuated, with a narrow ocular area and a broader, round thoracic area (Fig. 10*C*).

(*2*) *Pars cephalica length*: 0, short; 1, long.
(L = 5; CI = 20; RI = 71)
The pars cephalica can be short, finishing just after the ocular area, or long, at least double the length of the ocular area (Fig. 10*B*, *C*).

(*3*) *Carapace profile (lateral view):* 0, convex (Fig. 10*D*); 1, flat (Fig. 10*E*); 2, higher in the ocular area and gradually sloping posteriorly (Fig. 10*F*); 3, higher in the ocular and thoracic area and abruptly sloping posteriorly (Fig. 10*G*); 4, similar to the one described in State 3, but also presents a median transverse depression (Fig. 10*H*).
(L = 17; CI = 23; RI = 18) (Silva Dávila 2003: char. 67)

(*4*) *Anterior eye row (anterior view):* 0, straight (Fig. 11*A*); 1, recurved (Fig. 11*B*); 2, procurved (Fig. 11*C*).
(L = 14; CI = 14; RI = 50)

(*5*) *Posterior eye row (dorsal view):* 0, straight (Fig. 11*D*); 1, recurved (Fig. 11*E*); 2, procurved (Fig. 11*F*).
(L = 14; CI = 14; RI = 58)

(*6*) *ALE relative to AME:* 0, similar size (Fig. 11*C*); 1, larger (Fig. 11*A*); 2, smaller (Fig. 11*B*).
(L = 15; CI = 13; RI = 56) (Silva Dávila 2003: char. 88)

(*7*) *Tapetum:* 0, canoe-shaped; 1, grate-shaped; 2, perforated with pores.
(L = 13; CI = 15; RI = 60) (Griswold 1993: char. 50)
A tapetum is defined as a reflecting layer in the indirect eyes, in our spiders appearing with a narrow middle line, typically longitudinal along the centre of the eyes (State 0, canoe-shaped), forming loops (State 1, grate-shaped), or with evenly distributed pores (State 2, perforated) (Homann 1971). Tapeta are present in at least the PME of most examined taxa. When the reflecting layer is opaque (see next character), i.e. as in oxyopids and *Stiphidion*, we record the pattern of receptors.

(*8*) *Tapetum crystals:* 0, shiny; 1, opaque.
(L = 3; CI = 33; RI = 33)
Some of the examined taxa have a grate-shaped arrangement of the photoreceptive cells, but this does not form a typical, shiny tapetum, e.g. *Oxyopes* and *Peucetia.* Opaque refers to the non-shiny condition.

(*9*) *Thoracic fovea:* 0, absent; 1, present.
(L = 5; CI = 20; RI = 33) (Silva Dávila 2003: char. 68)
Most of terminal taxa present a thoracic fovea. It is absent only in *Megadictyna*, *Parazygiella*, *Apollophanes*, *Metaphidippus*, *Cheiracanthium mildei* and Thomisidae.

(*10*) *Chilum:* 0, absent; 1, present.
(L = 4; CI = 25; RI = 40) (Silva Dávila 2003: char. 70)
The chilum, a small sclerite between the clypeal margin and base of the paturon, is present in most of the terminal taxa, absent only in *Oxyopes*, *Peucetia*, *Senoculus*, the two *Argoctenus* species, *Megadictyna* and *Parazygiella*.

(*11*) *Shape of chilum:* 0, entire, undivided; 1, divided in middle.
(L = 7; CI = 14; RI = 40) (Silva Dávila 2003: char. 71)
An undivided sclerotised plate is present in Thomisidae, *Apollophanes*, *Metaphidippus*, *Anyphaena*, *Cheiracanthium*, *Cambridgea* and *Odo bruchi*. Two sclerotised plates that are separated medially are present in most of the terminal taxa.

(*12*) *Precoxal sclerites:* 0, absent; 1, present.
(L = 2; CI = 50; RI = 66)
Precoxal sclerites, triangular and strongly sclerotised structures within the membranes between the sternum and the coxae, are present only in *Trachelas*, *Anyphaena* and *Cheiracanthium.*

(*13*) *Sternum extending between coxae IV:* 0, no; 1, yes.
(L = 8; CI = 12; RI = 73) (Griswold 1993: char. 45; Silva Dávila 2003: char. 76)

Chelicerae and mouth parts

(*14*) *Number of promarginal teeth of chelicerae:* 0, zero; 1, one; 2, two; 3, three.
(L = 10; CI = 40; RI = 0) (Silva Dávila 2003: char. 73)

(*15*) *Number of retromarginal teeth of chelicerae:* 0, zero (Fig. 12*A*); 1, one (Fig. 12*B*); 2, two (Fig. 12*C*); 3, three (Fig. 12*D*); 4, four (Fig. 12*E*); 5, five (Fig. 12*F*).
(L = 19; CI = 31; RI = 50) (Silva Dávila 2003: char. 75)

(*16*) *Texture of proximal edge of the movable chela of chelicerae (fang):* 0, smooth (Fig. 12*C*); 1, serrate (Fig. 12*A*, *B*, *D–F*).
(L = 8; CI = 12; RI = 22)
The proximal edge of the movable chela (fang) is serrate in most terminal taxa.

(*17*) *Number of retrolateral thick setae at fang base:* 0, zero; 1, one (Fig. 12*C–F*); 2, two or more (Fig. 12*A*, *B*).
(L = 4; CI = 50; RI = 60)
The thick setae are positioned at the prolateral base of the fang and are curved, directed to the tip of the fang, and usually apically serrated.

(*18*) *Serrula of endite:* 0, absent; 1, present.
(L = 2; CI = 50; RI = 0)

(*continued next page*)

Appendix 2. (*continued*)

The serrula consists of a single row of strongly to weakly developed teeth ventrally near the endite apex. It is present in most of the terminal taxa, except *Desis* and *Argoctenus*.

(*19*) *Serrula position (endite):* 0, apical; 1, subapical.
(L = 10; CI = 10; RI = 67) (Silva Dávila 2003: char. 79)

Male palp

(*20*) *Patellar process:* 0, absent; 1, present (Fig. 15*D*).
(L = 4; CI = 25; RI = 0) (Silva Dávila 2003: char. 2)
Most examined taxa present an unmodified patella, but a few taxa (*Tmarus*, *Senoculus*, *Cybaeus* and *Coelotes*) have a retrolateral projection. All these processes appear to be independently derived.

(*21*) *Retrolateral tibial apophysis (RTA):* 0, absent; 1, present (Figs 13*C*, *E*; 14*D*; 15*B*, *F*).
(L = 3; CI = 33; RI = 60) (Griswold 1993: char. 1; Silva Dávila 2003: char. 12)
The presence of a retrolateral tibial projection in the male palp is synapomorphic for a large group of spiders, called the 'RTA clade' (Coddington and Levi 1991). The RTA is absent in the outgroup of the RTA-clade, here comprising *Megadictyna*, *Parazygyella* and *Vidole*. Although some, i.e. *Megadictyna* and *Vidole*, have a dorsal tibial process (DTA), we do not consider this a homologue of the RTA but rather a separate homology (Griswold *et al*. 2005, characters 105, 108: 63–64). For example, *Callobius* has both the RTA and DTA, refuting the single homology. The RTA optimises as secondarily lost in *Psechrus*, *Allopecosa* and *Draposa*.

(*22*) *Ventral tibial apophysis (VTA, or Type 1 ventral process):* 0, absent; 1, present.
(L = 6; CI = 16; RI = 44) (Griswold 1993: char: 3)
This is an additional projection ventral to the RTA (see below for discussion).

(*23*) *Ventral tibial process (VTP, or Type 2 ventral process):* 0, absent; 1, present.
(L = 8; CI = 12; RI = 63)
The process is formed by the apical border of the tibia, and usually can touch the cymbium. Most character descriptions and matrices make no distinction between the ventral tibial apophysis (VTA, Type 1) and the ventral tibial process (VTP, Type 2), but both features are present in at least three terminals, *Callobius nevadensis*, *Titiotus californicus* and *Kilyana hendersoni*, failing the conjunction test of a single homology.

(*24*) *Dorsal tibial apophysis (DTA):* 0, absent; 1, present (Fig. 13*A*).
(L = 3; CI = 33; RI = 33)
A projection on the dorsal tibia occurs in *Megadictyna*, *Vidole*, *Callobius* and *Tmarus*. The independence of this feature from the RTA was proposed by Griswold *et al*. (1999) and discussed by Griswold *et al*. (2005); here at least *Callobius* has both a DTA and RTA, failing the conjunction test of a single homology and corroborating these two apophyses as different homologies.

(*25*) *Shape of cymbium:* 0, piriform (or 'attenuate'); 1, rounded to oval.
(L = 10; CI = 10; RI = 43)
Most terminal taxa present a pyriform cymbium, which is elongated at the apex. An oval cymbium with a blunt apex occurs in several species of the Zoropsidae clade.

(*26*) *Cymbial retrolateral process:* 0, absent; 1, present (Fig. 15*D*).
(L = 16; CI = 6; RI = 28) (Silva Dávila 2003: char. 25)
The cymbial retromargin may be smooth or present projections. These cymbial modifications, although common, represent in many cases independent autapomorphies or apomorphies at the suprageneric or generic levels. In some spider groups, e.g. Orbiculariae (*Parazygiella*), the process is called paracymbium.

(*27*) *Cymbial retrolateral groove:* 0, absent; 1, present (Fig. 13*E*, *F*).
(L = 2; CI = 50; RI = 75) (Silva Dávila 2003: char. 22)
Most terminal taxa have a smooth retrolateral cymbium, but *Cheiracanthum*, *Mituliodon* and *Argoctenus* have it with a deep to shallow groove.

(*28*) *Cymbial dorsal scopulae patch:* 0, absent; 1, present.
(L = 5; CI = 20; RI = 42) (Griswold 1993: char. 4)
The cymbial scopulae is formed by a dense dorsal patch of erect, stout setae of equal size, which differ from the other setae on the cymbium (Griswold 1993, fig. 7; Griswold *et al*. 2005, fig. 185F). This is found in most Griswoldiinae (Zoropsidae), and also in *Uduba*, *Zoropsis* and *Psechrus*.

(*29*) *Subtegulum lobe (locking lobe):* 0, absent; 1, present.
(L = 8; CI = 12; RI = 65) (Silva Dávila 2003: char. 28)
The subtegulum can present a ventrally directed lobe or projection. This lobe usually interlocks with a corresponding projection near the base of the embolus (Griswold *et al*. 2005, fig. 186F).

(*30*) *Subtegulum with a shallow excavation (cup-shaped) (locking lobe):* 0, absent; 1, present.
(L = 6; CI = 16; RI = 0; Silva Dávila 2003: char. 28)
Additionally to the lobe in the subtegulum, some terminal taxa can also present an excavation above the lobe, which also interlocks with the corresponding projection in the base of the embolus.

(*31*) *Lobe or condyle at base of embolus (locking lobe):* 0, absent; 1, present.
(L = 5; CI = 20; RI = 83) (Silva Dávila 2003: char. 27)
The condyle occurs at the base of the embolus, which can be visible in an unexpanded palp or hidden by the tegulum, and it interlocks with the subtegular retromargin (Griswold *et al*. 2005, fig. 186F).

(*32*) *Lycosoid tegular notch:* 0, absent; 1, present (Fig. 15*E*).
(L = 3; CI = 33; RI = 50) (Silva Dávila 2003: char. 29)
A proximal tegular notch makes the subtegulum visible in ventral view: its presence seems to be synapomorphic for Lycosidae and Pisauridae.

(*33*) *Distal tegular protuberance (DTP):* 0, absent; 1, present (Fig. 14*D*).

(*continued next page*)

Appendix 2. (*continued*)

(L = 3; CI = 33; RI = 0) (Griswold 1993: char. 20; Silva Dávila 2003: char. 32)
A tegulum that projects into a DTP associated with the apical division (Sierwald 1990) occurs in *Thaumasia*, *Hala* and *Nilus*.

(*34*) *Median apophysis:* 0, absent (Figs 13*A*, 14*A*); 1, present (Figs 13*B–F*, 15*A*, *C–F*).
(L = 12; CI = 8; RI = 8) (Griswold 1993: char. 12; Silva Dávila 2003: char. 44)
The median apophysis is a tegular sclerite that arises in the centre or near the base of the tegulum and is articulated by a flexible membrane (Griswold 1993: 10; Sierwald 1990: 21; Lehtinen 1967: 295). This morphology is absent in *Megadictyna*, *Psechrus*, *Senoculus*, *Trachelas*, *Metaphidippus*, *Apollophanes*, *Tmarus*, *Architis*, *Hala* and most Fused Paracribellar clade species.

(*35*) *Shape of median apophysis:* 0, convex or hook-shaped (Fig. 13*D–F*); 1, cup-shaped.
(L = 5; CI = 20; RI = 42) (Griswold 1993: char. 14)
The shape of the median apophysis can be classified in two groups: a hook-shaped median apophysis, convex in all surfaces or with concavities forming only narrow grooves (0); or cup-shaped, with a prolateral surface with an oval concavity that is closed distally and a retrolateral surface that is arched or convex (1).

(*36*) *Hooked median apophysis apex:* 0, simple; 1, bifid (Fig. 15*A*; Platnick and Ubick 2008: figs 8, 9).
(L = 2; CI = 50; RI = 50) (Griswold 1993: char. 17; Silva Dávila 2003: char. 49)
Titiotus, *Zoropsis* and *Kilyana* share a similar median apophysis with an apical split.

(*37*) *Position of median apophysis:* 0, opposite to embolus (Fig. 13*B*); 1, at distal margin of embolic base (Fig. 13*E*, *F*).
(L = 1; CI = 100; RI = 100) (Silva Dávila 2003: char. 45)
In most examined taxa, the median apophysis is positioned at the side of the embolic base. In contrast, Miturgidae and Viridasiidae present a unique configuration having the median apophysis arising on top of the distal margin of the embolic base.

(*38*) *Median apophysis angle:* 0, longitudinal; 1, transversal (Fig. 15*A*).
(L = 3; CI = 33; RI = 33) (Griswold 1993: char. 18)

(*39*) *Sierwald conductor:* 0, absent; 1, present (Figs 13*E*, *F*, 15*A*, *B*, *E*, *F*).
(L = 8; CI = 12; RI = 50)
Sierwald (1990: 37) recognised a peculiar membranous (hyaline) conductor in a retroapical position as a synapomorphy of at least *Dolomedes* and *Thalassius* (currently *Nilus*) within the Pisauridae. A structure in this position, wholly or partially hyaline, is more widespread in spiders. We propose the term 'Sierwald conductor' to contrast this with other types of conductor that arise near the embolic base and accompany or embrace the embolus for part or all of its length, e.g. in *Desis* or *Stiphidion*. The term 'Sierwald conductor' refers to a structure arising at the retroapex of the tegulum; it may or may not support the embolus. If we follow the pathway made by the spermatic duct, which starts in the subtegulum, extends into the tegulum and ends in the embolus, the Sierwald conductor is the first process to arise from the tegulum. The shape and size of the conductor varies broadly among all examined taxa. At least some taxa (e.g. *Vidole*) have processes that arise near the embolic base (i.e. a typical conductor) and at the retroapex of the tegulum (i.e. a 'Sierwald conductor'): this corroborates the separate homologies of these structures (for example, see Griswold (1990, fig. 19b), showing the structures labelled EBA and M at the embolic base, like a typical conductor, and the structure labelled C at the tegulum retroapex, which is a 'Sierwald conductor').

(*40*) *Sierwald conductor texture:* 0, hyaline; 1, sclerotised; 2, partially sclerotised.
(L = 3; CI = 66; RI = 50)

(*41*) *Tegular process at Sierwald conductor base:* 0, absent (0); present (1).
(L = 1; CI = 100; RI = 100)

(*42*) *Additional tegular process:* 0, absent; 1, present.
(L = 9; CI = 11; RI = 69)
In addition to a median apophysis, a conductor embracing the embolus, and Sierwald conductor, the tegulum can have yet another apophysis, the additional tegular process, which can be either membranous or sclerotised. This process arises between the base of the embolus and the median apophysis.

(*43*) *Shape of additional tegular process:* 0, convex, simple; 1, apically enlarged, T-shaped (Fig. 14*A*, *B*).
(L = 2; CI = 50; RI = 80)
The additional tegular process can be apically enlarged and supporting the embolus, in a T-shaped configuration. It is present in the Fused Paracribellar clade. Forster and Wilton (1973: 21) referred to this as a T-shaped conductor, characteristic of New Zealand Agelenidae.

(*44*) *Embolus base:* 0, fixed (Fig. 14*A*, C); 1, flexible (Fig. 13*E*, *F*).
(L = 13; CI = 7; RI = 50) (Griswold 1993: char. 23)
Fixed embolus presents a sclerotised attachment to the tegulum. Flexible embolus is attached to the tegulum by membranous cuticle and has some degree of movement perpendicular to the tegulum.

(*45*) *Embolus origin:* 0, retrolateral or 3 o'clock (Fig. 13*E*); 1, middle of the tegulum; 2, prolateral or 9 o'clock (Fig. 14*A*): 3, apical or 12 o'clock (Fig. 14*C*); 4, basal or 6 o'clock (Fig. 13*A*).
(L = 21; CI = 14; RI = 21) (Silva Dávila 2003: char. 50)
We refer to the embolus origin, on the left palp in ventral view, by analogy to the old-style clock with hour and minute hands, which convention has been used for generations to express relative direction. Whereas the origin of the embolus may vary within a single genus, in some groups the origin appears to be more stable.

(*46*) *Embolus arising from basal lobe:* 0, no; 1, yes (Fig. 13*E*, *F*).
(L = 4; CI = 25; RI = 40) (Griswold 1993: char. 24)
The embolus origin can arise gradually from the tegular surface or present a basal lobe, which can be firmly or flexibly attached to the tegulum.

(*47*) *Embolus direction of curve:* 0, clockwise (Fig. 15*A*); 1, counterclockwise (Fig. 15*E*).
(L = 9; CI = 22; RI = 22) (Griswold 1993: char. 26)
Again we use analogy to the old-style clock with hour and minute hands, as applied to the left palp in ventral view. The embolus curving in a clockwise direction occurs in most terminal taxa. The counterclockwise embolus occurs only in *Megadictyna*, *Parazygiella*, *Uduba*, *Draposa*, *Alopecosa*, *Tmarus*, *Nilus* and *Architis*.

(*48*) *Embolus shape in cross section:* cylindrical (0); oval (1); laminar (2).

(*continued next page*)

Appendix 2. (*continued*)

(L = 15; CI = 13; RI = 27)
The shape refers to a cross-section in the middle of the embolus

(*49*) *Pars pendula:* 0, absent; 1, present.
(L = 1; CI = 100; RI = 100)
Pars pendula is a membranous strip that may accompany the sclerotised truncus of the embolus. Whereas this structure is widespread in spiders, it is conspicuous in only a few of our exemplars, i.e. the viridasiids *Viridasius* and *Vulsor*.

Walking legs

(*50*) *Inferior tarsal (third) claw (ITC) on leg I:* 0, absent; 1, present (Fig. 16*A*, *C*, *E*).
(L = 6; CI = 16; RI = 72) (Silva Dávila 2003: char. 110)
Three tarsal claws are regarded to be a plesiomorphic condition for spiders (Platnick and Gertsch 1976; Coddington and Levi 1991). The third claw (inferior tarsal claw, ITC) is present in most of our terminal taxa, including the *Cheiracanthium* species from Madagascar (Dionycha) and most of the Ctenidae. Dionycha means 'two tarsal claws', but the presence of a third small claw is not uncommon in Salticidae, Anyphaenidae and Miturgidae. Ctenidae are usually regarded as having only two tarsal claws, but several species placed in this family present an inferior tarsal claw on at least the first leg.

(*51*) *Teeth on third claw (leg I):* 0, absent (Fig. 16*B*, *C*); 1, present (Fig. 16*E*).
(L = 9; CI = 11; RI = 55) (Silva Dávila 2003: char. 112)

(*52*) *Adhesive setae on tarsus:* 0, absent (Fig. 16*E*, *F*); 1, present (Fig. 16*C*, *D*).
(L = 8; CI = 12; RI = 74)
Wolff and Gorb (2012) provided a detailed and precise discussion of leg setae, especially scopular setae, and provided a new classification of these setae. Adhesive setae (Fig. 16*D*) are defined by the presence of spatulate microtrichia (Wolff and Gorb 2012). Those setae can be distributed as a tuft on the tip of the tarsus, close to the claws, which is commonly called a 'claw tuft'; as a scopula on ventral tarsus; or a combination of both. The presence of large quantities of non-adhesive friction setae can form claw tufts or scopulae on the tarsus (Figs 16*E*, *F*), but the function of the friction setae is different from the adhesive setae (Wolff and Gorb 2012).

(*53*) *Adhesive setae on tip of the tarsus (claw tufts):* 0, absent; 1, present (Fig. 16*C*, *D*).
(L = 2; CI = 50; RI = 50)
The adhesive setae can be organised on the tip of the tarsus, as clusters, named claw tufts. The use of the term 'claw tufts' is widespread, and in the literature this term can also be used to describe a cluster of serrate setae in the tip of the tarsus. Here we are considering only a restricted definition: the clusters formed by adhesive setae (Wolff and Gorb 2012).

(*54*) *Tenant plates (bearing claw tufts):* 0, absent; 1, present (Fig. 16*B*, *C*).
(L = 3; CI = 33; RI = 33) (Silva Dávila 2003: char. 106)
Tenant plates are movable plates at the tip of the tarsus that bear adhesive setae.

(*55*) *Adhesive setae on ventral tarsus (tarsal scopulae):* 0, absent; 1, present.
(L = 7; CI = 14; RI = 0) (Silva Dávila 2003: char. 104)
The adhesive setae can be distributed ventrally on the tarsus, forming a dense patch. As is the case with the claw tufts, the term 'tarsal scopula' is also used in the literature to describe setae that are not adhesive. Here we score tarsal scopula as present only when this structure is formed by adhesive setae (Wolff and Gorb 2012).

(*56*) *Tarsus I structure:* 0, entire; 1, pseudosegmented (Fig. 16*A*, pointed by arrow).
(L = 9; CI = 11; RI = 27)
Some species present a ring of less sclerotised cuticle close to the tip of the tarsus. This ring allows the tip of the pseudosegmented tarsus to be mobile.

(*57*) *Tarsal organ, opening shape:* 0, round to oval (Fig. 17*A*); 1, stellate (Fig. 17*B*); 2, tear drop or keyhole (Fig. 17*C*); 3, narrow slit (Fig. 17*D*).
(L = 5; CI = 60; RI = 71)

(*58*) *Position of tarsal organ:* 0, close to the tip of tarsus; 1, distant from the tip (Fig. 18*A*, *B*).
(L = 4; CI = 25; RI = 40)
Most examined taxa present the tarsal organ in a distal position, close to the tip of the tarsus. *Parazygiella*, *Oxyopes*, *Peucetia*, *Griswoldia* and *Kilyana* have the tarsal organ distant from the tip of the tarsus, in the proximal half (Fig. 18*A*, *B*).

(*59*) *Tarsal trichobothria:* 0, absent; 1, present (Fig. 18*A*–*F*).
(L = 1; CI = 100; Ri = 100)

(*60*) *Tarsal trichobothria rows number:* 0, one (Fig. 18*A*); 1, two or more (Fig. 18*B*).
(L = 7; CI = 14; RI = 45)

(*61*) *Tarsal trichobothria lengths:* 0, all equal; 1, becoming longer distally.
(L = 6; CI = 16; RI = 61)

(*62*) *Tarsal trichobothrial distribution:* 0, row(s) starting close to the tip of tarsus, at or anterior to tarsal organ; 1, row(s) starting distant from the tip, proximal of the tarsal organ (Fig. 18*A*; arrow points to the tarsal organ position).
(L = 1; CI = 100; RI = 100)

(*63*) *Tarsal trichobothrium, proximal and distal plates:* 0, without distinction (Fig. 18*C*); 1, well differentiated (Fig. 18*D*–*F*).
(L = 2; CI = 50; RI = 50)

(*64*) *Tarsal trichobothrium proximal plate texture:* 0, smooth (Fig. 18*F*); 1, transverse ridges (Fig. 18*E*); 2, longitudinal ridges (Fig. 18*D*).
(L = 12; CI = 16; RI = 47) (Silva Dávila 2003: char. 115)

(*65*) *Number of longitudinal rows of dorsal trichobothria on the metatarsus:* 0, one or two; 1, three or more.
(L = 1; CI = 100; RI = 100)

(*66*) *Distal spine of ventral metatarsus:* 0, absent; 1, present.
(L = 10; CI = 10; RI = 52)

(*continued next page*)

Appendix 2. (*continued*)

(*67*) *Number of ventral spines on metatarsus I:* 0, zero; 1, one pair; 2, two pairs; 3, three pairs; 4, four pairs.
(L = 18; CI = 22; RI = 30) (Silva Dávila 2003: char. 98)
In general, the leg spination exhibits great variation at family level.
(*68*) *Male tibial crack (autospasy suture):* 0, absent; 1, present.
(L = 4; CI = 25; RI = 62) (Griswold 1993: char. 52; Silva Dávila 2003: char. 93)
The legs of some males can break following a suture line at the base of tibia, just distad of the basal pair of ventral spines (Griswold 1993, figs 3, 4). It occurs in the Ududidae and some species of Zoropsidae, e.g. *Phanotea*, *Griswoldia*, *Kilyana* and *Zoropsis*.
(*69*) *Number of ventral spines on tibia I:* 0, three pairs or fewer; 1, four pairs; 2, five pairs; 3, six or more pairs.
(L = 12; CI = 25; RI = 68) (Griswold 1993: char. 59; Silva Dávila 2003: char. 97)
As in character 67, the leg spination on ventral tibia exhibits great variation at family level.
(*70*) *Tibia I with ventral spines overlapping:* 0, no; 1, yes.
(L = 10; CI = 10; RI = 18) (Silva Dávila 2003: char. 99)
This refers to spine length: we classify tibia I as having ventral spines overlapping when the proximal spines are long enough to reach and pass the origin of the next, distal spines.
(*71*) *Scales on legs (smooth or feathery):* 0, absent; 1, present.
(L = 7; CI = 14; RI = 53) (Griswold 1993: char. 58)
Scales may be recognised by having the shaft bent near its socket. Most scales identified in this analysis are of the feathery type. Only *Metaphidippus* presents a smooth scale.
(*72*) *Calamistrum:* 0, absent; 1, present.
(L = 9; CI = 11; RI = 27) (Griswold 1993: char. 64)
(*73*) *Calamistrum shape:* 0, linear; 1, oval (Griswold 1993: fig. 1).
(L = 1; CI = 100; RI = 100) (Griswold 1993: char. 65; Silva Dávila 2003: char. 103)
Oval refers to a calamistral arrangement comprising a patch of setae not arranged in rows, or a group of several, ill-defined rows (Griswold 1993: fig. 1). This character is non-applicable to the numerous ecribellate taxa in our dataset. If we apply acctran optimisation, the oval calamistrum optimises as an ambiguous synapomorphy for a large clade, including Dionycha, which has no calamistrum. Deltran optimisation specifies the oval calamistrum as a synapomorphy for a less inclusive clade, a more realistic outcome.
(*74*) *Distal border of trochanter leg I:* without notch (0); deeply notched (1); asymmetric and shallowly notched (2).
(L = 14; CI = 14; RI = 63) (Griswold 1993: char. 55; Silva Dávila 2003: char. 94)
This character refers to the distal border of the trochanter, which exhibits a range of variation of shapes.

Opisthosoma

(*75*) *Pedicel lorum I and II junction:* 0, separate; 1, fused (Fig. 19*A–F*).
(L = 3; CI = 33; RI = 80)
In many spiders the pedicel connecting the carapace and abdomen has two separate, dorsal sclerites: the anterior lorum I and posterior lorum II. A fused lorum I and II occurs only in *Parazygiella* and some families of Lycosoidea (Lycosidae, Pisauridae, Thomisidae and Oxyopidae), with a secondary reversion to separated in *Cupiennius*.
(*76*) *Lorum I projected over II:* 0, no; 1, yes.
(L = 1; CI = 100; RI = 100)
This is a synapomorphy for Stiphidiidae (*Stiphidion*).
(*77*) *Epiandrous spigots:* 0, absent; 1, present.
(L = 3; CI = 33; RI = 86) (Silva Dávila 2003: char. 125)
The presence of modified setae (spigots) in the epigastric region of males that are connected to the epiandrous glands is a plesiomorphic condition in Araneomorphae (Griswold *et al*. 2005). Epiandrous spigots are absent in the Oval Calamistrum clade.

Epigynum

(*78*) *Epigynum configuration:* 0, anterior and posterior folds (Fig. 20*A*); 1, median and lateral folds (Fig. 20*B*, *C*); 2, single fold (Fig. 20*D*).
(L = 7; CI = 28; RI = 61) (Griswold 1993: char. 28; Silva Dávila 2003: char. 52)
Several outgroups present an epigynum formed by anterior and posterior folds. A longitudinal development of the epigynum results in median and lateral folds of the epigynum, which can be well differentiated or partly fused (Sierwald 1989). State 2 refers to an epigynal cuticle fused, either well or lightly sclerotised.
(*79*) *Epigynum median fold:* 0, convex; 1, concave.
(L = 2; CI = 50; RI = 66)
The median fold of the epigynum can be concave, forming a depression.
(*80*) *Epigynum lateral sector form:* 0, convex; 1, with tooth (Fig. 20*C*).
(L = 9; CI = 11; RI = 33) (Griswold 1993: char. 30; Silva Dávila 2003: char. 57)
The epigynal lateral folds may have toothlike outgrowths. The shape of this lateral sector apophysis varies greatly and is often species-specific.
(*81*) *Epigynum lateral sector form:* 0, convex; 1, with pocket (Fig. 20*D*).
(L = 7; CI = 14; RI = 0) (Silva Dávila 2003: char. 58)
The epigynal lateral folds may present shallow lateral depressions.
(*82*) *Spiraled copulatory ducts (some Pisauridae):* 0, absent; 1, present (Fig. 20*E*).
(L = 1; CI = 100; RI = 100)
(*83*) *Copulatory ducts with elongated gland tubes:* 0, absent; 1, present (Fig. 20*F*).
(L = 5; CI = 20; RI = 20)

(*continued next page*)

Appendix 2. (*continued*)

Here we define these as any tube (short or long) originating from a hole in the copulatory ducts.

(*84*) *Bennett's gland:* 0, absent; 1, present (Fig. 21*A–D*, indicated by arrows).
(L = 5; CI = 20; RI = 20)
These large, barrel-shaped, vulval perforations with numerous small pores were first recognised by Bennett (1992) in cybaeids, members of Forster's (1970) Dictynoidea. Bennett (1992) accordingly called these 'Dictynoid' pores. In fact, they are absent in all Dictynidae: hence we use the replacement name 'Bennett's gland'.

(*85*) *Head of spermatheca texture:* 0, entire, imperforate; 1, with pores.
(L = 4; CI = 25; RI = 0)

(*86*) *Head of spermatheca with gland tubes:* 0, no; 1, yes (Fig. 21*A*, *E*, *F*).
(L = 16; CI = 6; RI = 28)
Here we define these as any tube (short or long) originating from a hole in the head of the spermathecae. The homology of these tubes is still uncertain.

(*87*) *Arrangement of gland tubes of the head of the spermathecae:* 0, scattered; 1, clustered (Fig. 21*E*, *F*).
(L = 3; CI = 33; RI = 66)

(*88*) *Texture of spermathecae Ududidae-like:* 0, absent, fine texture smooth (Fig. 21*E*, *F*).; 1, present, fine texture with small convex projections (Fig. 22*A–D*).
(L = 2; CI = 50; RI = 80)
In Ududidae the vulval cuticle surface is formed by unique small convex projections, usually covering the spermathecae and sometimes (like in *Uduba*) also covering the copulatory ducts.

Spinnerets

(*89*) *Minor ampullate gland spigots:* 0, together on mound; 1, not on a mound, separated by their diameter; 2, not on a mound, separated by less than their diameter.
(L = 3; CI = 66; RI = 83) (Silva Dávila 2003: char. 137)

(*90*) *Anterior median spinnerets (as cribellum or colulus):* 0, absent, no cribellum or colulus; 1, present.
(L = 4; CI = 25; RI = 50)

(*91*) *Anterior median spinnerets shape:* 0, colulus; 1, cribellum.
(L = 9; CI = 11; RI = 27) (Silva Dávila 2003: chars 128–129)
The presence of a cribellum is considered a synapomorphy to all Araneomorphae (Platnick 1977: 7). However, the loss or reduction to a colulus occurred several times in the spider phylogeny.

(*92*) *Cribellum shape:* 0, divided; 1, entire, not divided.
(L = 3; CI = 33; RI = 33) (Griswold 1993:char. 41; Silva Dávila 2003: char. 129)

(*93*) *Posterior lateral spinnerets:* 0, short; 1, elongated.
(L = 3; CI = 33; RI = 33) (Silva Dávila 2003: char. 131)
Most of examined taxa present short posterior lateral spinnerets. Some miturgids present posterior lateral spinnerets with the distal segment greatly elongated and often more slender than the basal segment. Ududid PLS are not as elongate as those of eutichurids, but are still relatively longer than in other families in our matrix.

Behaviour

(*94*) *Nursery web:* 0, absent; 1, present.
(L = 2; CI = 50; RI = 66) (Griswold 1993: char. 67; Silva Dávila 2003: char. 145)

(*95*) *Lycosidae parental care:* 0, absent; 1, present.
(L = 1; CI = 100; RI = 100) (Silva Dávila 2003: char. 145)
Lycosid females transport their young on the abdomen until the spiderlings disperse (Foelix 2011: fig. 7.35).

(*96*) *Egg sac:* 0, fixed (web or in the environment); 1, carried by the chelicerae; 2, carried attached to the spinnerets.
(L = 5; CI = 40; RI = 40)